NGL 33-018-033

COMPOSITE STRUCTURAL PROGRAM

RENSSELAER POLYTECHNIC INSTITUTE TROY, N.Y. 12181

(NASA-CR-163377) COMPOSITE STRUCTURAL MATERIALS Semiannual Report, Sep. 1979 - Apr. 1980 (Rensselaer Polytechnic Inst., Troy, N. Y.) 152 p HC A08/MF A01 CSCL 01C

N80-28339

Unclas

G3/05 28239

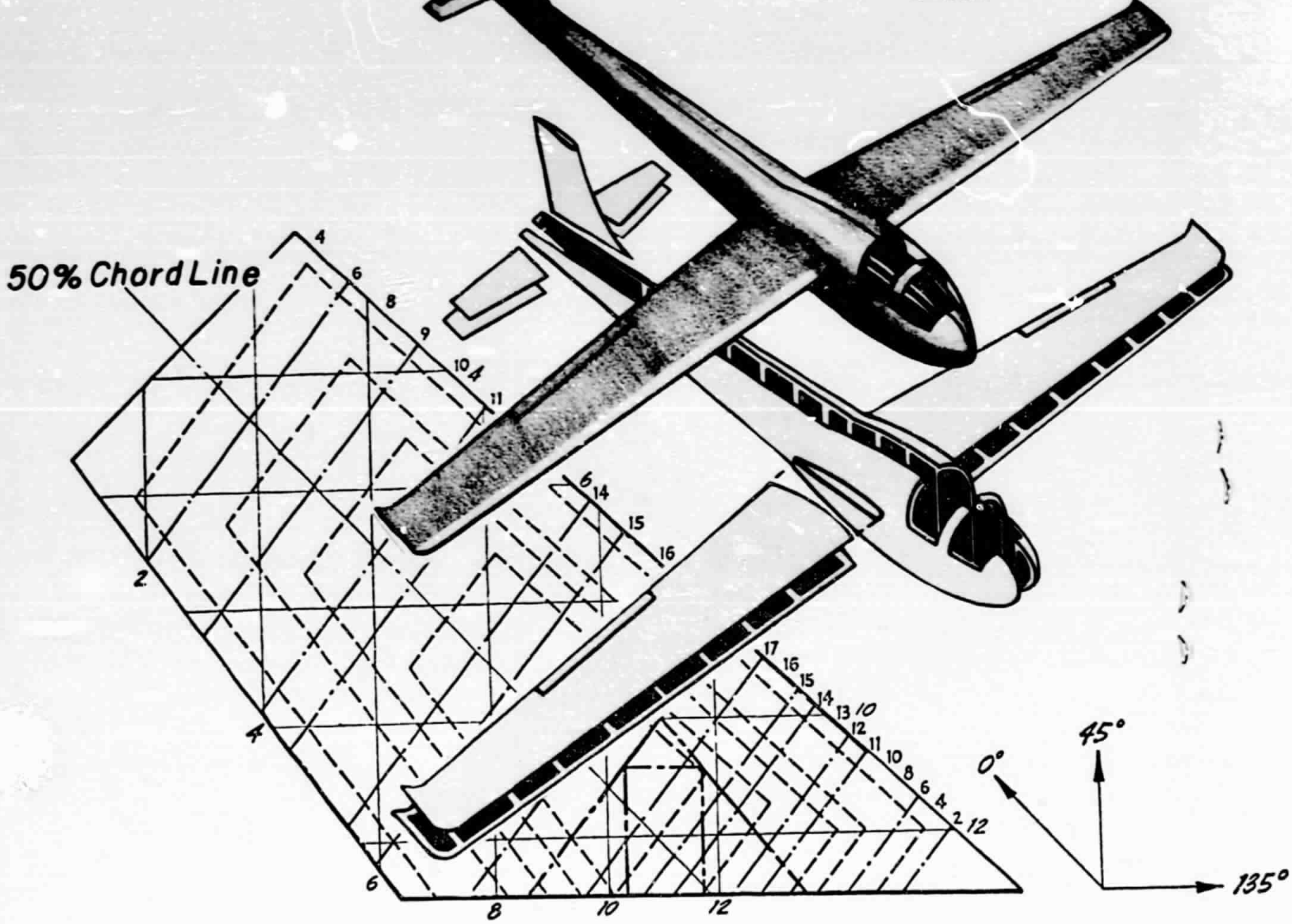

SKIN DESIGN

SPONSORED BY NASA/AFOSR

Semi-Annual Progress Report

September 1979 - April 1980

COMPOSITE STRUCTURAL MATERIALS

Air Force Office of Scientific Research

and

National Aeronautics and Space Administration

Grant No. NGL 33-018-003

Co-Principal Investigators:

George S Ansell
Dean, School of Engineering

Robert G. Loewy
Institute Professor

and

Stephen E. Wiberley
Professor of Chemistry

Rensselaer Polytechnic Institute

Troy, New York 12181

NASA Technical Officer

Leonard A. Harris
Materials and Structures Division

NASA Headquarters

38th Semi-Annual Report June 1980

Semi-Annual Progress Report

September 1979 - April 1980

COMPOSITE STRUCTURAL MATERIALS

Air Force Office of Scientific Research

and

National Aeronautics and Space Administration

Grant No. NGL 33-018-003

Co-Principal Investigators:

George S Ansell
Dean, School of Engineering

Robert G. Loewy
Institute Professor

and

Stephen E. Wiberley
Professor of Chemistry

Rensselaer Polytechnic Institute

Troy, New York 12181

NASA Technical Officer

Leonard A. Harris
Materials and Structures Division

NASA Headquarters

38th Semi-Annual Report June 1980

CONTENTS

LIST OF TABLES

LIST OF FIGURES

INTRODUCTION

INTRODUCTION

The promise of filamentary composite materials, whose development may be considered as entering its second generation, continues to generate intense interest. Such interest is well founded, having been generated by the possibility of using brittle materials with high modulus, high strength, but low density in composites which fail in a non-catastrophic manner. Such fiber reinforced composite materials offer substantially improved performance and potentially lower costs for aerospace hardware. While much progress has been achieved since the initial developments in the mid 1960's, however, only a very few applications to primary aircraft structure have been made, and those are in a material-substitution mode and on military aircraft.

To fulfill the promise of composite materials more completely, requires a strong technology base. NASA and AFOSR have realized that to fully exploit composites in sophisticated aerospace structures the technology base must be improved. This, in turn, calls for expanding fundamental knowledge and the means by which it can be successfully applied in design and manufacture. Not the least of this effort is to learn how to design structures specifically to capitalize on the unique properties of composite materials. It also calls for expanding the body of engineers and scientists competent in these areas. As part of their approach to accomplishing this, NASA and AFOSR have funded the current composites program at Rensselaer. The purpose of the RPI composites program is to develop advanced technology in the areas of physical properties, structural concepts and analysis, manufacturing, reliability and life prediction. Concommitant goals are to educate engineers to design and use composite materials as normal or conventional materials. A multifaceted program has been instituted to achieve these objectives. The major elements of the program are:

1. CAPCOMP (Composite Aircraft Program Component). CAPCOMP is primarily a graduate level project being conducted in parallel with a composite structures program sponsored by NASA and performed by a private, aerospace manufacturing contractor. The first component redesign is being done in conjunction with the Boeing Commercial Airplane Company. The main spar/rib region on the Boeing 727 elevator, near its actuator attachment point, was selected, with Boeing's advice and the concurrence of NASA/AFOSR, for study in CAPCOMP. The magnitude of the project - studying, designing, fabricating and testing of a relatively small but highly stressed region on the elevator - is both consistent with Rensselaer's capabilities and a significant challenge. The selection of a portion of a full-scale flight hardware structure assures relevance to this project's direction.

Visits to Boeing were conducted in the Fall of 1978 by Professor Hoff and several of his students, and the first serious design work began shortly thereafter. Two alternative designs were pursued to the point of preliminary analysis and testing. One of these was selected for more detailed analysis, redesign, complete fabrication and testing. Further progress on fabrication planning and fabrication facilities and test fixture development is reported in Part I.

2. CAPGLIDE (Composite Aircraft Program Glider). This undergraduate demonstration project has as its objectives the design, fabrication and testing of a foot-launched, ultralight glider using composite structures. A flight vehicle was selected to maximize student interest and to provide the students with a broad-based engineering experience. For those students continuing with graduate work at RPI, CAPGLIDE is intended to provide natural progression to CAPCOMP. The progress on the CAPGLIDE project to date has been very good. Seven professors and approximately 30 students were actively engaged in the project during this period; that is, the '79-'80 semesters. High point of the project to date was final assembly of the complete glider, dubbed "RP-1", and its exhibition during the site visit to Rensselaer by a team of scientists/engineers from NASA and industry. A description of the status of the CAPGLIDE project to the end of the current reporting period is given in Part II.

3. COMPAD (Computer Aided Design). A major thrust of the composites program is to develop effective and efficient tools for the analysis and design of composite structures. Rensselaer and NASA Langley have jointly implemented the use of the SPAR code on minicomputers, and the work at Rensselaer

has made "virtual memory" available to those using SPAR. Attention for the current period has continued to be focused on preprocessor developments; details are reported in Part III.

4. Composites Fabrication and Test Facility. Structural design engineers, educated only by course work and design projects limited to paper, often fail to sense or appreciate problems involved in fabrication. The actual fabrication and testing of composite structural components provides this training and the final validation for the designs in our CAP projects. RPI's Composites Fabrication and Test Facility is located in the laboratory and high bay areas of the Jonsson Engineering Center. Equipment is available for compression molding parts as large as 19" x 19" and vacuum bagging parts of much larger size. Panels approximately 4' x 20' have been made by vacuum bagging. Specifics are given in Part II, CAPGLIDE. A pressure vessel for small parts and spars has been designed and built. A second one capable of higher pressures was designed and parts ordered in the current period; assembly of all components but air circulation is now complete. More information on this development is contained in Part I, CAPCOMP.

5. INSURE (Innovative and Supporting Research). The criteria for selection of research projects to be conducted under this program are (a) that they must anticipate critical problem areas which may occur in the CAP or NASA/AFOSR programs or (b) that solutions to existing problems are not

yet satisfactorily in hand. During the reporting period seven such projects were conducted as part of the program. Results from the ongoing projects are reported in Part IV.

6. Curriculum Revisions. The goal of educating engineers to think of composites as normal or conventional materials has required changes in curriculum. Since the initiation of this program, almost all Rensselaer engineers take introductory courses which incorporate the concepts of anisotropy and composite materials. In addition, six specialized courses in composites have been offered during the past three years to develop those special skills required of students involved in the composites program. A new course was introduced in the Fall of '78 semester on composite design and analysis using programmable hand calculators, a central mini and full frame computers. A new graduate level advanced topics course with the title "Advanced Finite Elements" was offered for the first time in September 1979.

The additions of the SAP and SPAR computer codes and the growing availability of interactive computer graphics under our COMPAD program element have reached the point where our engineering students are using these facilities as everyday working tools for design, analysis and visualization purposes. We have thus achieved one of the principal goals of the curriculum development activities.

7. Technical Interchange.

a) Mr. Hiromitsu Otsuka joined the faculty at RPI as a Visiting Research Associate. Mr. Otsuka is a member of the staff of the Industrial Products Research Institute of the Ministry of International Trade and Industry where he was engaged in developing a light weight wheelchair of fiber reinforced plastic materials. At RPI he has been conducting acoustic emission studies of composites under load, together with RPI's Professor H. Scarton, during this period.

b) Technical Meetings: Technical meetings, on- and off-campus, provide important opportunities for interchange of technical information. Because of the large number of composites meetings, a central catalog with all upcoming meetings is being maintained and distributed periodically. In this way we help assure that a Rensselaer staff member will participate in important meetings. The calendar for this reporting period is shown in Table I. Meetings attended by RPI composites program faculty/staff during the reporting period are shown in Table II. Some meetings particularly relevant to composites, held on-campus with off-campus speakers, are listed in Table III. A list of composite-related visits to relevant organizations by RPI faculty/staff/students, with the purpose of each visit outlined, is presented in Table IV.

In summary, the NASA/AFOSR Composites Aircraft Program is a multi-faceted program whereby aeronautical, mechanical and materials engineers must interact to achieve its goals. "Hard-nosed" engineering of composite aircraft structures is balanced against research aimed at solving present and future

TABLE I
CALENDAR OF COMPOSITES-RELATED MEETINGS
for the period September '79 to April '80

1979	
10/1-3	Tests Methods and Design Allowables for Fibrous Composites, Dearborn, Mi. "Sponsored by ASTM."
10/7-10	Fall Meeting of Society for Experimental Stress Analysis, Mason, Oh.
10/8-11	Advanced Techniques in Failure Analysis Symposium and Exposition, Los Angeles, Ca.
10/10-11	Conference on Engine Structures, NASA Lewis Research Center.
10/10-12	3rd SAE International Conference on Vehicle Structural Mechanics, Troy, Mi. "Sponsored by SAE."
10/16-18	50th Shock and Vibration Symposium, Colorado Springs, Co.
10/22-23	Grumman/University Technical Forum, Bethpage, N. Y. "Sponsored by Grumman."
10/23-25	SAMPE Technical Conference, Boston, Ma. "Sponsored by SAMPE."
10/28	Annual Meeting of the Society of Rheology, Boston. Ma.
10/30-11/1	5th Annual Mechanics of Composites Review, Dayton, Oh. "Sponsored by the Air Force Materials Lab."
10/30	U. S. National Committee for Theoretical and Applied Mechanics, Boston, Ma.
11/6-8	Helicopter Propulsion System Specialists' Meeting, Williamsburg, Va. "Sponsored by AHS."
11/13-16	Supersonic Cruise Research Conference, Hampton, Va. "Sponsored by NASA Langley."
12/2	9th International Symposium on Acoustical Imaging, Houston, Tx.
12/2-7	ASME Winter Annual Meeting, N. Y. C., N. Y. "Sponsored by ASME."

TABLE I (continued)

1980	
1/6-11	Engineering Foundation Conference on Fatigue Crack Initiation, Asilomar, Ca.
1/14-16	18th Aerospace Sciences Meeting, Pasadena, Ca. "Sponsored by AIAA."
1/20-26	Gordon Research Conference on Deformation and Failure in Composites, Santa Barbara, Ca.
2/4-8	35th Annual Reinforced Plastics/Composites Institute Conference, New Orleans, La. "Sponsored by the Society of Plastics Industry.
2/10-13	3rd Annual Meeting of Adhesion Society, Savannah, Ga.
2/24-26	109th AIME Annual Meeting, Failure Modes in Composites V, Las Vegas, Ne. "Sponsored by AMMRC."
3/25-27	Specialists Meeting on Fatigue Methodology, St. Louis, Mo. "Sponsored by AHS."
4/14-15	Symposium on Short Fiber Reinforced Composite Materials, Minneapolis, Mn. "Sponsored by ASTM/SAE/ASCE."
4/14-18	Practical Applications and Design of Fibrous Composites, Los Angeles, Ca. "Sponsored by UCLA."
4/22-24	Conference on Propeller Propulsion, Dayton, Oh. "Sponsored by University of Dayton, AIAA, AHS, Society of Auto Engineering."

TABLE II

COMPOSITES-RELATED TECHNICAL MEETINGS ATTENDED OFF-CAMPUS

for the period September '79 to April '80

1979	
10/1-3	ASTM Meeting on Test Methods and Design Allowables for Fibrous Composites (Prof. Helwig), Dearborn, Mi.
10/10-11	Conference on Engine Structures (Prof. Loewy), NASA Lewis Research Center.
10/28	Annual Meeting of the Society of Rheology, (Prof. Sternstein and D. Taggart), Boston, Ma.
10/30-11/1	Mechanics of Composites Review (Prof. Kudva), Dayton, Oh.
10/30	U. S. National Committee for Theoretical and Applied Mechanics (Prof. Hoff), Boston, Ma.
12/2	9th International Symposium on Acoustical Imaging (Prof. Das), Houston Tx.
1980	
1/6-11	Engineering Foundation Conference on Fatigue Crack Initiation (Prof. Stoloff), Asilomar, Ca.
1/20-26	Gordon Research Conference on Deformation and Failure in Composites (Profs. Diefendorf and Sternstein*), Santa Barbara, Ca.

* Presented a paper titled, "Swelling Stress in Epoxy Composites".

TABLE III
COMPOSITES-RELATED MEETINGS/TALKS HELD AT RPI
(September '79 - April '80)

Topic	Date	Speaker(s)
Aromatic Polyamides: Development and Uses	10/10/79	Paul W. Morgan, formerly Research Associate, E. I. duPont de Nemours and Co.
New Methods in High Temperature Structural Design	10/11/79	Donald Griffin, Westinghouse Corp.
World Trends in Computer-Aided Manufacturing	10/25/79	M. Eugene Merchant, Director of Research Planning, Cincinnati Milacron, Inc.
Effects of Moisture on Epoxy Composites	11/29/79	James B. Whiteside, Head, Applied Mechanics Laboratory, Grumman Aerospace Company
An Integrated Shell Analysis System with Interactive Computer Graphics	11/13/79	John F. Abel, Cornell University
New Thoughts on the Problem of Bending and Twisting of Beams	12/13/79	Eric Reissner, University of California at San Diego
Microscopic Fracture of Fibrous Composites	1/15/80	Byron Pipes, Director, Center for Composite Materials, University of Delaware
Some Topics of Low-Cycle Fatigue Design of Heavy Duty Components	1/17/80	Y. Asada, University of Tokyo
Preliminary Design Study of a Space Telescope Using Composites	2/7/80	Donald E. Skoumal, Lead Engineer, Structural Development, Boeing Aerospace Co.
Acoustic Scattering in Random Inhomogeneous Media	2/18/80	Mark Beran, Tel-Aviv University
Challenges of Opportunities of In-situ Composites	3/6/80	F. Lemkey, United Technologies Corp.
Forces Acting on Lattice Defects in Generalized Coordinates	3/13/80	Richard K. T. Hsieh, Royal Institute of Sweden
Reacting to Things That Fall Apart in Service	4/17/80	Oscar Orringer, Transportation Systems Center, Department of Transportation, Cambridge, Ma.

TABLE IV
COMPOSITES-RELATED VISITS TO RELEVANT ORGANIZATIONS
by RPI Faculty/Staff/Students

Visited	Date	by Prof(s)	Purpose
ASTM Committee Meetings E-9 and E-24, Pittsburgh, Pa.	10/30-11/1	N. Stoloff	Meetings concerning fatigue toughness and fracture toughness testing
Lockheed California Co.	11/6	S. Sternstein	To discuss processing science aspects of curing composites
Boeing Commercial Airplane Company: J. L. Lundry Supervisor-Aero Methodology	11/12-13	G. Helwig H. Hagerup	To apply Boeing Airfoil Composite Design Methodology to CAP-GLIDE RP-2
NASA Langley: Structures Division	4/9/80	N. Hoff	To present results of theoretical developments regarding stresses around holes in composites

problems. In the following sections, detailed descriptions of the CAPCOMP, CAPGLIDE, COMPAD and INSURE programs are presented.

PART I

CAPCOMP (Composite Aircraft Program Component)

CAPCOMP (Composite Aircraft Program Component)
(N. Hoff, R. Loewy)

CAPCOMP is a program to design flight critical structures to take the maximum advantage of composite materials. By combining the efforts of experienced faculty with bright and well trained but inexperienced graduate students in an environment relatively free of traditional design and manufacturing processes, we intend to devise new and hopefully useful design concepts.

There is sufficient information available to prove that many structural elements can be made lighter by using advanced composites today than by using metals. But if such elements have to be joined by methods other than adhesive bonding, difficulties and uncertainties arise which can be eliminated only through conservative designs with their attendent penalties in weight or by extensive and expensive programs of "cut and try". This stands as one important impediment to full adoption of composites by the aerospace industry.

On the basis of these considerations Rensselaer Polytechnic Institute began, as the first task aimed at new structural concepts, the design using composites of a joint used in an airplane elevator. To make the design realistic, an existing metal airframe component was chosen for redesign in composites. The existing design chosen was that of the Boeing 727 elevator actuator attachment. We conc .ve of this work as carrying forward a Structures Demonstration Program using the joint of the 727 elevator, paralleling that of NASA and its aerospace engineering contractor, the Boeing Commercial Airplane Company. Our design, fabrication and test effort emphasizes design ideas specifically suited to advanced composite construction for the purpose of minimizing the weight of the structure, but on a scale consistent with the university context and funding level. The staff of RPI is very grateful to the Boeing Company and its engineers for their wholehearted support of the work at RPI.

During the reporting period, one of two different designs reported previously (July and December 1979) as suitable for replacing the largely metal attachment produced by Boeing was selected for further analysis, redesign, fabrication and testing. We call it the "Berg Design", and it makes use of quasi-isotropic, graphite-epoxy laminates. The second design, called the "Muser Design", which made a deliberate attempt to use uniaxial graphite-epoxy tape to as great an extent as possible, was suspended. It has led, however, to more generic research efforts to maximize the load carrying ability of pin-loaded holes in composite membranes and plates. These efforts are directed at improving the design of the attachment of the rib flanges to the elevator skin through mechanical (i.e., pin-type) fasteners and at maximizing the efficiency of the movable, heavily loaded, actuator attachment points in CAPCOMP. In addition, however, and increasingly, these generic effects are motivated by the general and widespread utility that will result from improvements in pin-loaded hole designs for composites.

These efforts have been jointly directed by Dr. Nicholas J. Hoff, in part time arrangement and by Dr. Robert G. Loewy. They are further described in the following paragraphs.

1. The Elevator and Its Attachment

To place the progress reported here in proper context, some descriptions used in earlier reports are repeated. The conventional aluminum alloy elevator of the Boeing 727 is shown in the upper half of Figure 1. The lower half of the figure is the new version of the elevator redesigned by Boeing in graphite epoxy; it is evident from the pictures that the latter is composed of fewer parts than the former. However, the actuator fitting of the new design is still manufactured of aluminum alloy. This fitting is shown in Figure 2. The fitting is attached to outboard and inboard portions of a new graphite-epoxy spar and to a graphite-epoxy nomex-honeycomb rib as indicated in Figure 3.

The attachment was designed by Boeing to carry loads up to 19,000 pounds. The direction of the load varies as the elevator rotates over an angle of 28 degrees from the full-down to the full-up position.

2. Berg's Design

Berg's design is shown in Figures 4 and 5. The first of these figures compares the Boeing composite design with

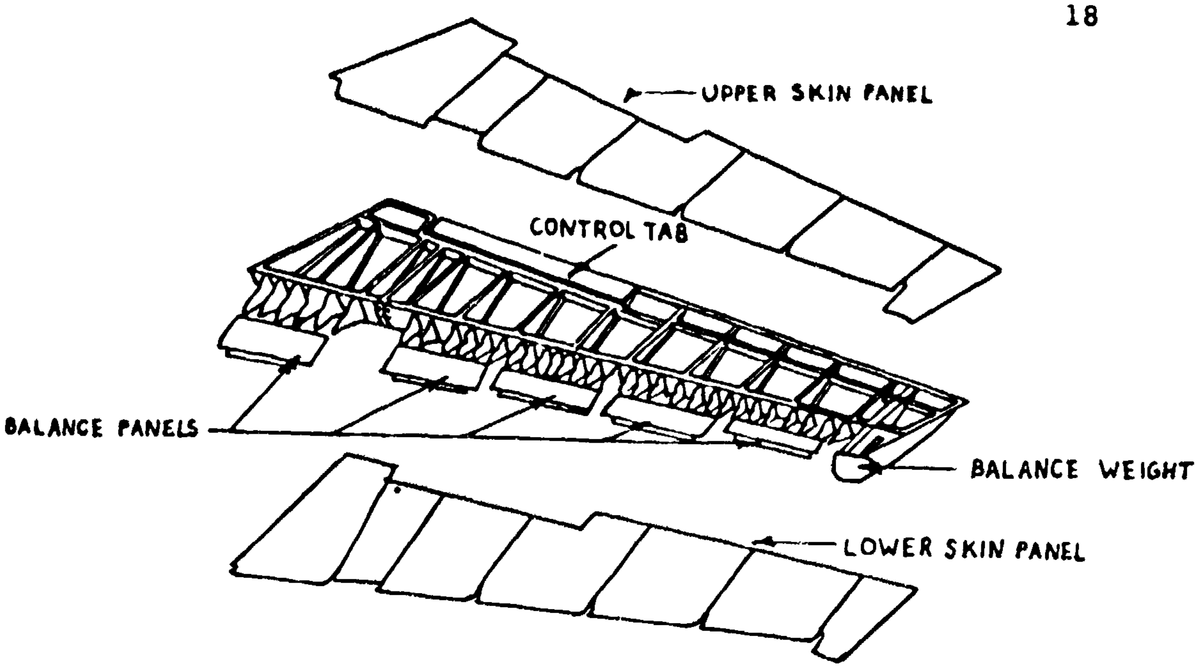

Conventional Aluminum Elevator

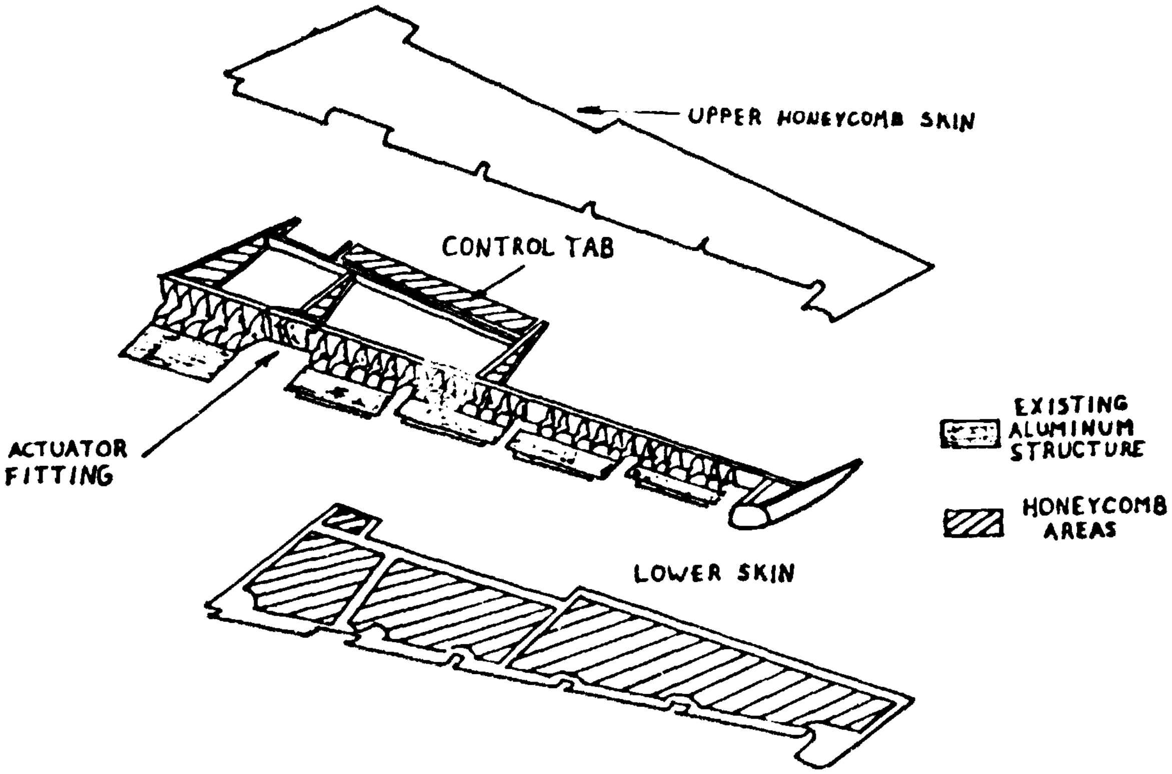

Advanced Composite Elevator

BOEING ELEVATOR ASSEMBLY

Figure 1

ALUMINUM ACTUATOR FITTING (Boeing Design)

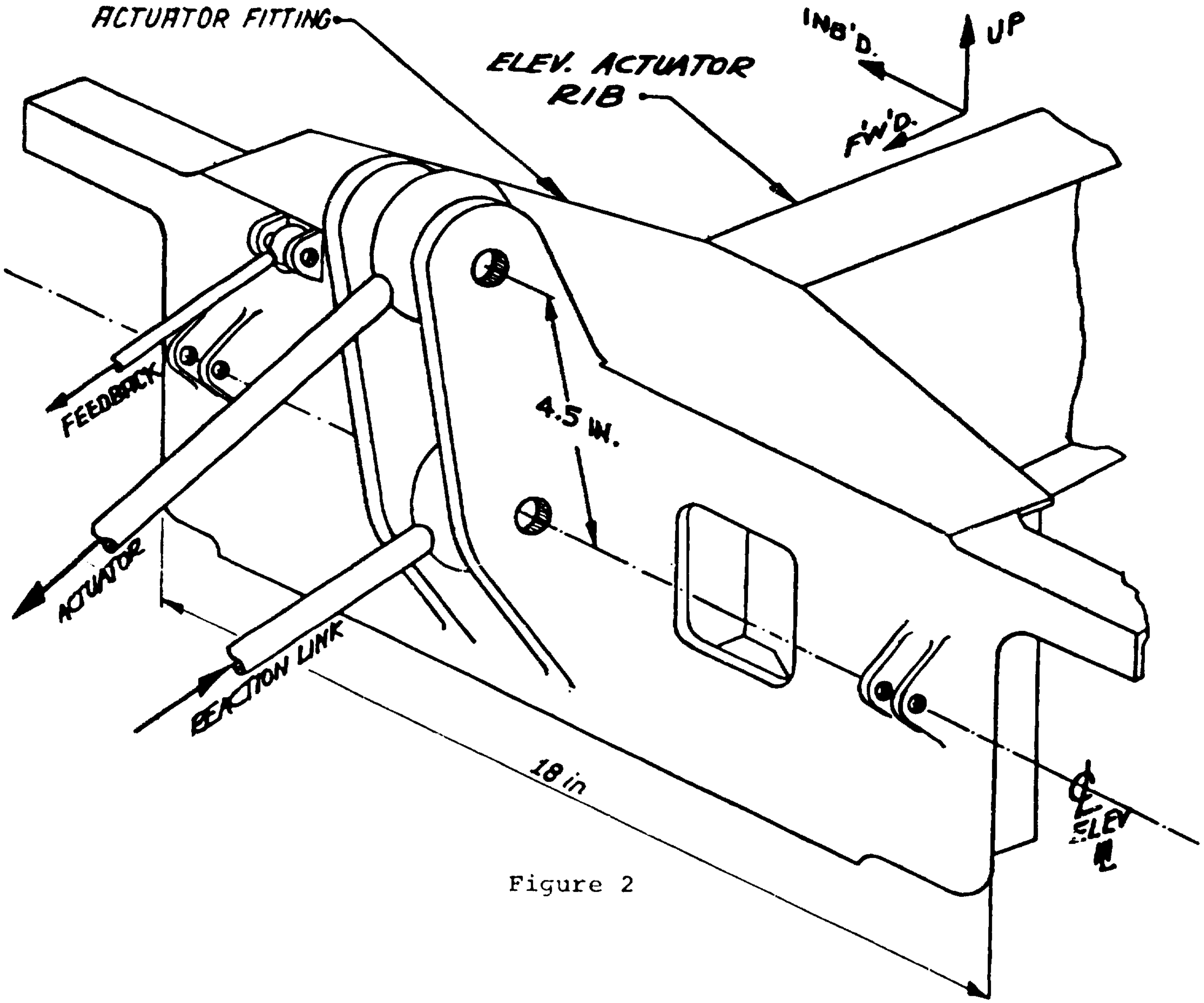

Figure 2

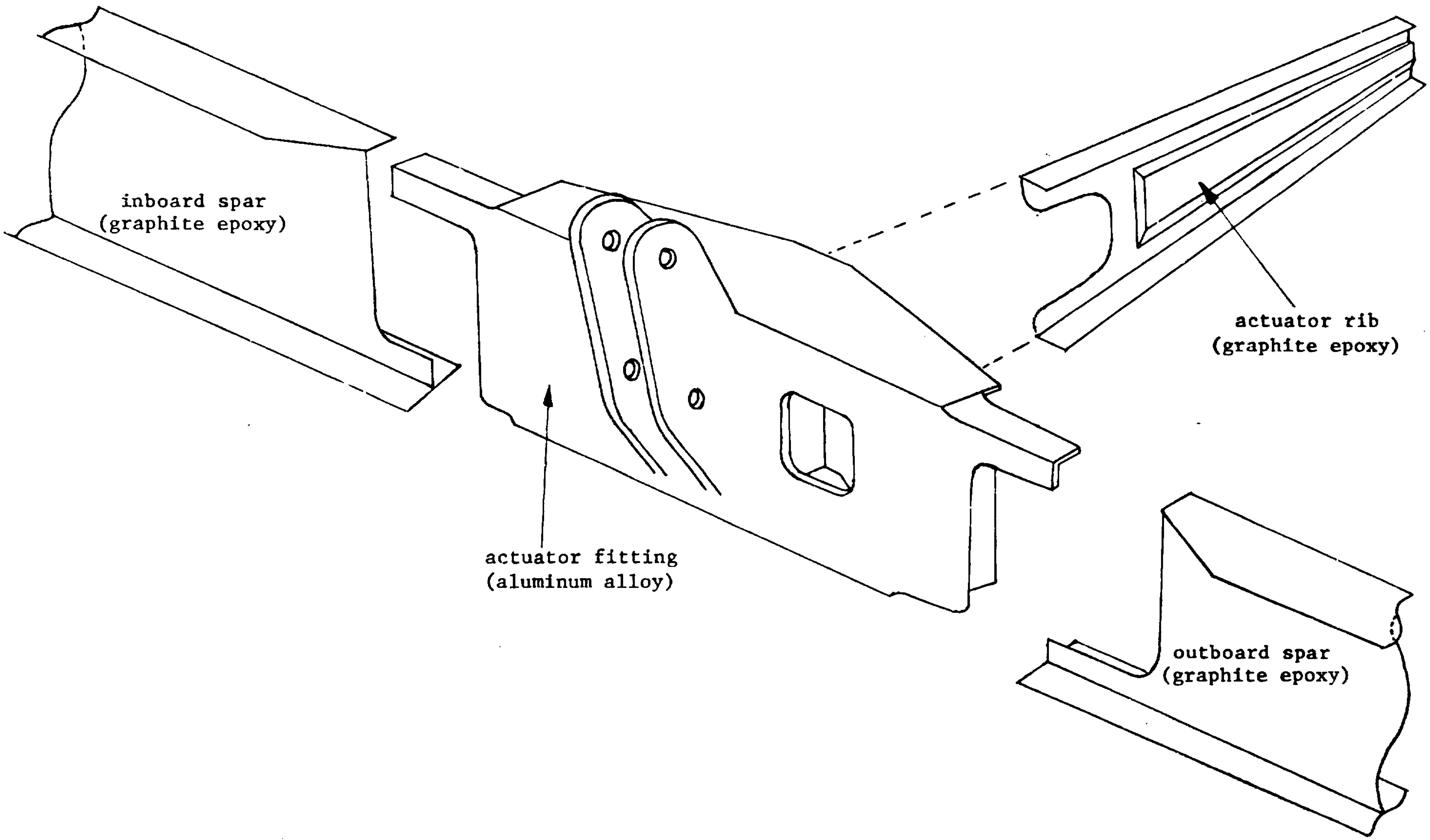

COMPOSITE ELEVATOR ACTUATOR ASSEMBLY (Boeing Design)

Figure 3

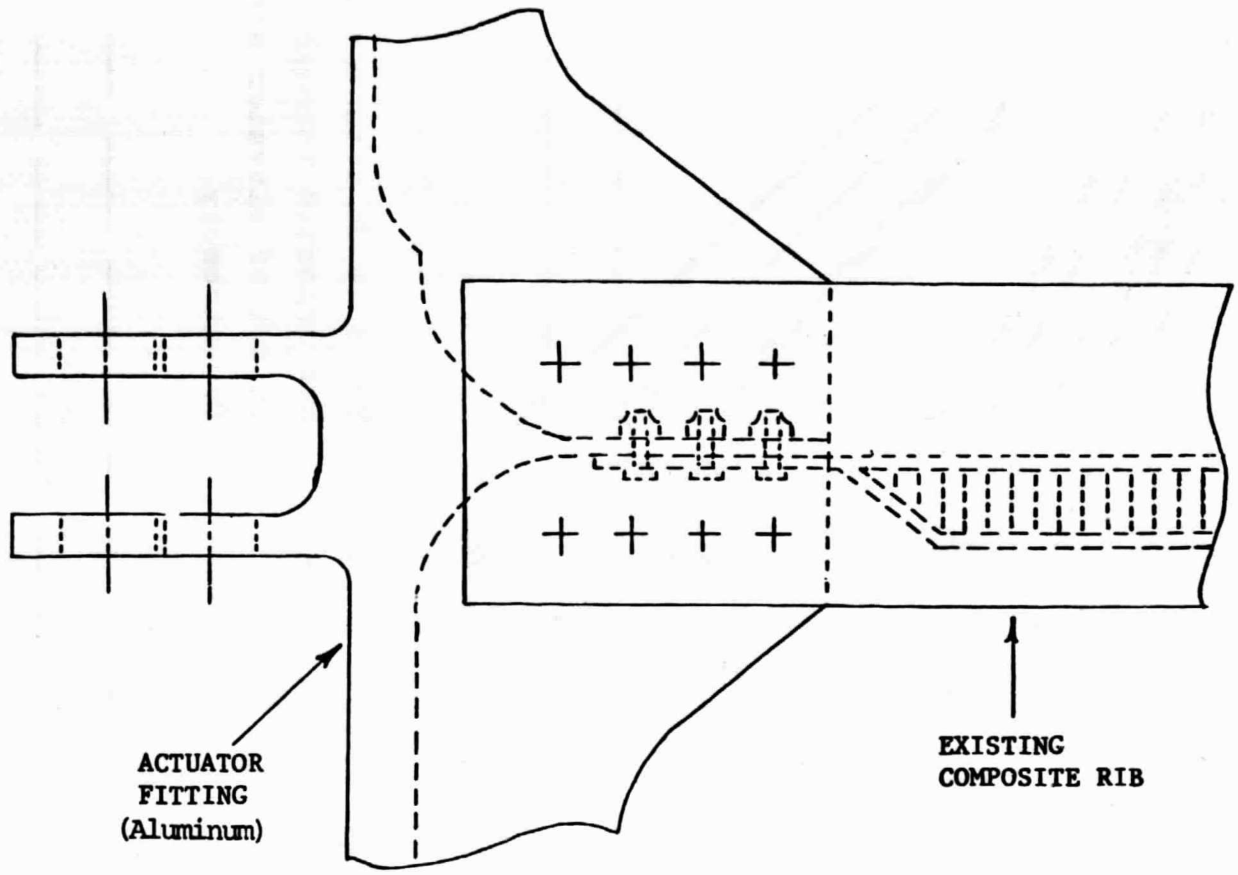

PRESENT DESIGN

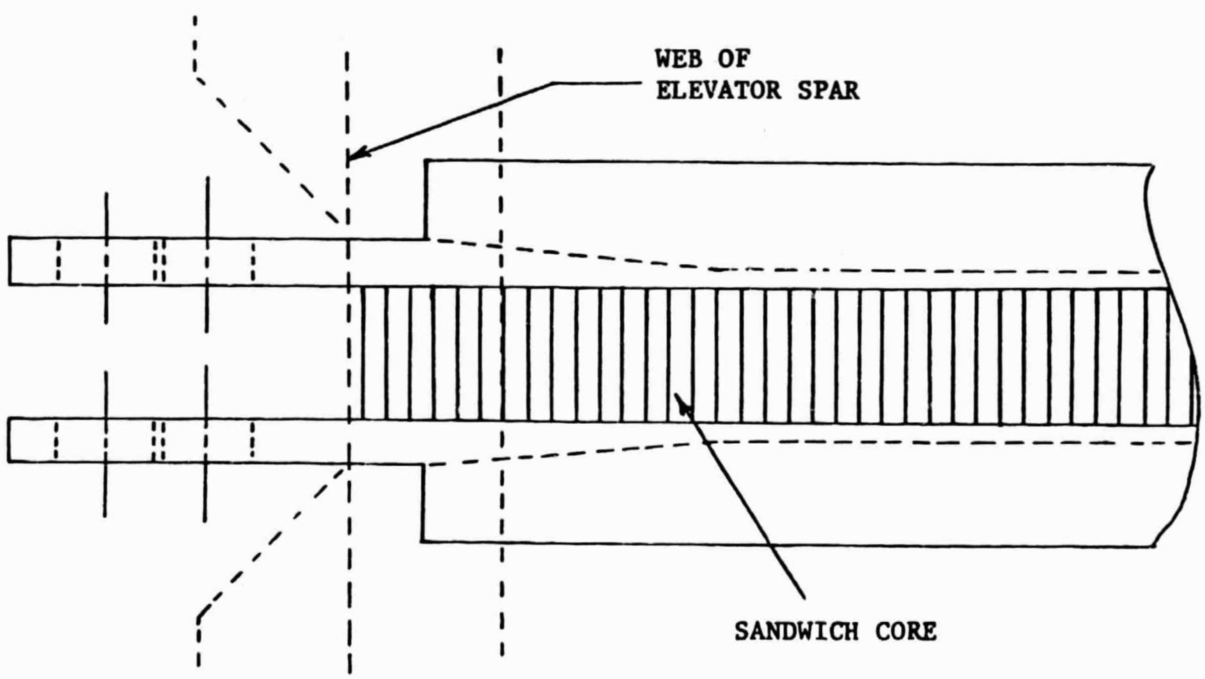

PROPOSED DESIGN (Berg)

ACTUATOR LUG TO RIB TRANSITION - TOP VIEW

Figure 4

PROPOSED SPAR AND RIB ASSEMBLY (Berg Design)

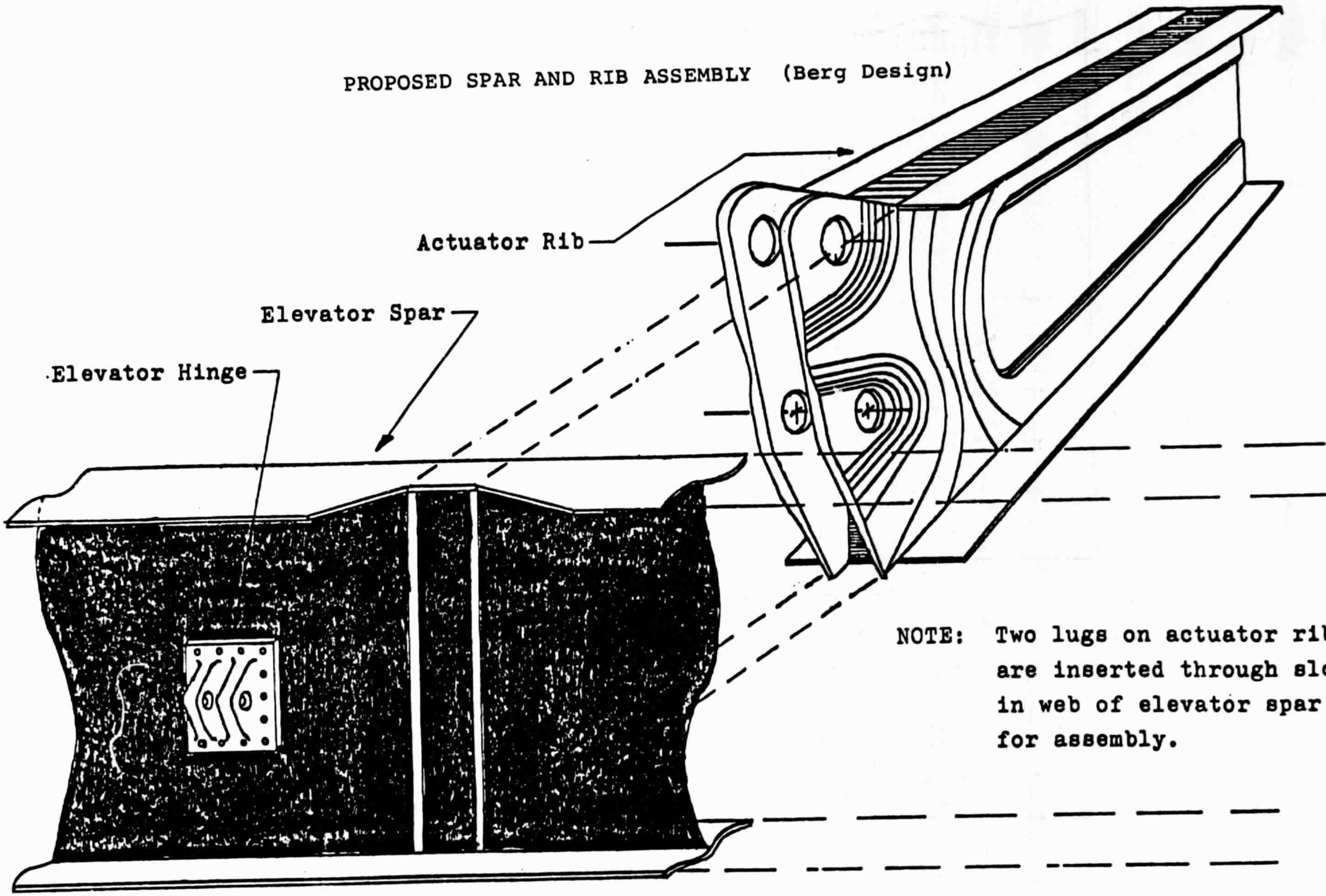

NOTE: Two lugs on actuator rib are inserted through slots in web of elevator spar for assembly.

Figure 5

Berg's design; both are shown. Figure 5 shows both how the the spar and new actuator rib would be assembled and also the build-up of thickness in the lug areas anticipated as needed to provide the required bearing strength. Note that the edges of some of the layers are bent 90 degrees to form flanges to which the upper and lower coverplates of the elevator can be attached. Attachment will be by means of titanium Hi-Loc fasteners. The right-hand and left-hand graphite-epoxy webs are stabilized by a layer of nomex-honeycomb between them.

The design analyses described in the previous report led to an elevator attachment rib with a variable thickness web. The distribution of hickness is predicted, by finite element methodology, to produce a relatively uniform stress level. It is shown in Figure 6.

Planning for fabricating the elevator attachment rib began with deciding on filament orientations. Two conflicting objectives emerged almost at once. It is clearly desirable that filaments be parallel to the edges of the flanges (Part A in Figure 7). It is also desirable that a layer of material be continuous from upper flange to web to lower flange. Since neither set of flanges is parallel to the web C_L or the other, these two characteristics are incompatible. This is illustrated in Figure 8a. The decision was made to have two sets of fiber directions, one keyed to the edges of the flanges and another to the centerline of the web. Layers providing continuity from upper flange to web to lower flange

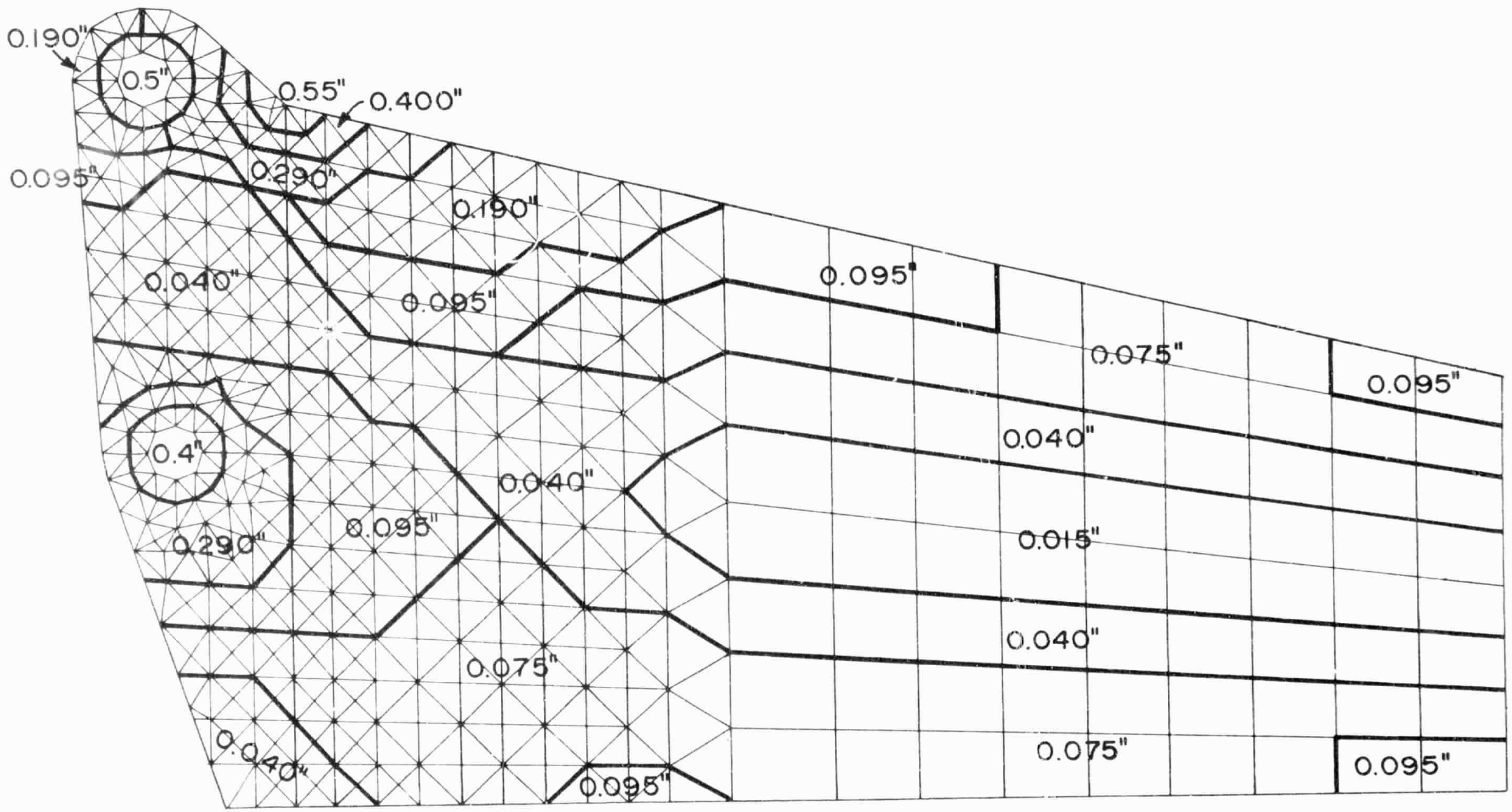

VARIABLE THICKNESS FINITE ELEMENT MESH

Figure 6.

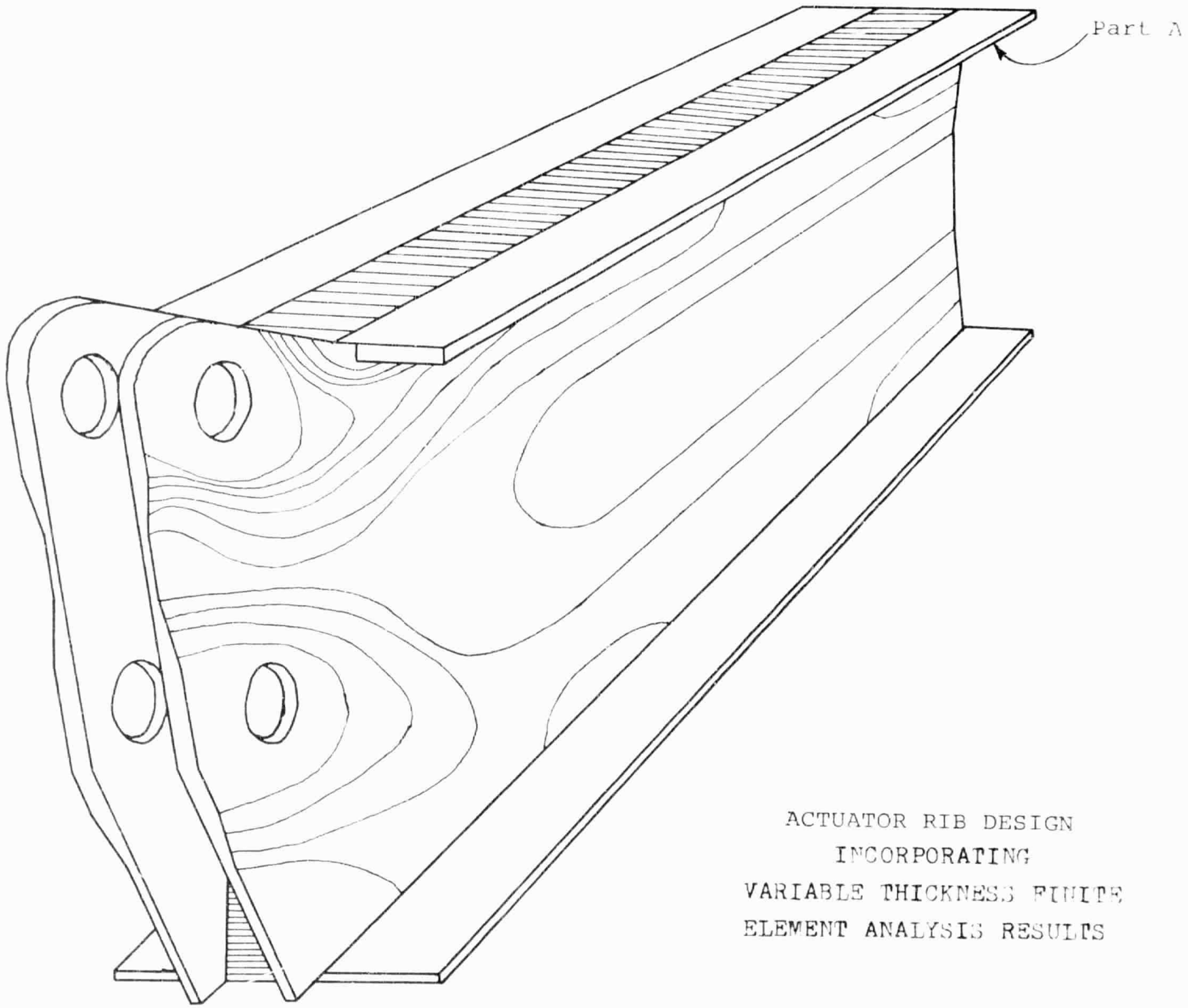

ACTUATOR RIB DESIGN
INCORPORATING
VARIABLE THICKNESS FINITE
ELEMENT ANALYSIS RESULTS

Figure 7

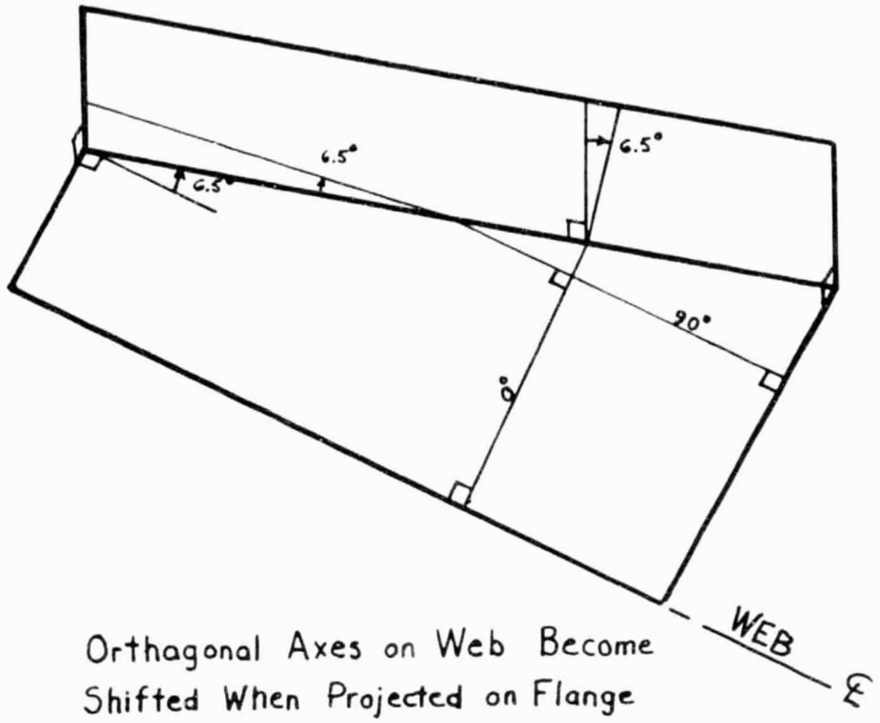

(a)

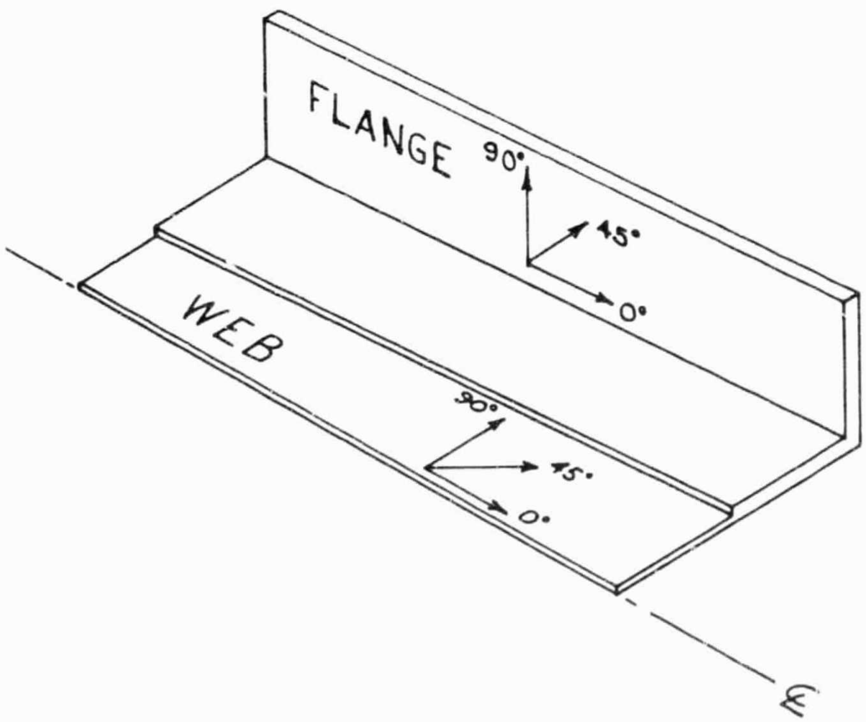

(b)

Figure 8. Reference Angles

would be oriented in the latter system; those basically providing flange reinforcement would be oriented to the former system. This is illustrated in Figure 8b.

The basis of the design is use of quasi-isotropic laminates. Furthermore, minimizing warpage imposed requirements for laminate symmetry about the midplane. The minimum number of layers satisfying these criteria is eight; for example

$$(90, +45, -45, 0)_s$$

Initial lay-up design, therefore, resulted in ply orientations as shown in Figure 9. (Note: The sharp "step" from flange thickness to web thickness actually is tapered as shown in later figures in this report.) Throughout the design, stress allowables are satisfied by going to the "next higher thickness" represented by eight layers of a symmetric laminate.

Experiments in fabricating flange-web angles were conducted following the steps shown in Figure 10, a through f. Materials and cure cycle (Figure 11) were those used by Boeing in completing the actual elevator attachment rib. The "web" portion of this sample consisted by 8 layers and the "flange" portion of 6 layers. The results were quite satisfactory, leading to a smooth flat sample (Figure 12).

Since the earlier test of the attachment lug (reported in the 36th Semi-Annual Report dated July 1979) was essentially a materials test which did not incorporate the proper edge distance for the hole in the actuator attachment lug,

PLY ORIENTATION

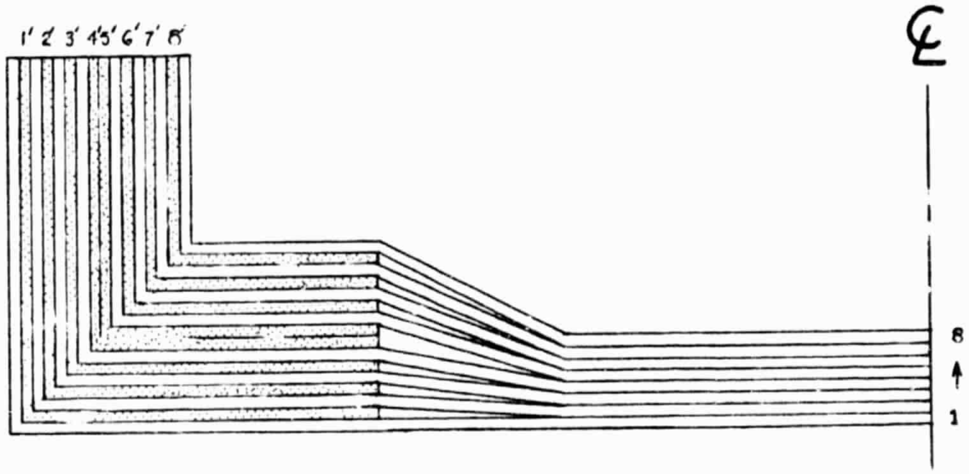

Layer		Angle	
1			0
	1'	90	
2			-45
	2'	+45	
3			90
	3'	-45	
4			+45
	4'	0	
	5'	0	
5			+45
	6'	-45	
6			90
	7'	+45	
7			-45
	8'	90	
8			0

Figure 9

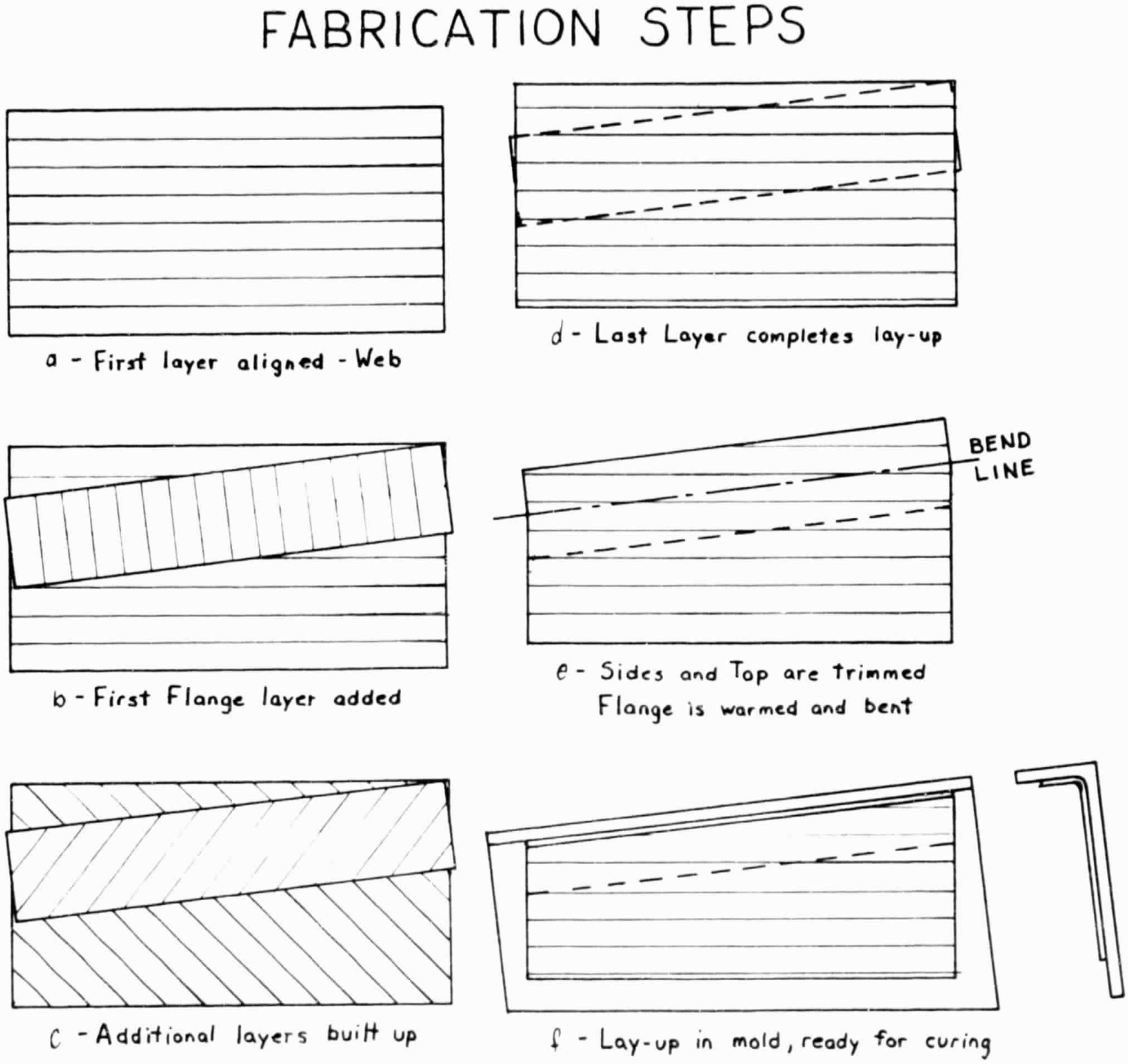
FABRICATION STEPS
a - First layer aligned - Web
d - Last Layer completes lay-up
BEND
LINE
b - First Flange layer added
e - Sides and Top are trimmed
Flange is warmed and bent
c - Additional layers built up
f - Lay-up in mold, ready for curing

Figure 10.

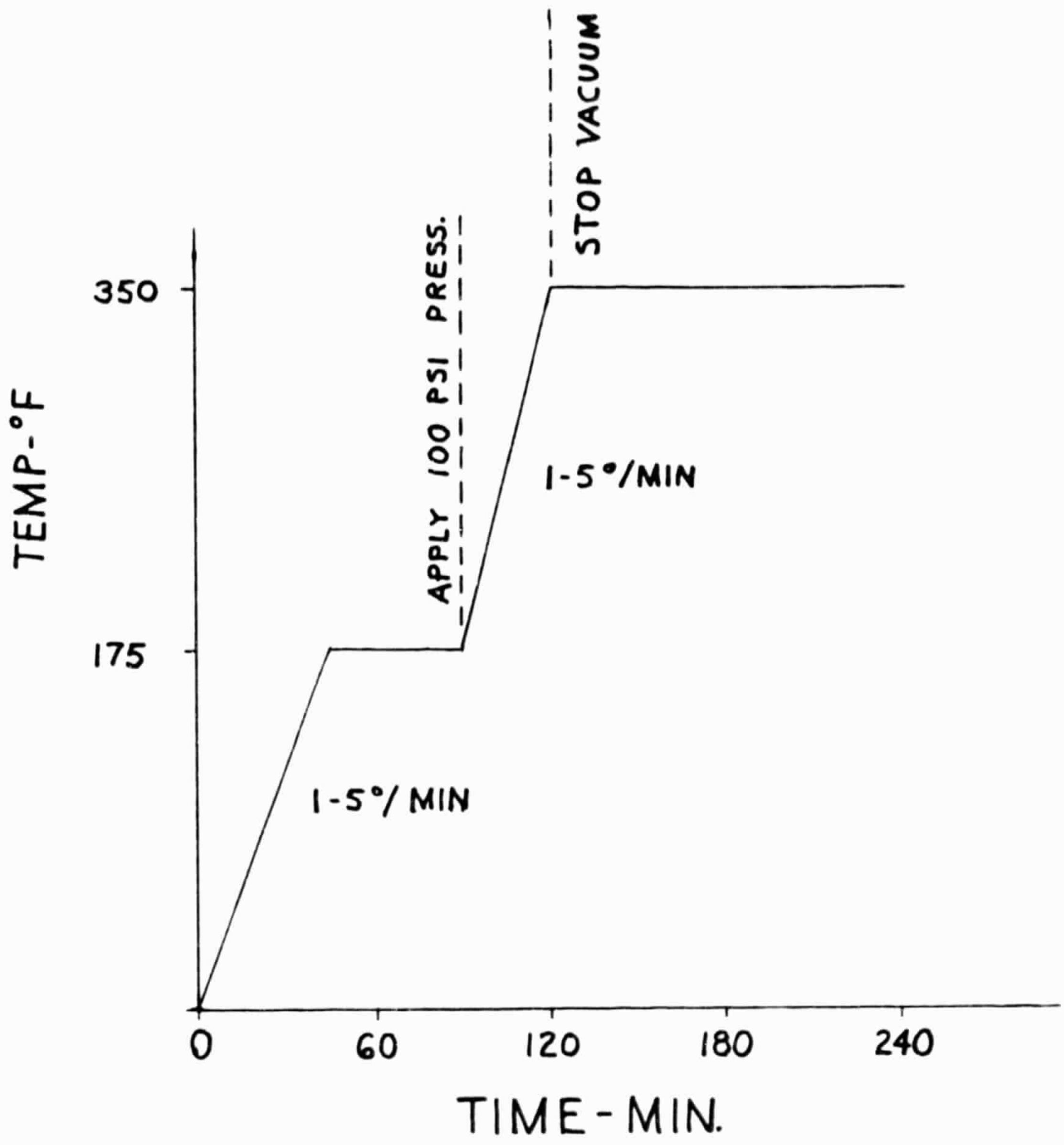

GRAPHITE-EPOXY CURE CYCLE

Figure 11

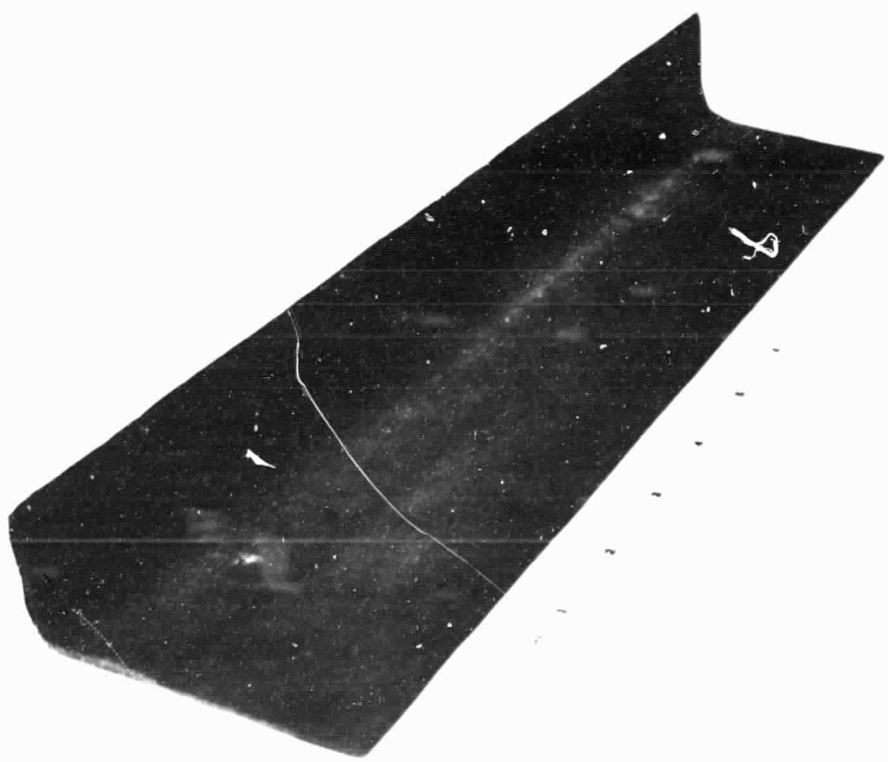

Figure 12. Photograph of Angle Sample

the test was repeated during this reporting period. It showed that additional layers were, in fact, required in the lug area (see Figure 13). The final laminate lay-up design is shown in Figure 14. Note that the maximum thickness is in the lug areas and is 64 layers (approximately 3/8") thick and that the minimum number of layers is 8 (as previously discussed) consisting of a mirror-image pair of 4-layer laminates. "Steps" in thickness all involve 4-layer "height" changes and taper is provided by "step-widths" estimated to be the minimum possible which will still avoid bonding voids. This "step-width" criterion to avoid bonding voids does create small areas where mirror-image pairs of 4-layer laminates don't exist. Only in these small areas, however, is there a lack of symmetry of fiber orientation through the thickness of the composite.

Note that the contours of varying thickness are formed by straight lines, to enhance ease of fabrication. Layers are cut to the patterns shown, in the quasi-isotropic groups of four. In Figure 14, the circled numbers indicate the number of layers in that area; uncircled numbers in the figure indicate the order in which layers are to be put down. Layers 1 and 16, therefore, encase all the intervening layers between them. The dotted lines indicate "fold" lines which establish the upper and lower flanges. Layers are put down in the female mold shown in Figure 15. The entire rib is then cured using the vacuum bag technique and the temperature cycle of Figure 11. The sides of the female mold

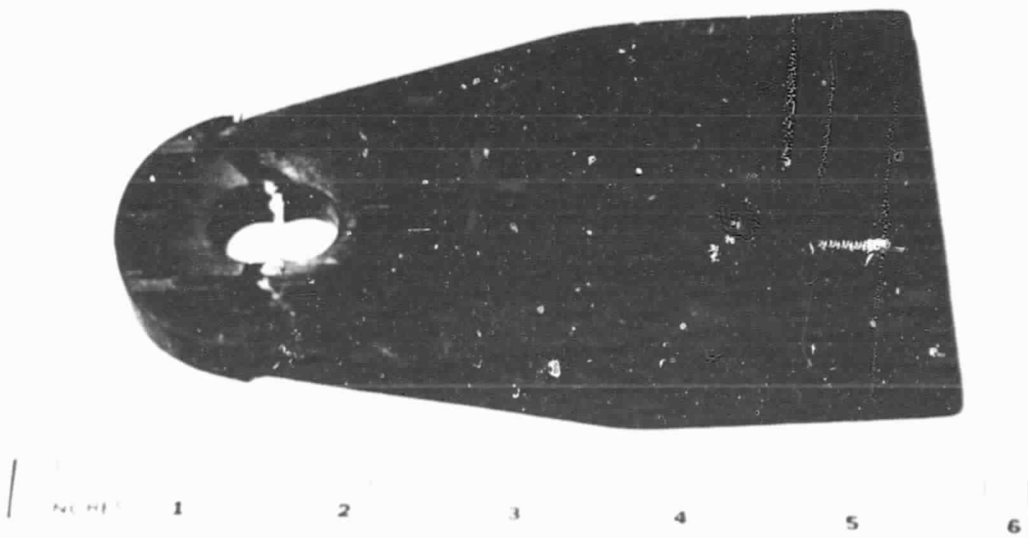

Figure 13. Photograph of Failed Lug

NOTE: Circled numbers show number of plies.
Uncircled numbers show step in lay-up sequence a particular 4-layer laminate is added.

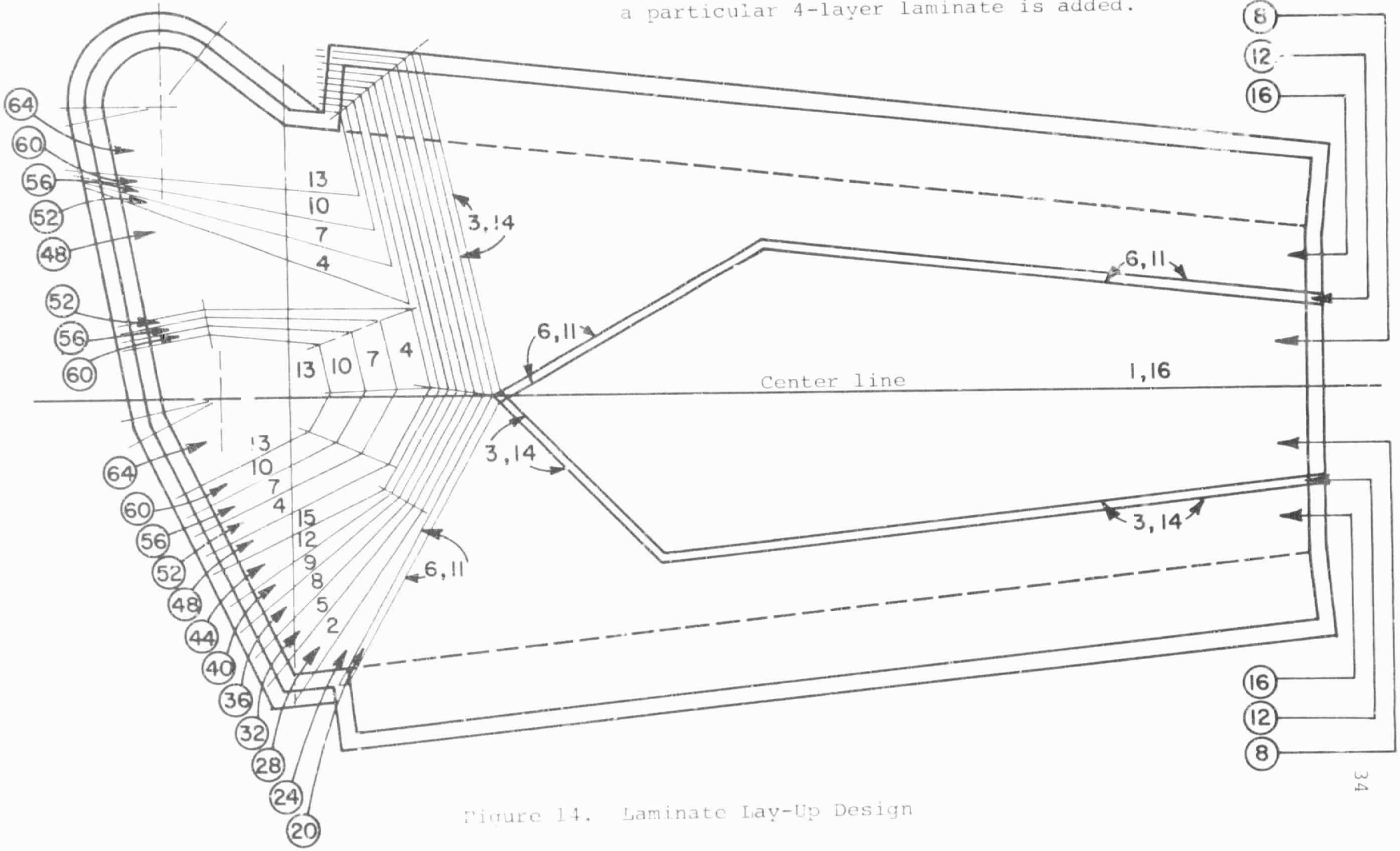

Figure 14. Laminate Lay-Up Design

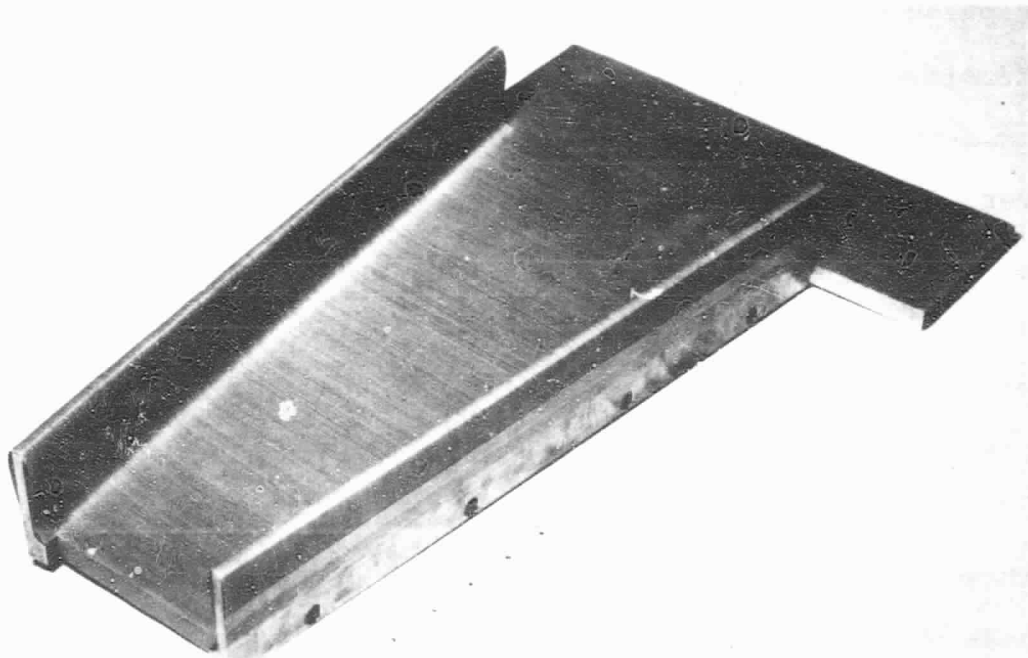

Figure 15. Female Mold for Rib Fabrication

(Figure 15) are reversible to allow both left hand and right hand ribs to be made with the same tool.

In parallel with fabrication planning and preliminary experiments, means by which the finished component can be tested were devised during the current reporting period. The Boeing Commercial Airplane Company provided a full description of the testing procedures they used to qualify their 727 elevator actuator attachment structure. The Boeing testing methodology could not simply be duplicated at RPI, however. Figure 16 shows the Boeing test set-up. Two hydraulic cylinders (mounted horizontally) provide the actuator load and reaction through a vertical bar which is bolted to the two elevator actuator attachment points. In the absence of hydraulic load generators at RPI, the equivalent loadings are to be generated in an Instron testing machine through linkages as shown in Figure 17. In the campus test set-up, loads will be applied vertically to a bar oriented horizontally which transmits the loads through two bolts to the elevator actuator attachment lugs. This linkage arrangement, which provides the equivalent of the Boeing load test, has been stress-checked and is about to be built.

Also shown in Figure 17 is the "strong-back" structure (items 9, 10 and 11) and the reinforcements of the elevator rib (items 12 and 13) to ensure reaction-load transfer to the "strong-back" structure. These test fixtures (i.e., items 9, 12 and 13) and the aft elevator skin reinforcements (item 14) are planned to be identical to those used in the

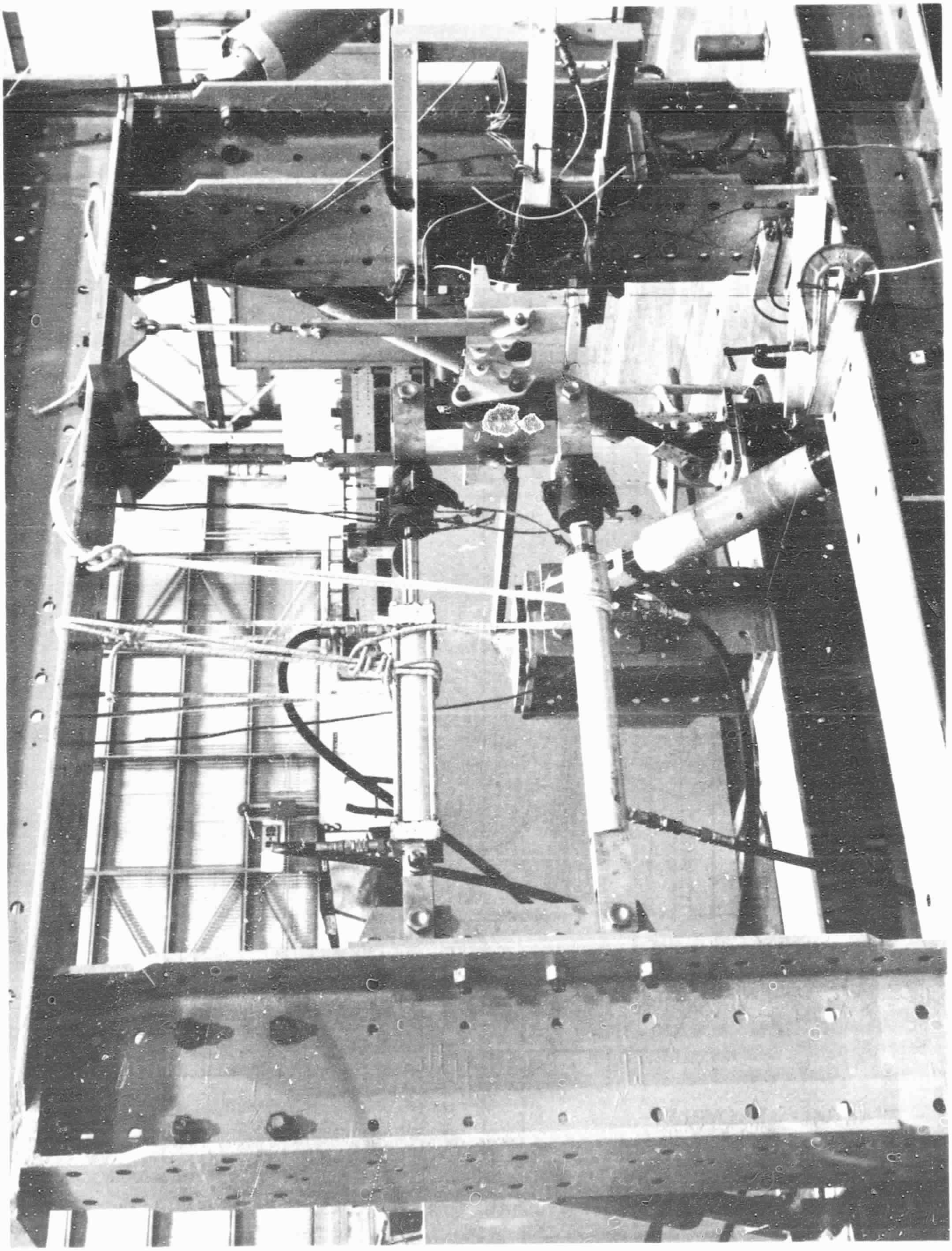

Figure 16.

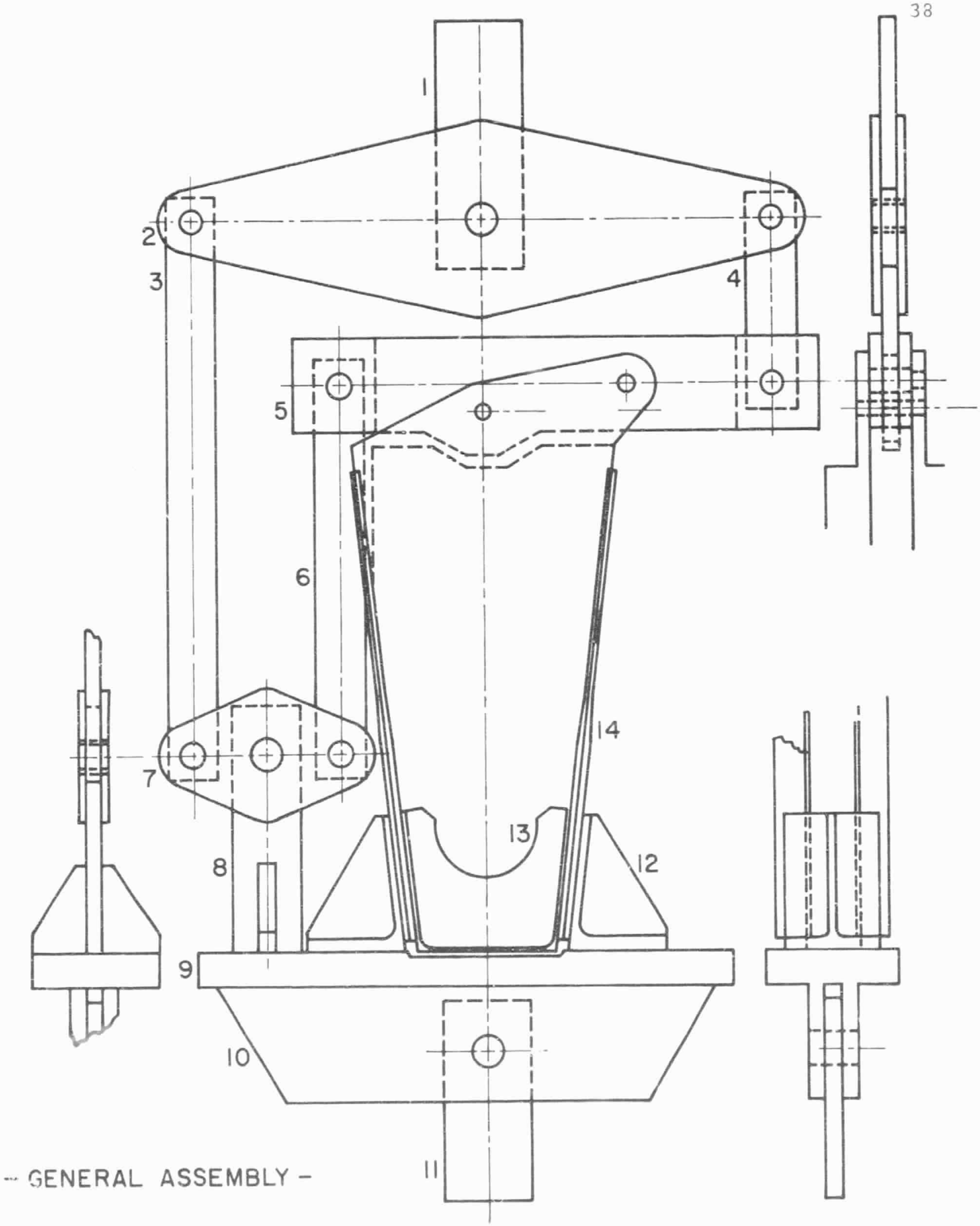

Figure 17. Rib Test Fixture

Boeing test. Thus, both loading conditions and reactions should be the same for both RPI and Boeing designs.

We expect the first full RPI component to be fabricated and proof-tested during the next reporting period.

3. Optimizing Fiber Orientations in The Vicinity of Heavily Loaded Joints
(N. Hoff and C. Muser)

It has often been noted that a basic advantage of fiber-reinforced materials lies in the possibility of "tailoring" the material to transmit forces most efficiently. Since the number of possible material choices and fiber directions is very large, suitable methods of analysis were initiated in the previous reporting period and continued in the current period to advance the methodology for minimizing weight in the design of attachments or joints.

For an optimal utilization of a composite material, empty holes as well as bolted attachments require different orientations of the fibers around the hole as compared to those far away from the hole. A simple example is a tension link with a hole near each of its ends into which bolts are inserted. At some distance from the holes, the best fiber arrangement is an essentially uniaxial one in which all the fibers are parallel to the straight line connecting the center of the holes (the centerline of the link). But this arrangement has a very low efficiency in the immediate vicinity of the hole.

For load transmittal by means of a tensile link, the tension loop has been proposed as described in the references 1 through 4 in Table V. The loop consists of fibers wrapped 180 degrees around the bolts and running substantially parallel to the axis of the link some distance away from the bolt holes. It has been found that the stress concentration factor is low with this arangement. In addition, matrix failure does not imply a catastrophic failure of the structural element; this is a significant advantage of the tensile loop.

A drawback of the tensile loop is that it is efficient only for a single direction of load application while, in practice, the direction of the load often varies. This is particularly true when the bolts transmit loads to plates rather than to load links. For plates, the designer often requires fiber arrangements resulting in quasi-isotropic properties at some distance from the holes. A multiple loop arrangement, combining several loops in a star pattern, may be suitable for this purpose.

A related structural arrangement utilizing prepreg layup techniques was proposed by N. Hoff and was described briefly in the previous progress report. It retains the main characteristics of the tension loop in that all fibers contacting the bolt are tangential to the circular cross section of the bolt. When an attachment containing a single bolt is constructed, unidirectional prepreg tape is arranged around a circle with fibers tangential to the circle. The

TABLE V

REFERENCES: USE OF TENSION LOOPS IN COMPOSITE LINKS

1. Puppo, A. and J. Haener, "Application of Micromechanics to Joints and Cutouts", U. S. Army Aviation Material Laboratories, TR 69-25, April 1969, AD 688168.

2. Grueninger, G., "Moeglichkeiten der Krafteinleitung in faserverstaerkte Bauteile", in: Kohlenstoff- und aramid-faserverstaerkte Kunststoffe, 1977, VDI-Verlag Duesseldorf, West Germany.

3. Conen, H., "Deformation und Versagen von GFK-Strangschlaufen", in" Kunststoffe Bd 56, Heft9, 1966, pp. 629.

4. Woerndle, R. and H. Bansemir, "Beitrag zur Statischen Berechnung von Krafteinleitungselementen aus faserverstaerkten Kunststoffen" in: Bericht ueber das DGLR-Symposium "Neue Bauweissen und Vertigungsverfahren in der Luftfahrt", Sep 1976, Munich, pp. 249.

overlapping of the tape causes variations in thickness and results in increasingly quasi-isotropic properties as the distance from the hole increases. Since the structural element so produced is thinnest near the hole, some tapered insert has to be incorporated to preserve substantially constant thickness.

Figure 18 shows the basic lay-up of the plate. The number of fiber directions are indicated by small rosettes at various distances from the hole. The pattern of the thickness change is presented more clearly in Figure 19, although the density of "cross hatching" in this diagram is roughly the inverse of the number of layers.

These two figures (18 and 19) show stacks or "sets" of prepreg tape consisting of a maximum of four layers. Thicker structural elements can be produced by combining a number of these sets of four layers each with the individual sets rotated relative to one another to obtain a more equal spread of fiber orientation. The insert itself can be a composite material, tapered disk made on a filament winding machine. The final product may have a cross section as shown in Figure 20.

The development of an efficient arrangement of the fibers has been undertaken at Rensselaer Polytechnic Institute, both experimentally and theoretically. A short description of the experimental work will be given here, followed by some of the results of the analysis.

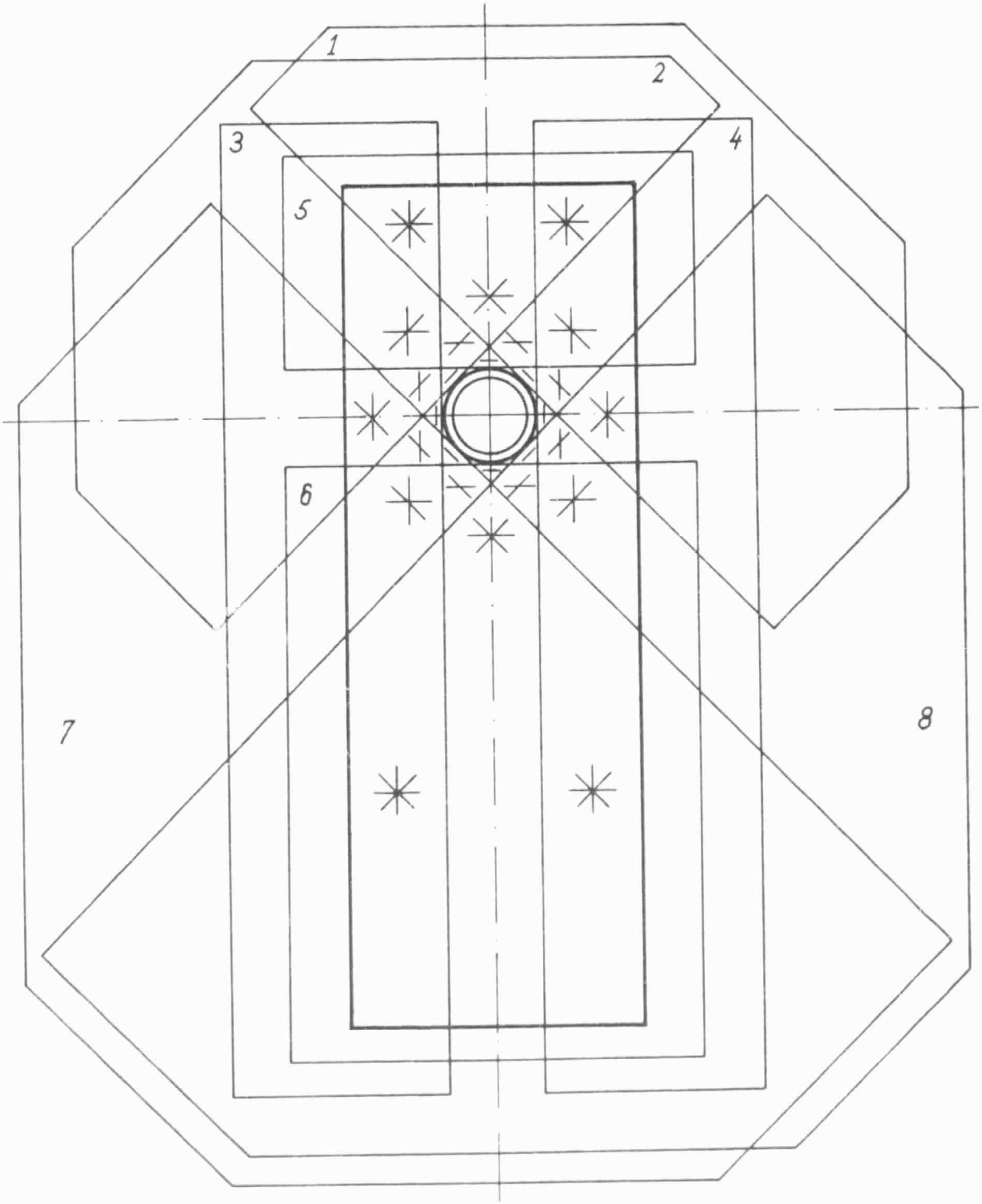

Figure 18. The Basic Lay-Up

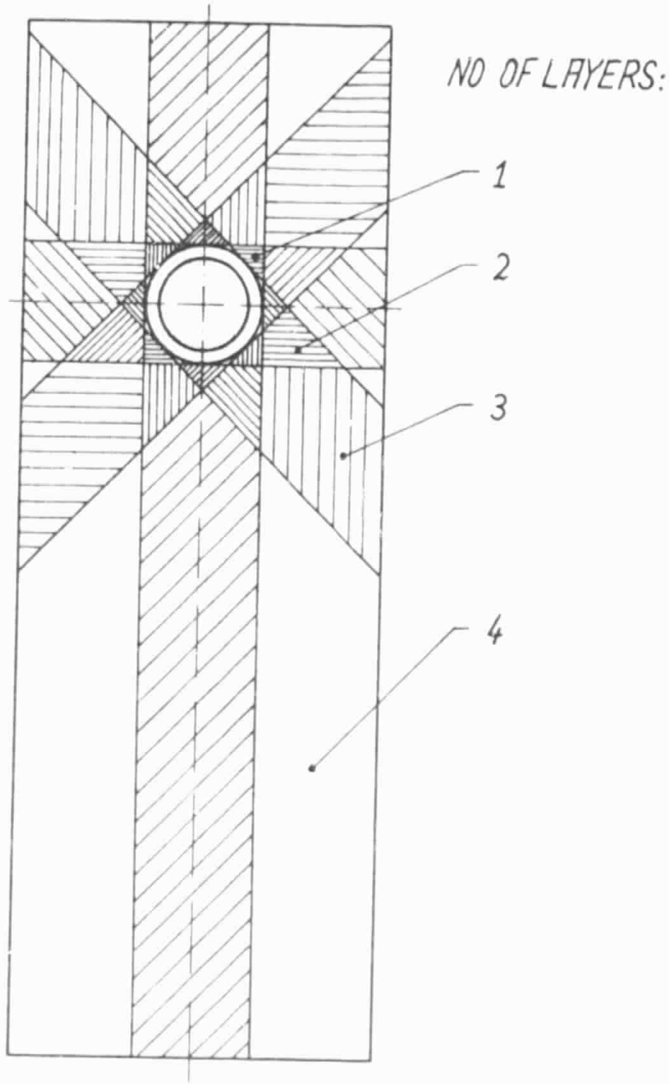

Figure 19. The Change of Thickness

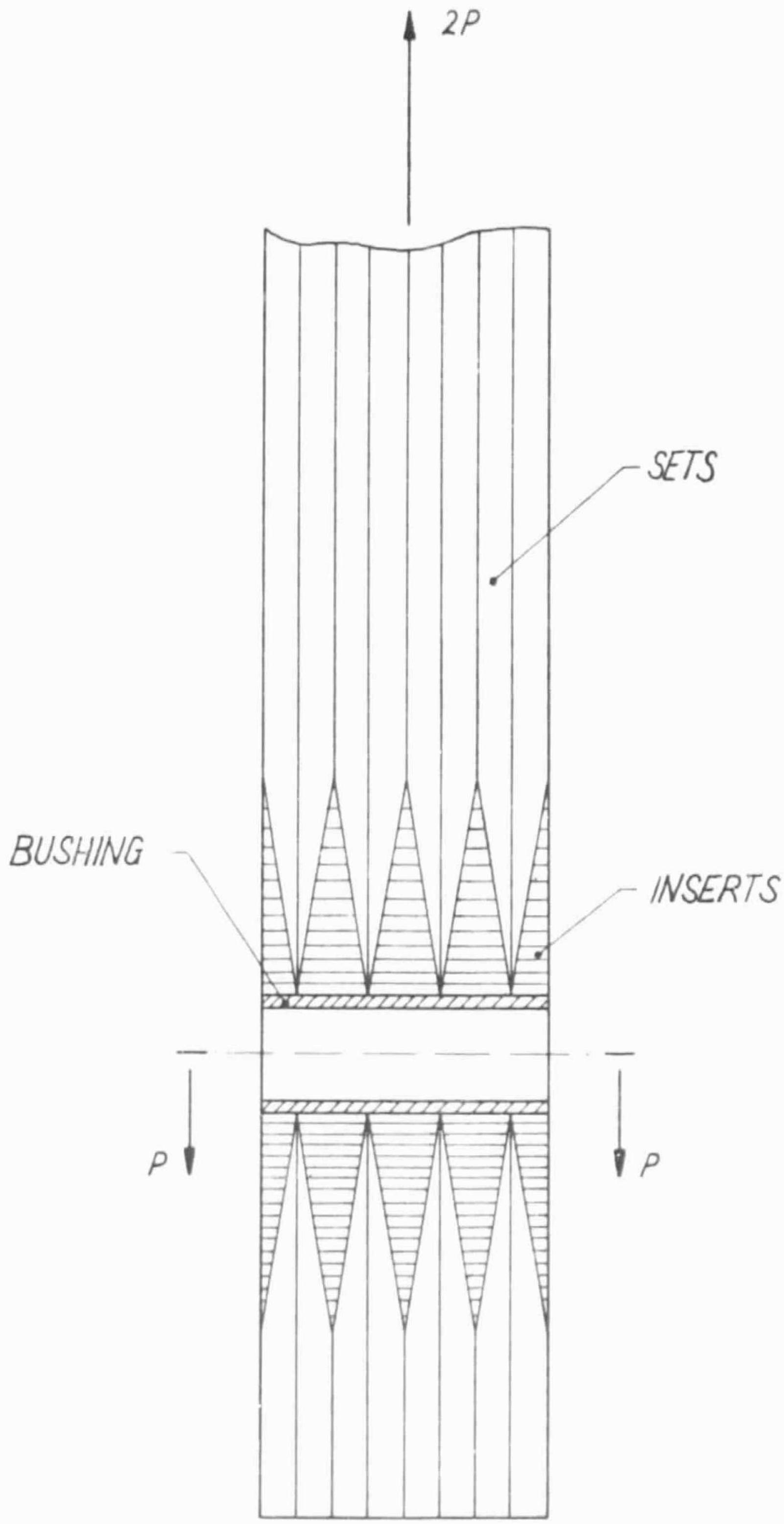

Figure 20. Cross Section

A. Experimental Work

The experimental approach to the solution of the problem consists of three phases:

Phase 1: Development of a manufacturing technique that produces satisfactory plate specimens consisting of 48 layers of tape, with a hole in the center of the specimen.

Phase 2: Development of a satisfactory insert and incorporating it in the plate specimen.

Phase 3: Testing the completed specimen, evaluating the results and suggesting modifications to the procedure on the basis of the test results.

In Phase 1, two specimens were built. Each was a 48 layer plate built up of 12 sets, of 4 layers each. The sets, basically as shown in Figures 18 and 19, were cut to the proper shape and stacked in a mold much as shown in Figure 20 but with only one insert. The specimen's material was graphite epoxy, and the single insert was a machined steel disk.

The first specimen, shown in Figure 21, was bonded in an autoclave. The second specimen, shown in Figure 22, was produced in a heated press. The main difficulty encountered in the manufacturing process was in providing a completely uniform pressure over an area which has small variations in plate thickness and non-uniformity in elastic constant

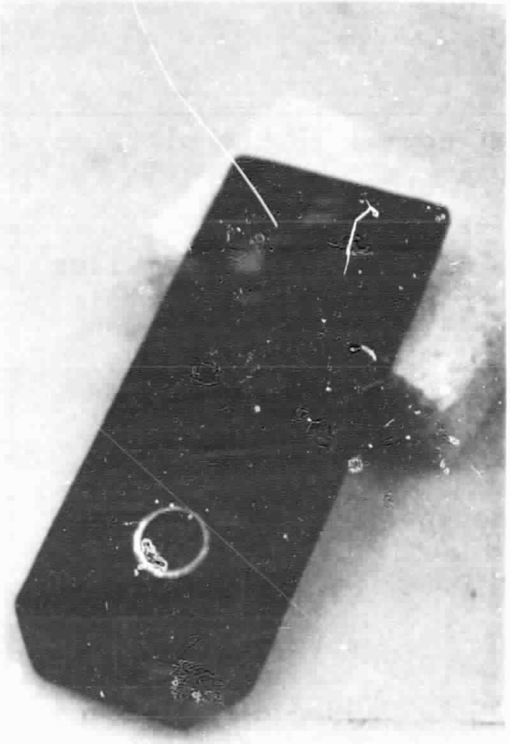

Figure 21. First Test Specimen

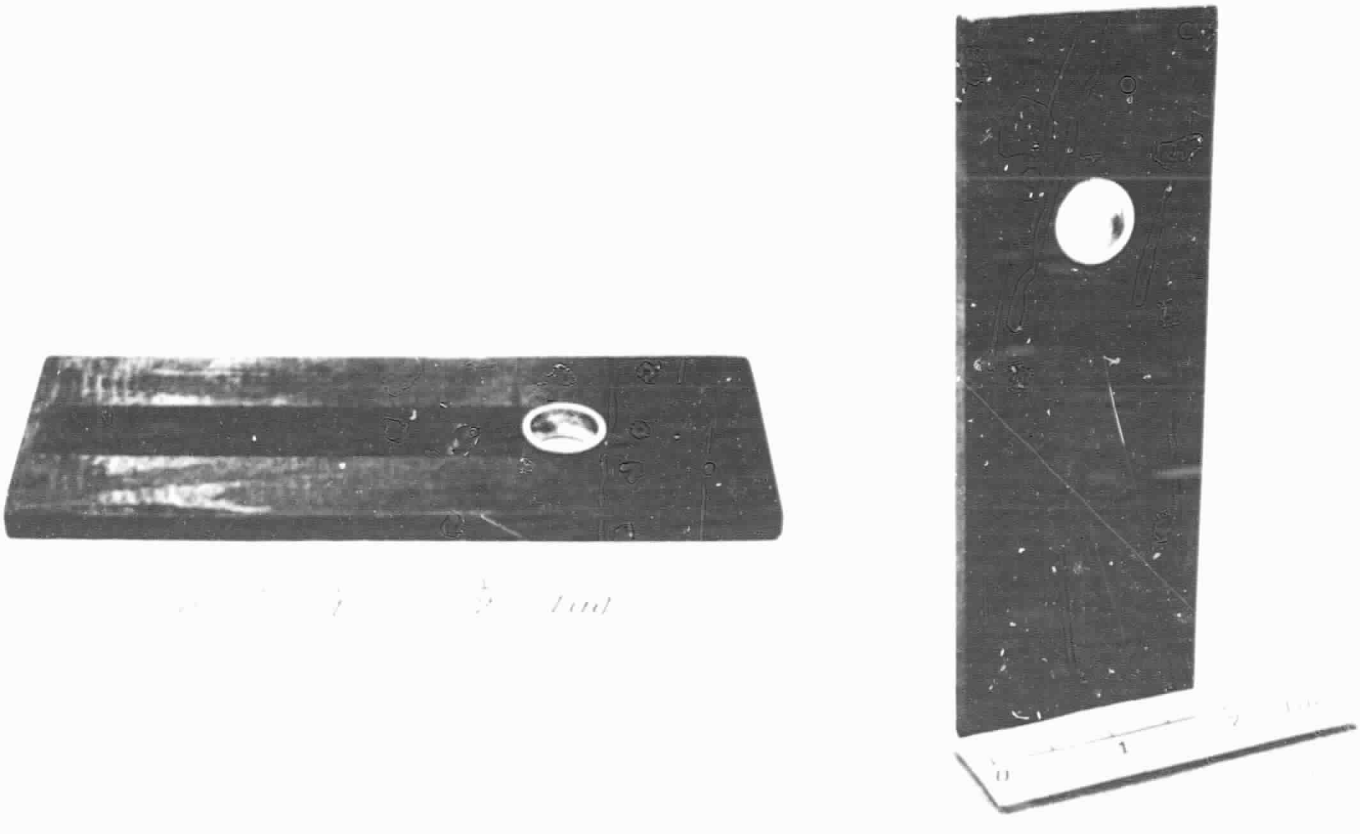

(a) (b)

Figure 22. Second Test Specimen

(Young's Modulus for the steel insert) normal to the plate over the area.

Both specimens were tested and broke under loads smaller than those obtained earlier with a quasi-isotropic specimen. The new specimens shattered near the steel inserts. Imperfect bonding between the steel and graphite epoxy is the likely source of these failures. Once loose, the insert acted like a wedge, splitting and crushing the composite material with which it came in contact. Pictures of the first two broken specimen are shown in Figures 23a and 23b.

In Phase 2, the insert was made of graphite epoxy rather than steel. To simplify the manufacturing process, the thickness of the insert was changed in steps instead of tapering it continuously. The insert was fabricated on a filament winder either using a wet filament, with the epoxy undergoing the same cure cycle as the prepreg material of the rest of the specimen, or using prepreg filaments. As the insert and the rest of the specimen were cured together, the result was a monolithic structure in which the joint (between a steel insert bonded to graphite epoxy) was essentially eliminated.

One specimen with a graphite epoxy insert showed the same type of failure as the two specimens with steel inserts (Figure 23c). We think, however, this happened for different reasons. One reason is that the prepreg used was old and did not bleed well. Another reason, perhaps, is that the volume of the insert was so small that the region around the hole

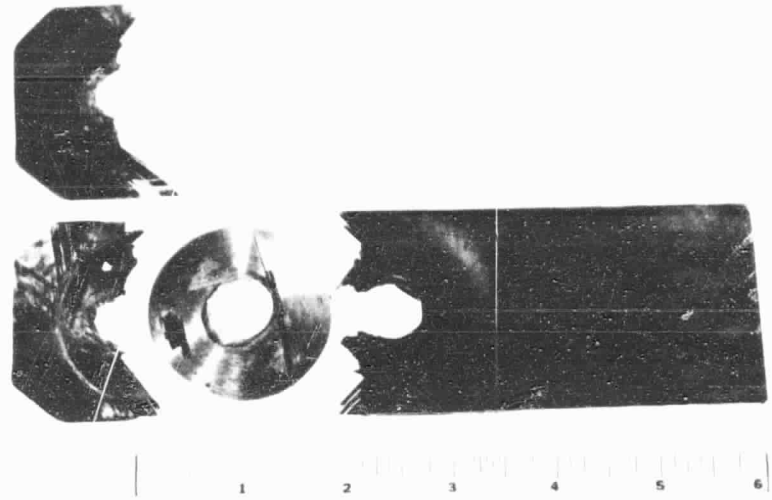

Figure 23a. First Specimen After Testing to Failure

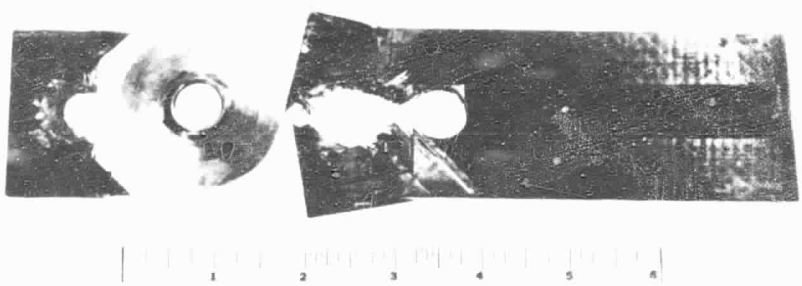

Figure 23b. Second Specimen After Testing to Failure

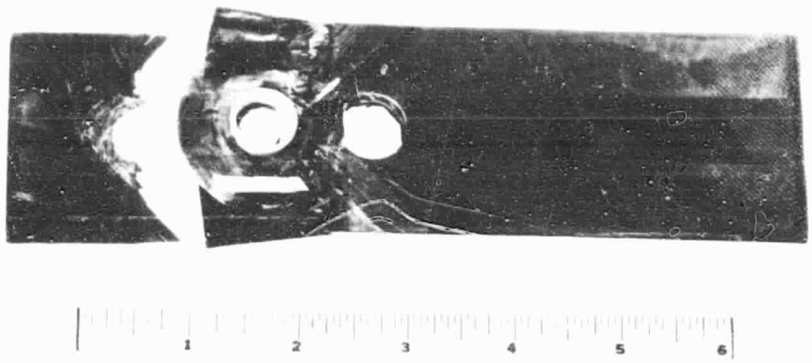

23c.

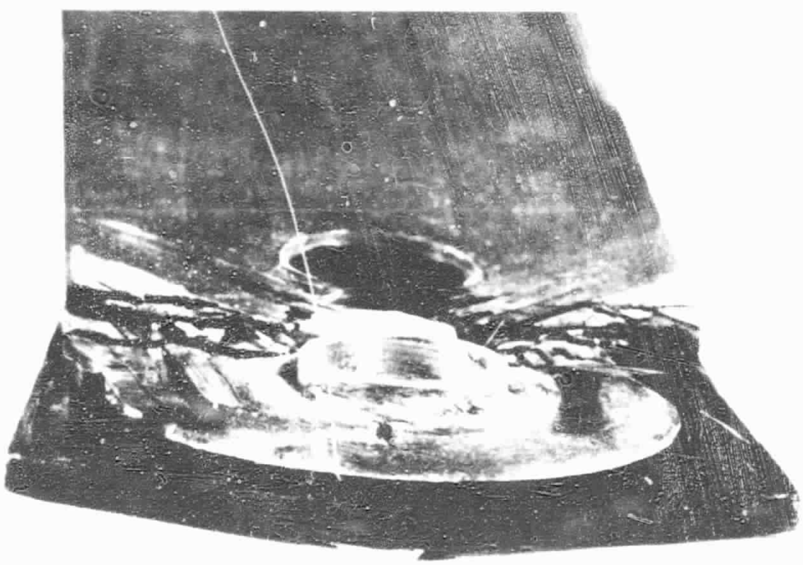

23d.

Figures 23c and 23d.
Specimen with Graphite Insert After Testing to Failure

was not subject to enough pressure when the piece was cured in the press. Better specimens with graphite epoxy inserts are being built and tested. Consideration is also being given to the use of glass fiber or Kevlar for the insert, since the lower modulus of these materials could contribute to further reduction of the stress concentration.

Work under Phase 3 is just beginning with the testing and evaluation of more accurately dimensioned and better bonded specimens. A change of the ratio of the insert diameter to the width of the specimen is being discussed also. The first specimens tested used a simple steel jig setup as shown in Figure 24 with the results already described. This method will have to be refined for more accurate tests.

B. Theoretical Analysis

There are many possible ways of arranging the fibers in the neighborhood of a hole in the hope of reducing the stress concentration. For the time being, only one class of fiber arrangement is being investigated in the analytical part of the project. In this class it is assumed that the fiber-reinforced plastic, or composite, plate is axially symmetric in its mechanical properties, and that these properties are functions of θ only. The plate is subjected to uniform, uniaxial tension in the χ - direction. It has a hole whose radius can be taken conveniently as unity (see Figure 25). The uniform tension in the χ - direction can be given in polar coordinates as

Figure 24. Test Set Up for Link with Heavily Loaded Hole

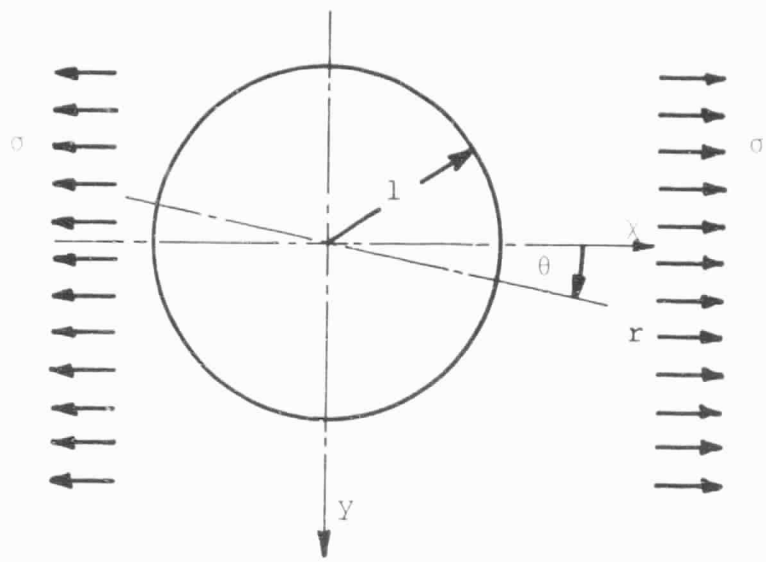

$$\sigma_r = (\sigma/2)(1 + \cos 2\theta)$$
$$\sigma_\theta = (\sigma/2)(1 - \cos 2\theta)$$
$$\tau_{r\theta} = -(\sigma/2)\sin 2\theta$$

Figure 25. Quantities for Theoretical Analysis

This uniform state of stress implies that tractions are applied to the edge of the circular hole. In their absence the state of stress is modified. The true state of stress can be obtained by superposing on the uniform state another state that is caused by the application to the edge of the hole tractions equal and opposite to those given above.

The part of the expressions given that is independent of θ represents a uniform state of stress $\sigma_r = \sigma_\theta = (\sigma/2)$. This corresponds to the situation existing when uniform radial stresses $\sigma/2$ are applied to the outer circular edge $r = R$ of a circular plate with $R > 1$. Superposition of the stresses arising from the application of $\sigma_r = -(\sigma/2)$ at the edge of the hole ($r = 1$) yields, for the circumferential stress at $r = 1$, the expression

$$\sigma_\theta = (\sigma/2)\left[1 + \sqrt{\bar{S}_{rr}}\right]$$

where $\bar{S}_{rr} = S_{rr}/S_{\theta\theta} = E_\theta/E_r$

Here S_{rr} and $S_{\theta\theta}$ are the compliances, and E_r and E_θ are Young's moduli, in the radial and circumferential directions, respectively.

The effect of the terms multiplied by cos 2θ has also been calculated. It was found that a state of stress

$$\sigma_r = (\sigma/2)\cos 2\theta \;;\; \sigma_\theta = -(\sigma/2)\cos 2\theta \;;\; \tau_{r\theta} = -(\sigma/2)\sin 2\theta$$

independent of r can exist only if the compliances satisfy the condition

$$2\bar{S}_{rr} - 2\bar{S}_{r\theta} - \bar{S}_{\theta\theta} = 0$$

where the symbols are again compliances non-dimensionalized through division by $S_{\theta\theta}$. When this condition is not satisfied, the state of stress does not correspond to compatible displacements. Superposition of the stresses caused by the application of tractions at $r = 1$, equal and opposite to those given above, yields for the circumferential stress at $r = 1$ the expression

$$\sigma_\theta = -(\sigma/2)\left[1 + 3\sqrt{\bar{S}_{rr}}\right]\cos 2\theta$$

Addition of this expression to the one given earlier representing terms independent of θ yields

$$\sigma_\theta = (\sigma/2)\left[1 + \sqrt{\bar{S}_{rr}} - [1 + 3\sqrt{\bar{S}_{rr}}]\cos 2\theta\right]$$

At $\theta = 0$ this reduces to

$$\sigma_\theta = -\sqrt{\bar{S}_{rr}}\,\sigma \quad ; \quad \theta = 0$$

At $\theta = \pi/2$ the expression becomes

$$\sigma_\theta = [1 + 2\sqrt{\bar{S}_{rr}}]\sigma \quad ; \quad \theta = \pi/2$$

All these expresseions reduce to the conventional ones for the isotropic case. This is characterized by $\bar{S}_{rr} = 1$.

$$\sigma_\theta = \sigma[1 - 2\cos 2\theta] \qquad \bar{S}_{rr} = 1$$

$$\sigma_\theta = -\sigma \qquad \bar{S}_{rr} = 1;\ \theta = 0$$

$$\sigma_\theta = 3\sigma \qquad \bar{S}_{rr} = 1;\ \theta = \pi/2$$

As has already been mentioned for arbitrary values of the compliances, a state of stress independent of r does not exist. Results have been calculated for this general case also, but difficulties have arisen with their interpretation. It appears that large changes occur in the stress concentration factor in consequence of small variations in the compliance values. Work is being continued to clarify this problem.

C. Supporting Research on Lightly Loaded Mechanical Joints

The work of graduate student Wonsub Kim continued to concentrate on stress distributions around pin-loaded holes in composite membranes and plates with no special fiber arrangements around the hole, the associated bearing strength and bearing failure mechanisms. Three different approaches were selected and are being pursued in parallel, as a way to increase understanding of the stress distributions. All of them are still under way. The first is photoelastic analysis, the second is finite element numerical analysis and the third is a theoretical analysis from first principles. The first two are discussed in more detail in the following paragraphs.

Beyond determining the stress distributions, to optimize such joints we need to determine their strength. Predicting the strength of a joint is possible, of course, only when both the state of stress and the fracture behavior of the material in that state is known. Fracture behavior of composite materials is a subject for which the state of the art is quite undeveloped. In our investigations, this subject has been put aside temporarily. An intensive literature survey has been conducted, however, and a series of microscopic investigations of failure surfaces has been carried out, including some with an electron microscope. This is also discussed later in a little more detail.

1) Photoelasticity: Our photoelastic method assumes that strains at a point on the surface of the laminated plate are uniform through the thickness and that laminated plate theory remains valid. If the strains on the surface are measured, then stresses in the individual lamina can be obtained. For example, from the following relation (σ_k) can be easily calculated once (ε_o) is measured, since $(\sigma_k) = [Q_k](\varepsilon_k) = [Q_k](\varepsilon_o)$; where (σ_k), $[Q_k]$ and (ε_k) are the stress vector, the matrix of moduli and the strain vector, respectively, at a point in the k-th layer, and (ε_o) is the constitutive strain vector at the same point on the laminate.

Additional useful results are expected from the photoelastic experiments. For instance, in both the finite element method and the theoretical analysis, the extent of the contact surface between the pin and the elastically deformed hole is not known, a priori. It is, therefore, not possible to define the boundary conditions along the edge of the hole, even if one knows with certainty the nature of the load distribution along the contact surface. The photoelastic approach to this problem is as follows:

> Isochromatic fringes on the photoelastic specimen represent the shear strain at a point. Thus, in the photoelastic experiment, we know the applied load and the distribution of the shear strain. On the other hand, in the finite element model idealization, the contact angle must be assumed. (See the section on the Finite Element Approach for details.) It follows that if the pattern of γ_{xy}, computed with a finite element program, matches well with the fringe patterns of the photoelastic experiment, it is probably safe to assume that the contact surface assumed in the finite analysis is correct. (The likelihood of compensating errors for a complete strain distribution is so remote as to be insignificant.) If the extent of contact surface can be obtained for a series of given loads, in this way, it may be useful information for the theoretical solutions.

As described in the previous progress report, five different types of laminated plates were selected in this investigation; they are shown in Table VI.

TABLE VI
LAMINATES USED IN PHOTOELASTIC TESTS

(Graphite/Epoxy; Union Carbide T300/Fiberite 948A)

Designation	Number of Layers	Total Thickness (nominal)	Layups
A	16	0.091 inch	$[0°/90°]_{8s}$
B	18	0.103 inch	$[\pm45°/0°]_{6s}$
C	18	0.103 inch	$[\pm45°/90°]_{6s}$
D	16	0.091 inch	$[\pm45°/0°/90°]_{4s}$
E	16	0.091 inch	$[\pm45°/\pm22.5°/\pm67.5°/0°/90°]_{2s}$

Fiberite's Hy-E 1048AE, epoxy resin preimpregnated graphite tape (Union Carbide's T300/Fiberite's 948A) was used for the test specimens. Laminated and cured plates were cut slightly larger than the designed specimen size and then finished with fine sandpaper to exact size. Specimens are shown in Figure 26. On both sides of the specimen, which were slightly abrated, Ps-1-C type photoelastic sheets (Photoelastic Inc., 0.04 inch nominal thickness), were glued with PC-1 type adhesive (Photoelastic Inc.) and were cured at room temperature for 24 hours. A square grid, spaced at 0.2 inch intervals, was engraved on the bonding to the specimen for improved photoelastic analysis.

A half-inch hole was then drilled at the appropriate location, using carbide tipped drill bits. In this drilling process, the delamination problems reported in the previous report were significantly reduced by applying a very slow feeding speed; i.e., taking 2 hrs. for 0.1 thickness. This was controlled by hand, since no drilling machine with so low a feeding speed is available. No delaminations were visible following use of this method.

Specimens were installed in a pair of specially prepared test fixtures and, in turn, on an Instron testing machine. Tests were begun but not completed, because of anomalies in the fringe patterns. According to the theory of photoelasticity, if the instrument is in position to be used as a crossed-plane polariscope and the applied load is not changed, then isoclinic fringes can be moved by rotating

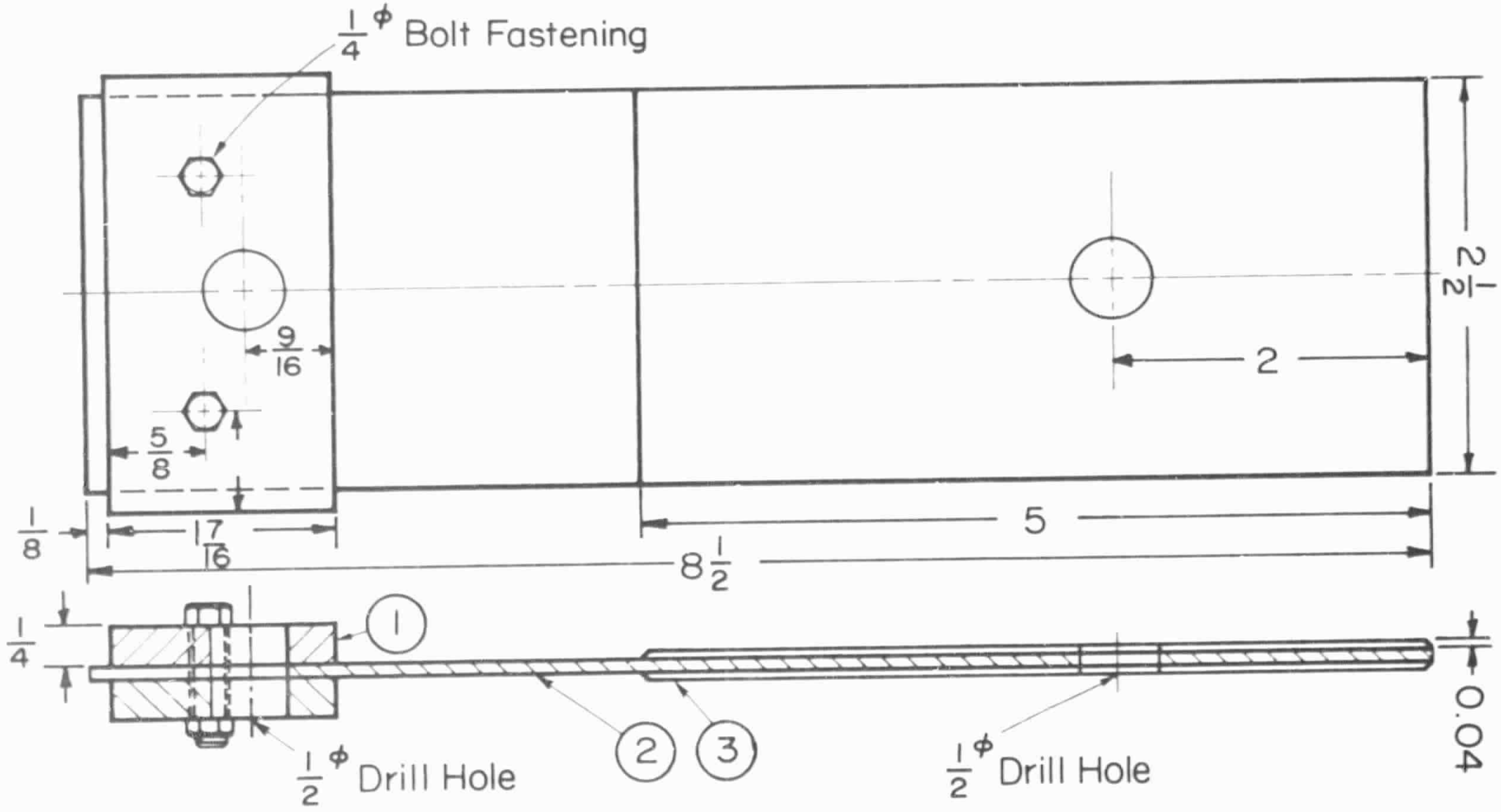

1. Alumnum Reinforcement
2. Graphite / Epoxy Plate
3. Photoelastic Sheet

Figure 26. Photoelastic Specimen

the polariscope angle. Under these circumstances, isochromatic fringes should not move. But in our experiments, both isochromatic fringes and isoclinic fringes moved as the polariscope was rotated. This problem remained at the end of the reporting period, and further photoelastic tests have been postponed until the phenomena has been explained.

2) Finite Element Approach: As indicated briefly in the previous section, both the load distribution and the extent of the contact surface between the pin and the hole are unknown. These uncertainties in boundary conditions must be overcome to obtain useful results. We plan to proceed as outlined in the following paragraphs.

The finite element model shown in Figure 27 has been postulated. A constant strain, triangular shaped element has been used and a total of 345 elements was generated by the program. As seen in Figure 27, elements are highly populated around the hole where higher stress gradients are expected. Even though work-equivalent nodal forces were used at the nodes along the edge where distributed load is applied (as discussed in the paragraphs to follow), a relatively large number of nodes was desired to simulate distributed loads, particularly on the hole where the contact area changes. The assumptions underlying this idealization are first, that the laminated plate theory is valid. This implies that no slips occur in the planes between layers; i.e., the strains through the thickness are constant. Second, we assume that the specimen may be considered to be in a state of plane stress

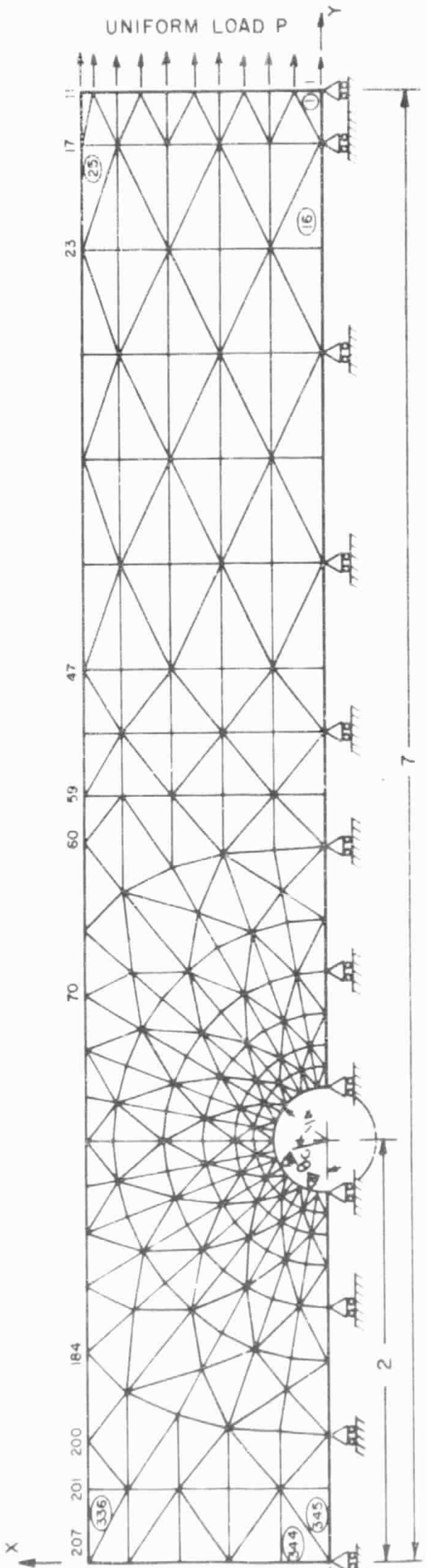

Figure 27. Finite Element Idealization and Boundary Conditions

all through the material domain, even at the points near the hole.

The boundary conditions for the program input are also shown in Figure 27. We wish to represent an evenly distributed load (P in Figure 27) at the far end of the specimen in the y-axis direction. Work equivalent tensile loads were, therefore, applied to represent the constant applied loads (nodes 1 to 11). Displacements at the nodes along this loaded edge are postulated as constant in the y-direction and are free in the x-direction.

At the loaded hole, we assume that the pin is perfectly rigid and fixed in the global coordinate system. This assumption leads to boundary conditions in which radial displacement of the nodes on the contact boundary at the edge of the hole are not allowed. Further, the contact surface between pin and hole is frictionless. This leads to circumferential boundary conditions on the contact boundary in which circumferential displacements are free; i.e., frictionless. The contact angle, θ_c, measured from the axis of symmetry (Figure 27), may (see Reference 3*) vary from 0° to 83° for isotropic material. The contact area, as indicated by this angle, θ_c, increases very rapidly with load until θ_c equals about 45°, and then the increase of θ_c, due to applied load, slows down markedly. Thus, for most cases θ_c can be expected to be between 45° and 85° (Figure 28). A

---

* All reference numbers in this section refer to Table VII.

TABLE VII
REFERENCES: LIGHTLY LOADED MECHANICAL JOINTS

1. Coker, E. G. and L. N. G. Fillon, "A Treatise on Photo-elasticity", Cambridge Press, 1957.

2. Theocaris, P. S., "The Stress Distribution in a Strip Loaded in Tension by Means of a Central Pin", J. of Applied Mechanics, March 1956.

3. Eshwar, V. A., "Analysis of Clearance Fit Pin Joint", J. Mechanical Science, Vol. 20, Pergamon Press, 1978, pp. 477-484.

4. Bickley, W. G., "The Distribution of Stress Round a Circular Hole in a Plate", Phil. Trans. of Royal Society of London, A227, 1924.

5. Tsai, S. W. and E. M. Win, "A General Theory of Strength for Anisotropic Materials", J. of Composite Materials, Vol. 5, 1971.

6. Hoffman, O., "The Brittle Strength of Orthotropic Materials", J. of Composite Materials, Vol. 1, 1967.

7. Narayanaswami, R. and H. M. Adelman, "Evaluation of the Tensor Polynomial and Hoffman Strength Theories for Composite Materials", J. of Composite Materials, Vol. 11, 1977.

8. Personal letter from Prof. Durelli, A. J. of Oakland University.

9. Abdul-Mihsein, M. J., Fenner, R. T. and C. L. Tan, "Boundary Integral Equation Analysis of Elastic Stresses Around an Oblique Hole in a Flat Plate", J. of Strain Analysis, Vol. 14, No. 4, 1979.

10. Mir Mohamad Sadegh, Ali R., "On the Problem of a Plane, Finite, Linear-Elastic Region Containing a Hole of Arbitrary Shape; Boundary Integral Approach", Ph.D. Thesis, Dept. of Metallurgy, Mechanics and Material Science, Michigan State University, 1978.

11. Quinn, W. J. and F. L. Matthews, "The Effect of Stacking Sequence on the Pin Bearing Strength in Glass Fiber Reinforced Plastic", J. of Composite Materials, Vol. 11, 1977.

12. Collings, T. A., "The Strength of Bolted Joints in Multi-Directional CFRP Laminates", Her Majesty's Stationary Office, London, 1977.

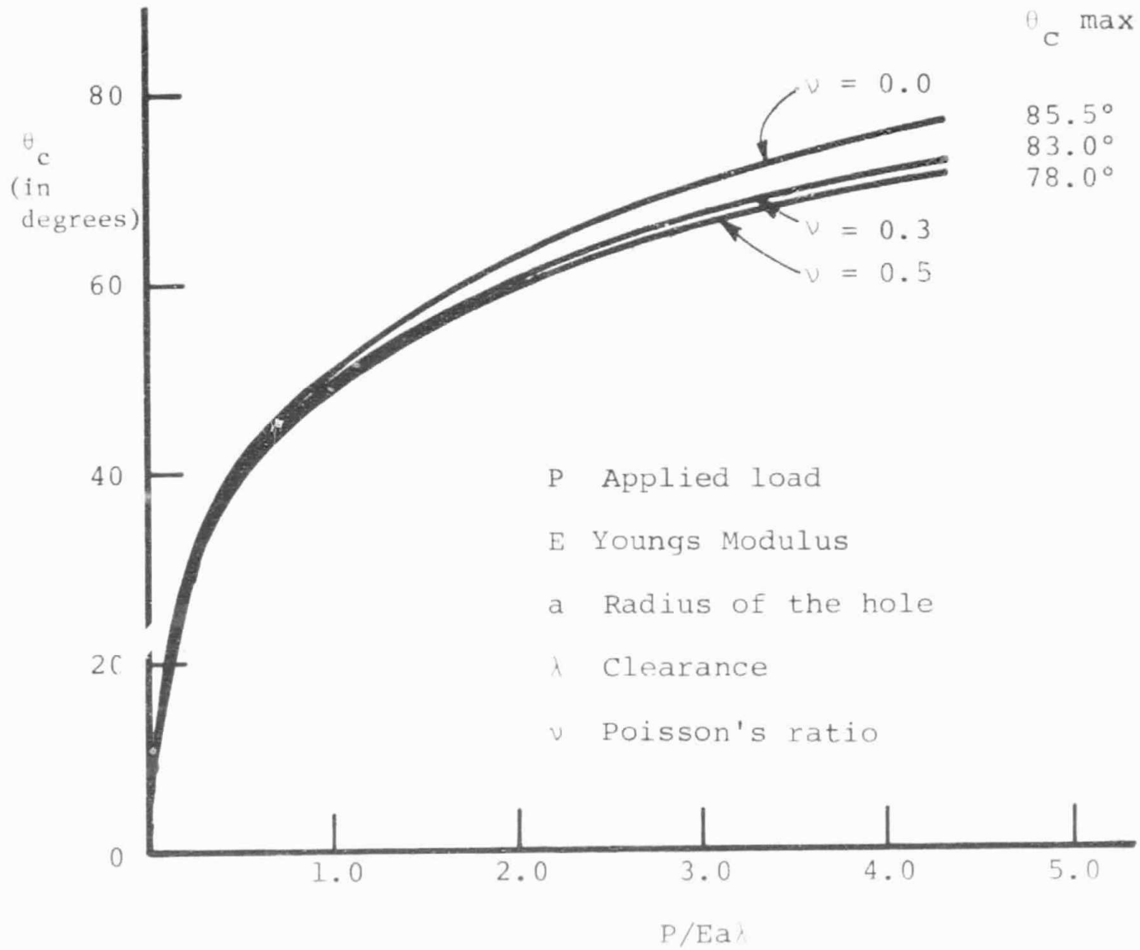

Figure 28. Eshwar's Analysis Results (Ref. 3, Table VII)

trial and error method which produces γ_{xy} distributions corresponding to photoelastic experimental results for the same applied load, therefore, can probably be restricted to this limited range, and the proper boundary condition decided. The "boundary" along the y-axis (the specimen centerline) in Figure 27 which represents symmetry conditons, is the equivalent of a simply supported boundary. That is, no x-displacements are allowed, but the "boundary" is free in the y-direction. All other boundaries (not mentioned above) are free.

The status of this finite element analysis is that first runs have been made and errors found in the program. Checkout continues.

3) Fracture Behavior and Criteria: Two types of investigation have been planned. The first is to determine a useful failure criterion for the material, and the second is to gain insight as to the failure mechanism in bearing. For the first task it was concluded, at the present time, that either the tensor polynomial criteria (Reference 5) or Hoffman's criteria (Reference 6) is adequate. A literature survey continues.

Investigation of the nature of the failure mechanism was limited to examination of the fractured surfaces by means of both optical and electron microscopes. Some optical results were reported earlier. While no final conclusions are available, several observations can be made using the nomenclature in Figure 29.

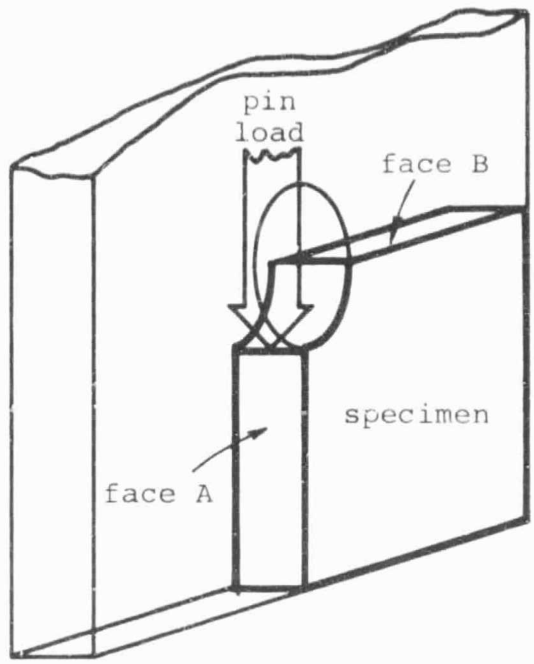

Figure 29. Failure Surface Nomenclature

Referring to failure Face A, three types of cracks are evident:

i. Layer separation (Figures 30a, 31a, 31b, 31c) usually appeared at the outer layers or at the ends of shear cracks.

ii. Shear cracks (Figures 30b, 31b, 31c) propagate in directions which are independent of fiber orientation in a layer.

iii. Buckling (Figures 30b, 31c) usually occurs in 0° layers and combines with shear-type failures.

Referring to failure Face B, all specimens showed layer separations. (Figures 30c)

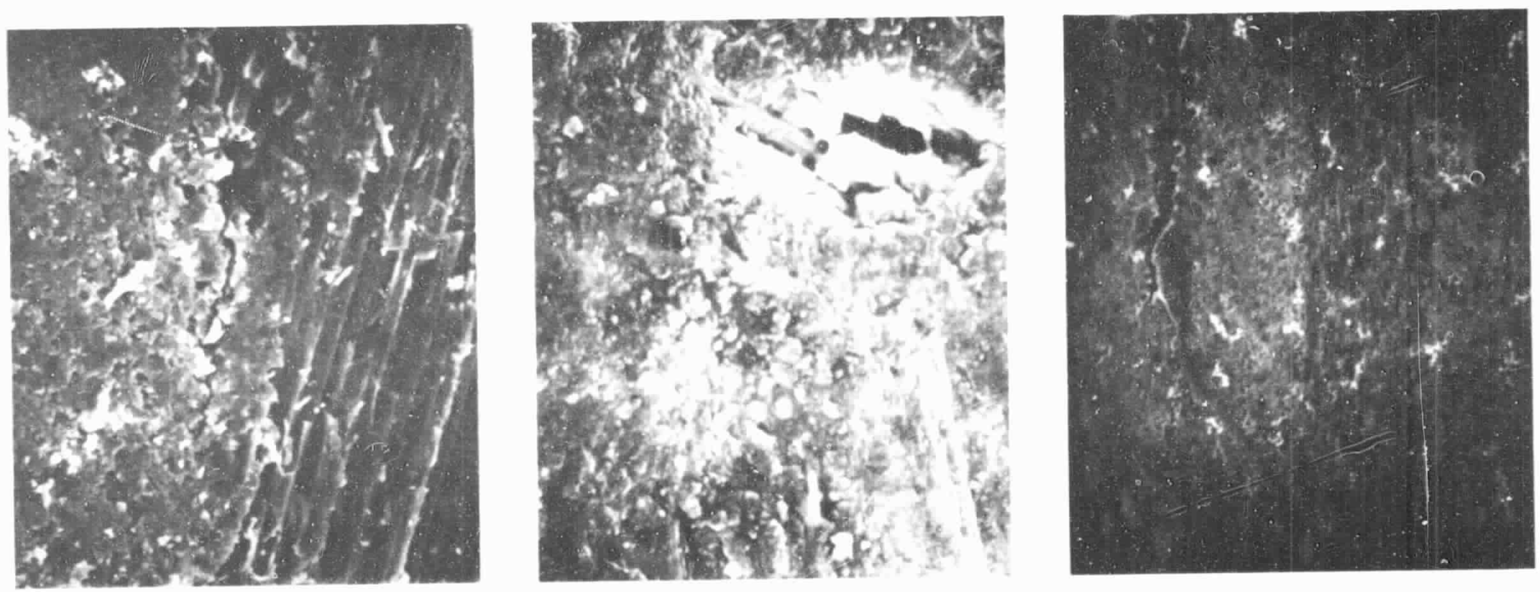

(a) Face A (Type B, x 500) (b) Face A (Type A, x 1000) (c) Face B (Type C, x 200)

Figure 30.

Cracks Due to Bearing Pressure
(Electronic Microscope)

(a) Type A (x 20)

(b) Type B (x 20)

(c) Type C (x 20)

Figure 31. Cracks Due to Bearing Pressure (Face A. Optical Microscope)

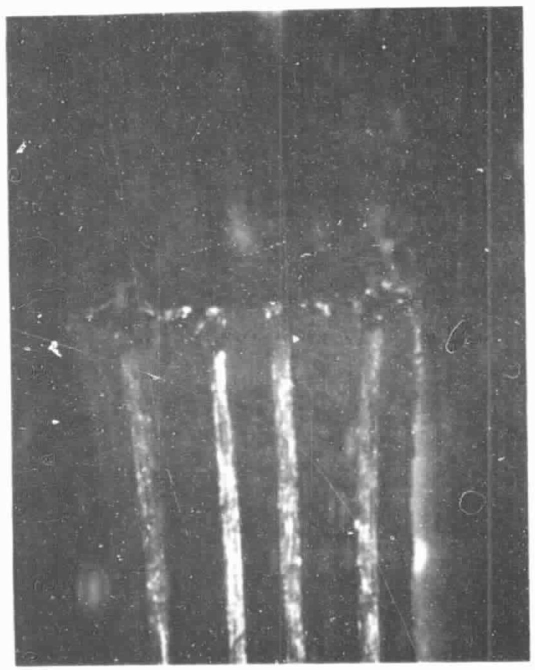

(d) Type D (x 15)

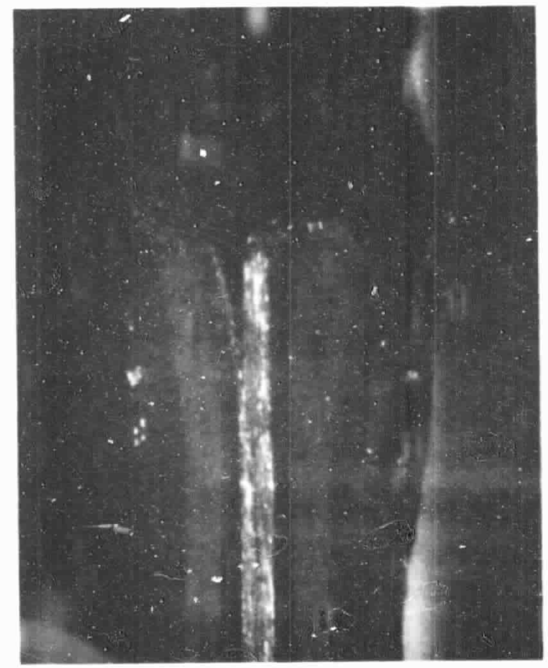

(e) Type E (x 20)

Figure 31. (continued)

at the 1980 SSA Convention in Seattle, Washington. Proof-testing of the RP-1 is in progress, and we expect the glider will be flown near the end of spring or early in the summer of 1980. As the glider neared completion, excitement increased, and as might be expected, the number of students doubled to 30 during the spring semester.

Two new gliders are now in the early design phase and are discussed later in this report. After completion of the RP-1 last fall, the main emphasis in the laboratory during the present reporting period was placed on fundamentals in composite structural techniques, rather than immediately on the design of the next glider. Thus, every student has been required to undertake a one-semester project, which includes calculation, fabrication and testing of a composite structural part. The variety of projects in progress during the spring semester can be seen in Table IX. The more advanced projects (marked with an *) are expected to motivate and prepare the student for more advanced studies and for research. These asterisked projects are described somewhat more fully in the following paragraphs.

<ins>Project 1</ins> deals with the determination of Young's modulus, Poisson's ratio and shear modulus. The structural element used is a tube of composite material. The test fixture and the mounting of strain gauges on the tubes are shown in Figure 33. For the shear modulus a separate torsion test is used.

TABLE VIII

CRACKS ON BEARING SPECIMENS

Type	Sketch of Fractured Shapes	Lay-Ups	Observation
A	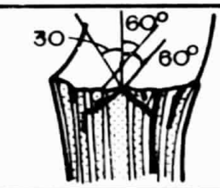	$[0°/90°]_{8s}$	1. The cracks are running across different layers of fiber orientation without changing directions. 2. Cracks ended where delaminations exist. 3. Local buckling on 0° layers.
B	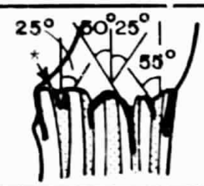	$[\pm45°/0°]_{6s}$	1. There are no inclined cracks on 0° layers. 2. Separation of a 0° layer appeared on (*). 3. Cracks ended at delaminations.
C	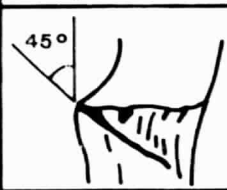	$[\pm45°/90°]_{6s}$	1. No visible delamination crossing the crack line. 2. Crack is continuous all across different fiber orientations.
D	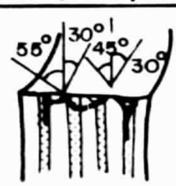	$[\pm45°/0°/90°]_{4s}$	1. Same pattern as A appears at middle section where fiber orientation is only [0°/90°]. 2. Cracks on the layers of ±45° fiber orientation did not cross 0° layers, but stopped at the boundaries between 0° layers and ±45° layers, where delamination occurred.
E		$[\pm45°/\pm22.5°/\pm67.5°/90°/0°]_{2s}$	1. Many delamination type cracks. 2. Separations in 0° layer and 67.5° layer.

1. ±45°, ±67.5°, ±22.5°, or 90° Layers
2. Major cracks
3. 0° Layers

investigate not only failed specimens but also those which are unfailed but loaded near the critical values. This may entail monitoring the initiation of failure during the test by means of acoustic emission or other techniques.

PART II

CAPGLIDE (Composite Aircraft Program Glider)

CAPGLIDE (Composite Aircraft Program Glider)
(R. J. Diefendorf, H. J. Hagerup, G. Helwig)

The present reporting period has seen the completion of the first all composite ultra-light glider, which has been named RP-1 (see Figure 32). RP-1 was on display during the project site visit in November, 1979.

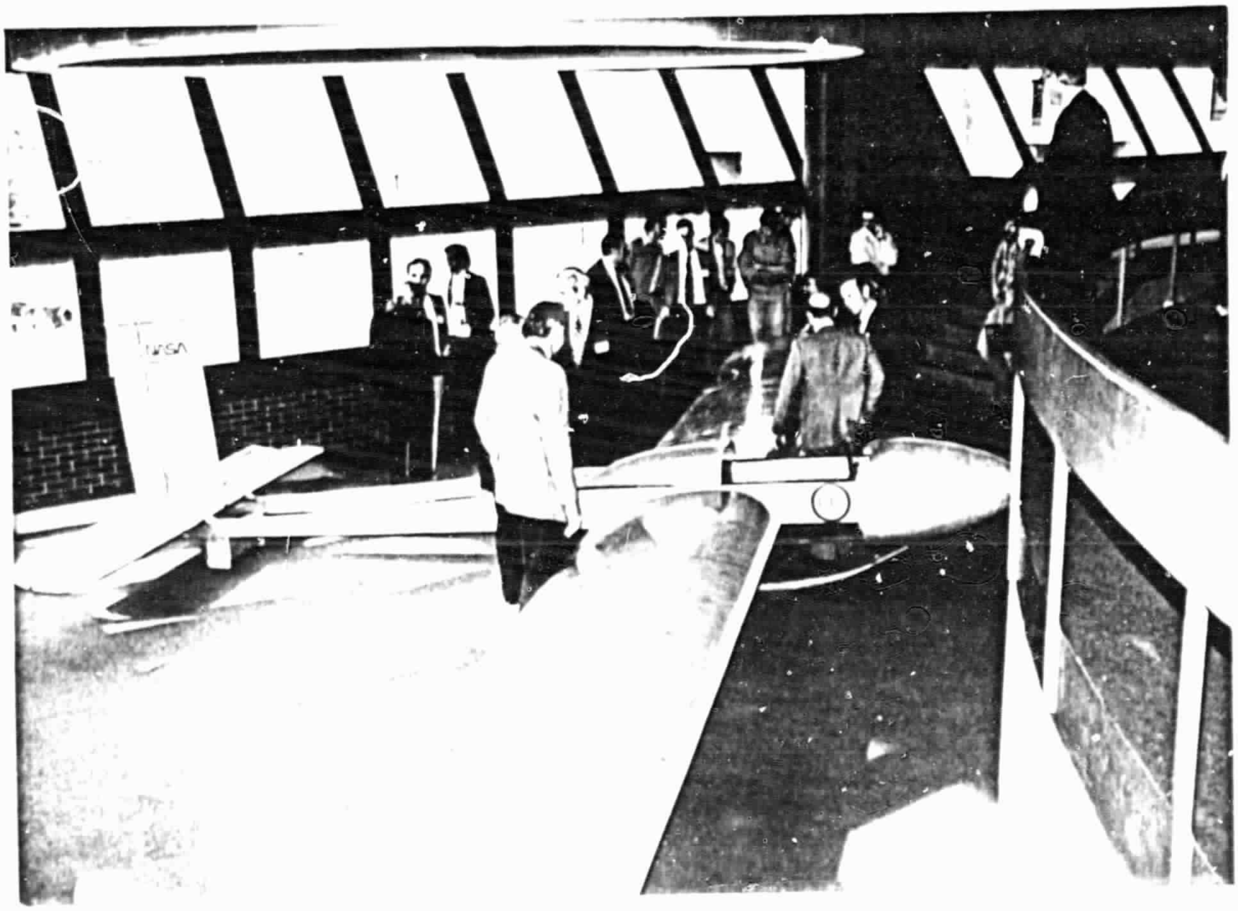

All Composite Glider, RP-1, on Display During Program Site Visit (November 1979)
Figure 32

A report on the RP-1 has been published in the membership journal of the Soaring Society of America (Soaring, February, 1980), and a presentation on the project was made at the 1980 SSA Convention in Seattle, Washington. Proof-testing of the RP-1 is in progress, and we expect the glider will be flown near the end of spring or early in the summer of 1980. As the glider neared completion, excitement increased, and as might be expected, the number of students doubled to 30 during the spring semester.

Two new gliders are now in the early design phase and are discussed later in this report. After completion of the RP-1 last fall, the main emphasis in the laboratory during the present reporting period was placed on fundamentals in composite structural techniques, rather than immediately on the design of the next glider. Thus, every student has been required to undertake a one-semester project, which includes calculation, fabrication and testing of a composite structural part. The variety of projects in progress during the spring semester can be seen in Table IX. The more advanced projects (marked with an *) are expected to motivate and prepare the student for more advanced studies and for research. These asterisked projects are described somewhat more fully in the following paragraphs.

Project 1 deals with the determination of Young's modulus, Poisson's ratio and shear modulus. The structural element used is a tube of composite material. The test fixture and the mounting of strain gauges on the tubes are shown in Figure 33. For the shear modulus a separate torsion test is used.

TABLE IX
PROJECTS IN FUNDAMENTAL COMPOSITE TECHNIQUES

Project No.	Description of Fabrication Exercise
1.	Graphite tubes*
2.	Hybrid specimen
3.	Pultrusion process
4.	Multi-way tube connection
5.	Kevlar tubes
6.	Graphite wing section
7.	Unidirectional Kevlar and graphite specimen*
8.	Variable camber wing section*
9.	Space structure beam
10.	Bi-composite
11.	Aeroelastic box-beam wing*
12.	Tapered graphite tube
13.	Shear test
14.	I-beam
15.	Wet-mold layup
16.	Delamination specimen
17.	Thermal coefficient of expansion*

* Advanced projects in composite structural techniques

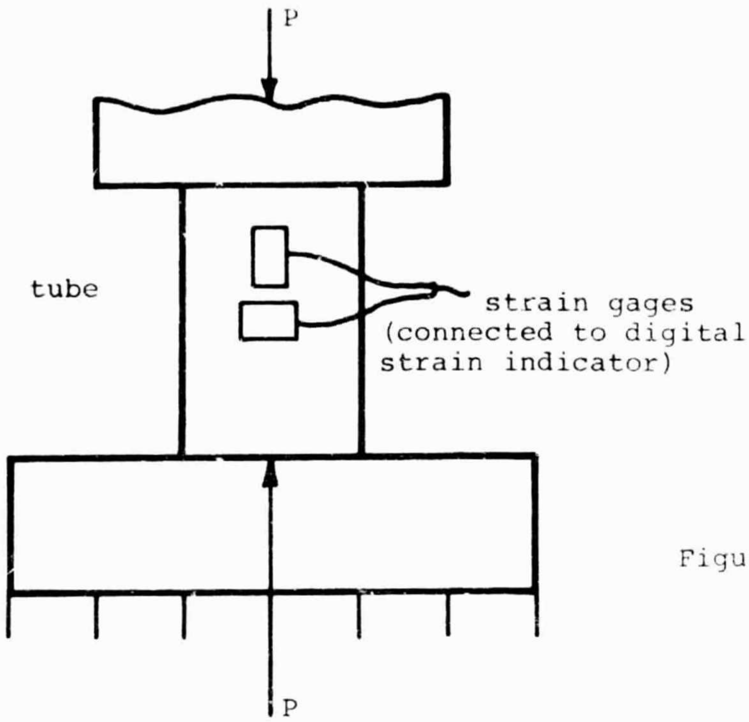

Figure 33. Test Set Up for Obtaining Elastic Properties Using a Composite Tube

Project 7 has been devised to obtain, with two simple out-of-axis tests, the four engineering constants of unidirectional materials. We have found that for the best accuracy, the two test specimens should be loaded off-axis by 15 and 75 degrees. Tests with graphite specimens gave the results shown in Table X.

TABLE X
PROJECT 7 RESULTS

Elastic Constant	Test	Nominal Value
E_1	21.30×10^6 psi	20.30×10^6 psi
E_2	1.40×10^6 psi	1.40×10^6 psi
ν_{12}	0.32	0.32
G_{12}	0.93×10^6 psi	1.00×10^6 psi

Project 8 is a study of a composite wing designed to have variable camber. The lower wing surface is a pre-stressed composite plate which can be "snapped through", so that the wing section changes from a high-lift to a high-speed configuration (Figure 34)*. A radio controlled model is under construction to test such a variable camber wing.

Project 11 investigates the coupling of bending and twisting in a box-beam type of wing with an aspect ratio of 10. This wing is built of graphite epoxy, and the design is shown in Figure 35. Measured stress and deformation data from tests of this wing will be compared with the results of a finite element calculation (Figure 36).

Project 17 is a development of a small computer-program to optimize the thermal expansion of a multi-layer laminate. The object function is

$$0 = \sqrt{\Sigma_{i,j,} (W_{ij}\sigma_{ij})^2} = \min(i,j, = 1,2)$$

where:

$W_{ij} \equiv$ weighting function

$\sigma_{ij} \equiv$ thermal coefficient of laminate.

The optimal result is used to make a test specimen whose thermal expansion characteristics are then measured.

---

* This concept emerged in a collaborative airfoil design design session at the Boeing Commercial Airplane Company on November 12 and 13, 1979 (see Table IV), and patent implications are being investigated in the names of the Boeing Company and G. Helwig, RPI.

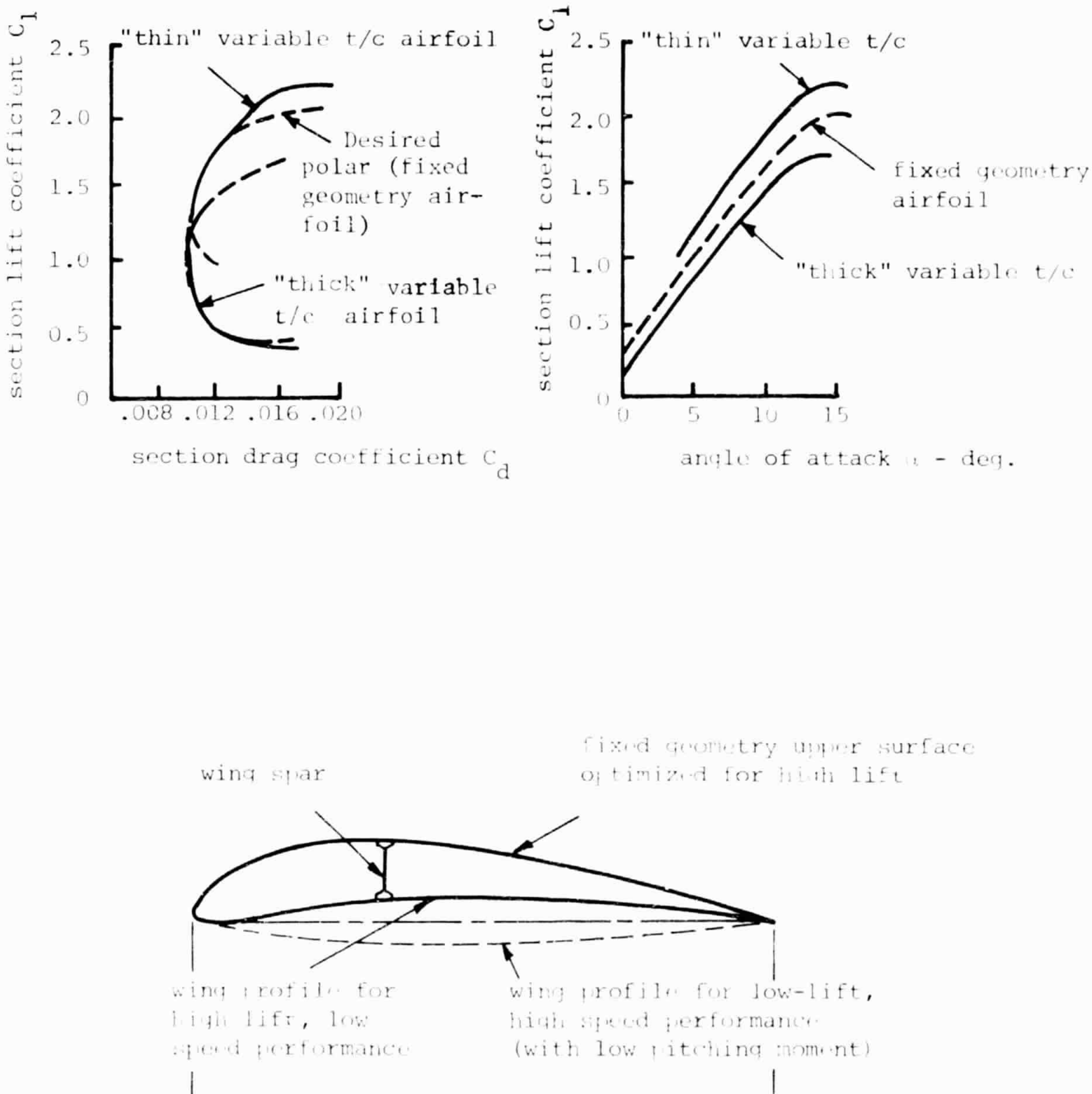

Figure 34. Variable Thickness/Chord and Camber Ultralight Glider Airfoil

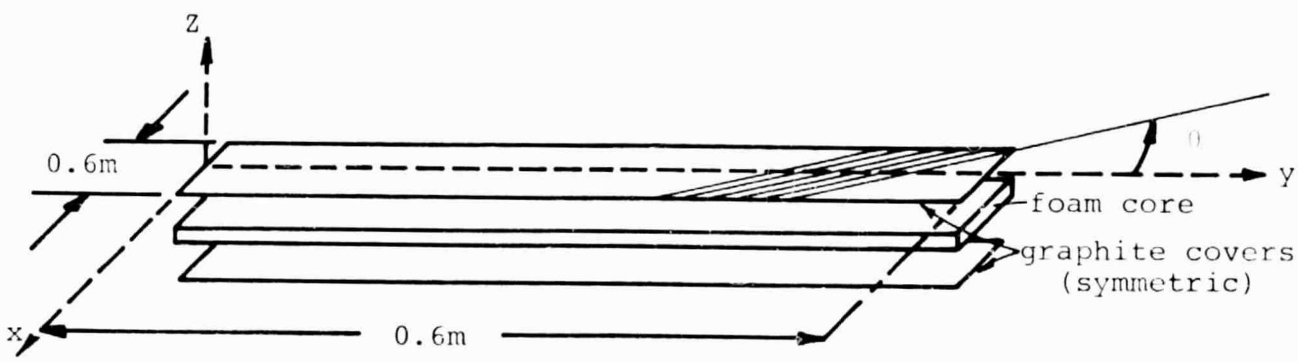

Figure 35. Build-Up of Box Beam Wing

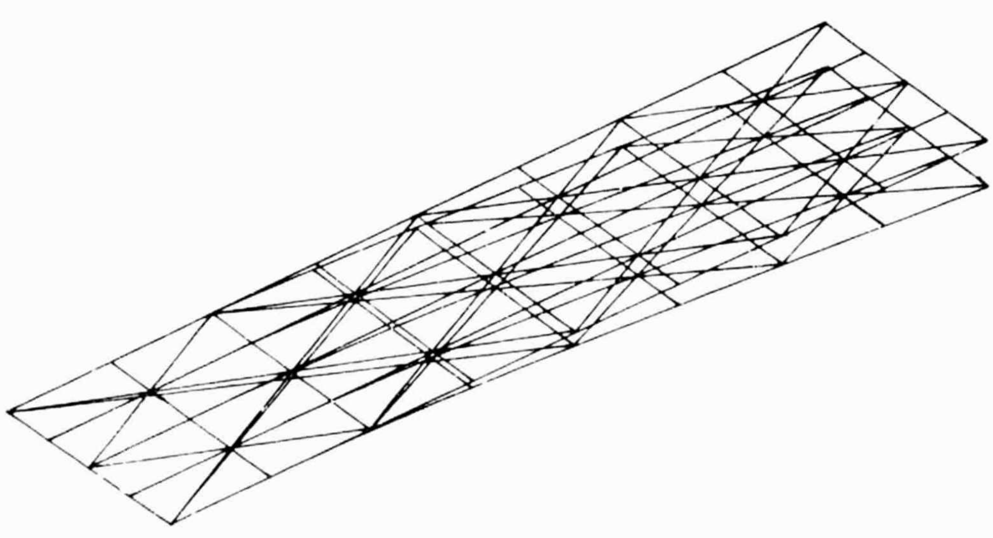

Figure 36. Finite-Element-Model of Box Beam Wing
(Deflection and Geometry Plot)

New Glider Projects

The concepts evolving for two new gliders are sketched in Figures 37 and 38. The super-ultralight composite glider, which should weigh about 70 pounds, will have a simple single-surface arc-wing section with a constant chord planform. The wing will be designed to be disassembled in four pieces and stacked for easy transportation on a car roof. The fuselage framework will be assembled with quick connections. The horizontal stabilizer is a flat plate, with an elevator. The winglets are rudder, aileron and airbrakes in one. A small motor and propeller are optional.

The second glider is a motorglider with a closed cockpit. The small motor (10 hp) is installed essentially in the cockpit and placed between the legs of the pilot. The driveshaft drives the propeller, which will be foldable and, therefore, can be retracted against the fuselage. The construction will be very similar to the RP-1. A new airfoil section, with a low pitching moment similar to that designated BHL in Figure 39, will be selected and is expected to make a lighter weight new wing possible.

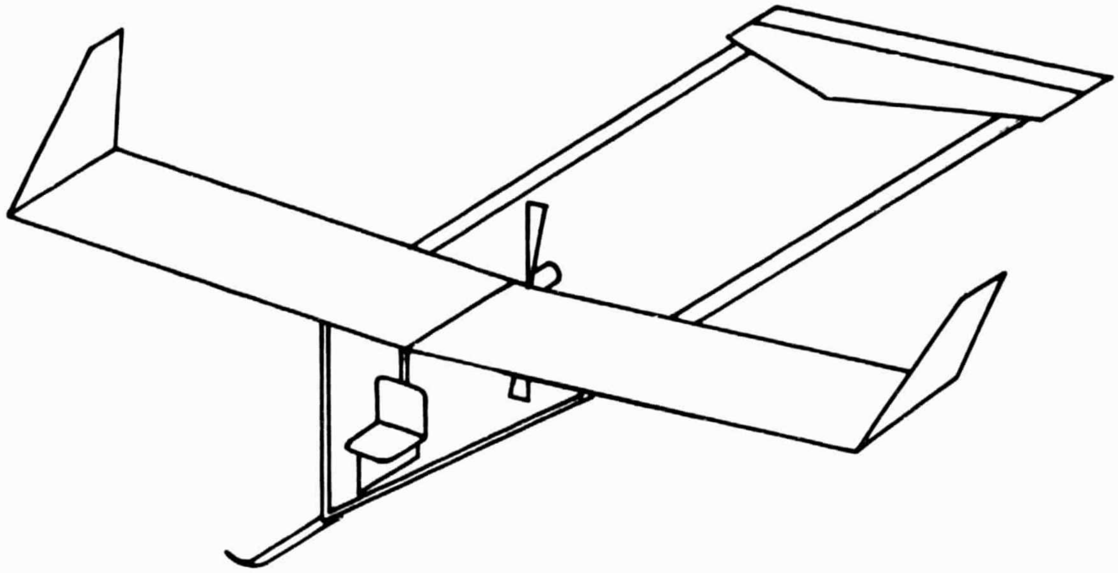

Figure 37. Super-ultralight glider

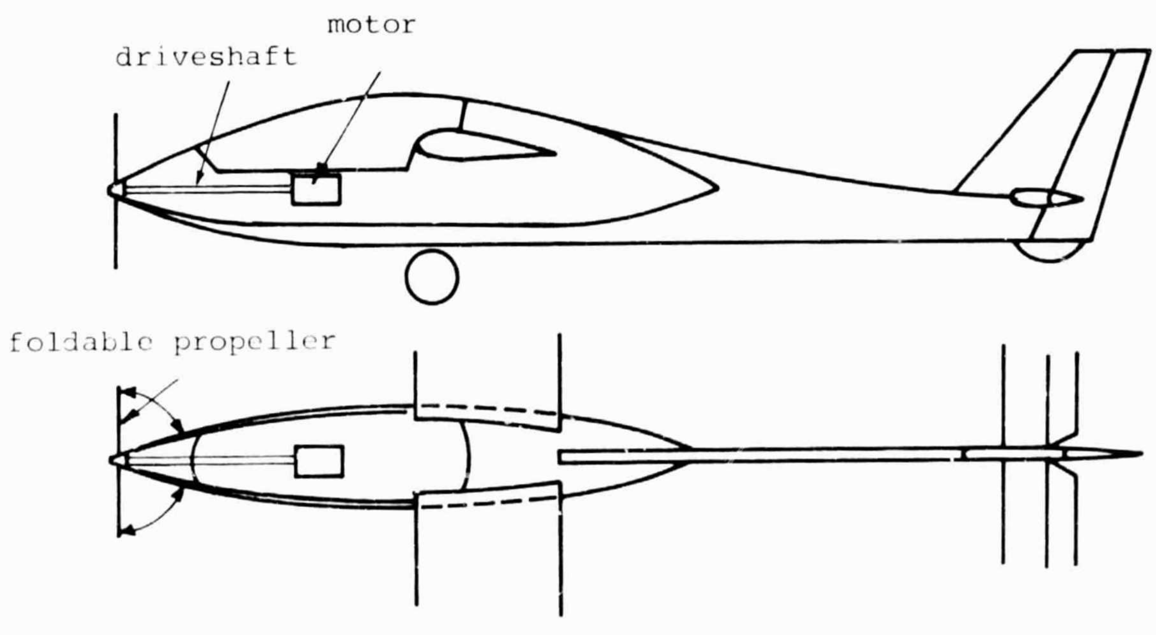

Figure 38. Composite Motorglider

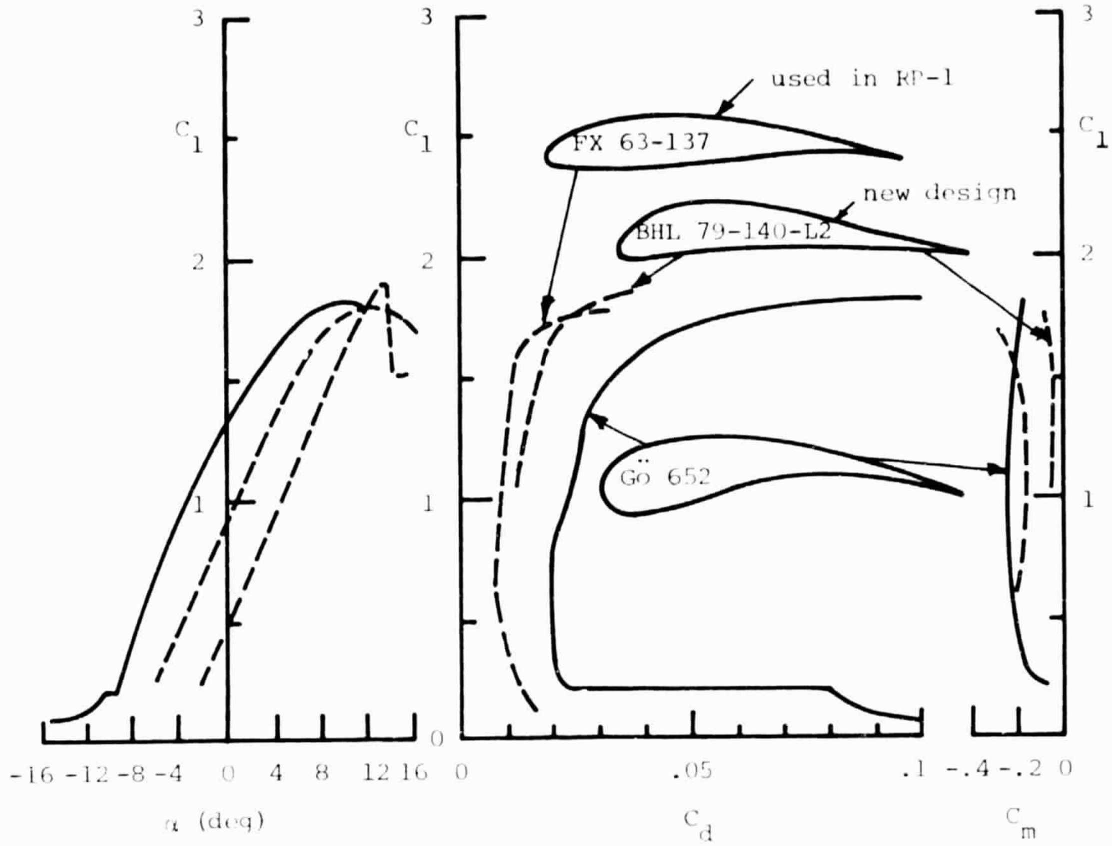

Figure 39. Comparison of three wing sections

PART III

COMPAD (Computer Aided Design)

COMPAD (Computer Aided Design)
(L. J. Feeser and M. S. Shephard)

During the current reporting period, the major emphasis within the computer aided design portion of the project has been on the continued development of the interactive finite element preprocessor. However, some effort was expended on other portions of the finite element system, referred to as RPIFEP (Rensselaer Polytechnic Institute Finite Element Package), which is discussed herein.

Continued work on the interactive two-dimensional finite element preprocessor has been concerned with three areas. They are;

1. adding a one-element-deep transitions mesh generator,
2. writing a mesh editing segment and
3. continued program testing for the purpose of detecting and correcting errors.

The function of the one element deep transition region is to allow for the grading from fine to course element meshes; the function of the element editor is to perform local modifications to the mesh on the element level. Program testing is almost always a time consuming task, which is, in this case, complicated by the fact that the preprocessor is a large, highly interactive program allowing for an infinite number of operation combinations.

To describe the one element deep transition capability, consider the simple example of a square plate shown in

Figure 40. Assume that it is known in advance that the lower left-hand corner is the most critical portion of the plate, and that, therefore, a fine mesh is desired in that area. Such a mesh can be generated using three subregions, as indicated in Figure 40. A fine mesh is generated in the lower left-hand corner, as shown in Figure 41. Next, the one element deep transition region, shown in Figure 42, is generated. This transition has 14 element edges on one side and 8 on the other. The transition is generated by placing the "best" possible set of triangular elements between the two sides. "Best" triangles are defined as those elements that are as near to equilateral as possible. Finally, the four-sided mesh (Figure 43) is generated, yielding the final mesh (Figure 44).

Although simple, the transition capability is important in the discretization of practical problems. For example, four transition regions were employed in the generation of a finite element mesh for the Berg Design of the actuator rib (see the CAPCOMP section of this report), as shown in Figure 45. Figure 46 shows the subregion boundary curves used to generate the mesh, while Figure 47 shows a close up of a portion of the mesh. It should be noted that the generation of the problem geometry and mesh in Figure 45 took under four hours, while the original hand generated model took several days.

The element editor allows the analyst to modify his mesh on an element by element basis and to generate one-

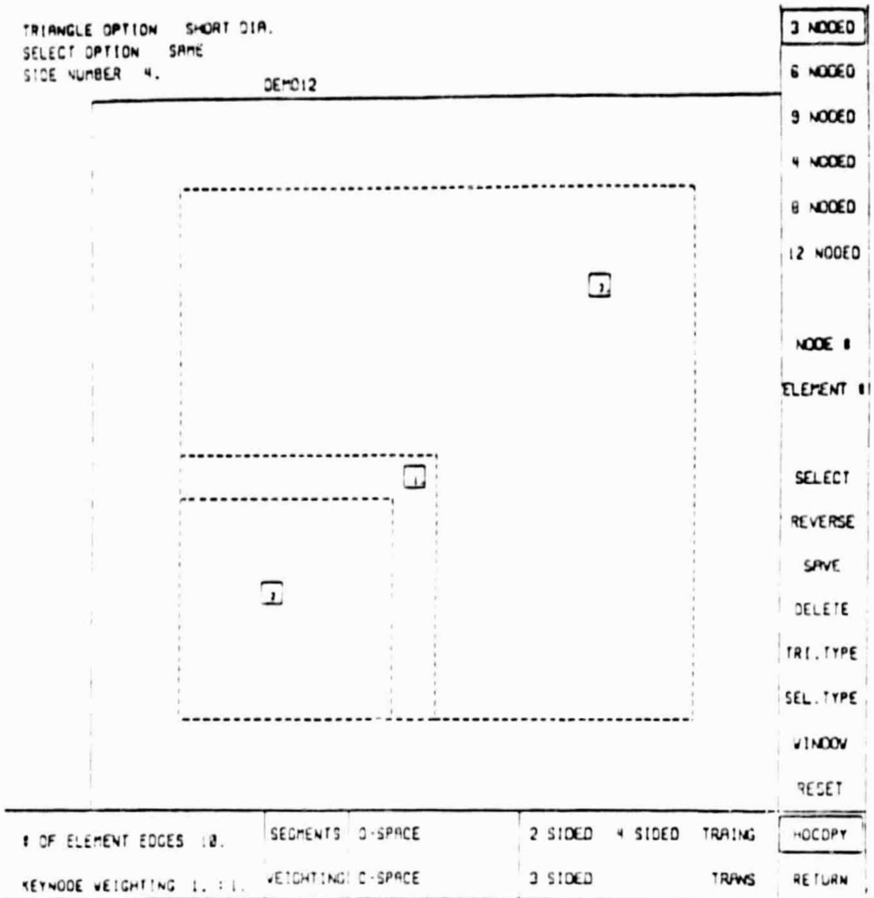

Figure 40. Boundary Curves for the Transition Region Example

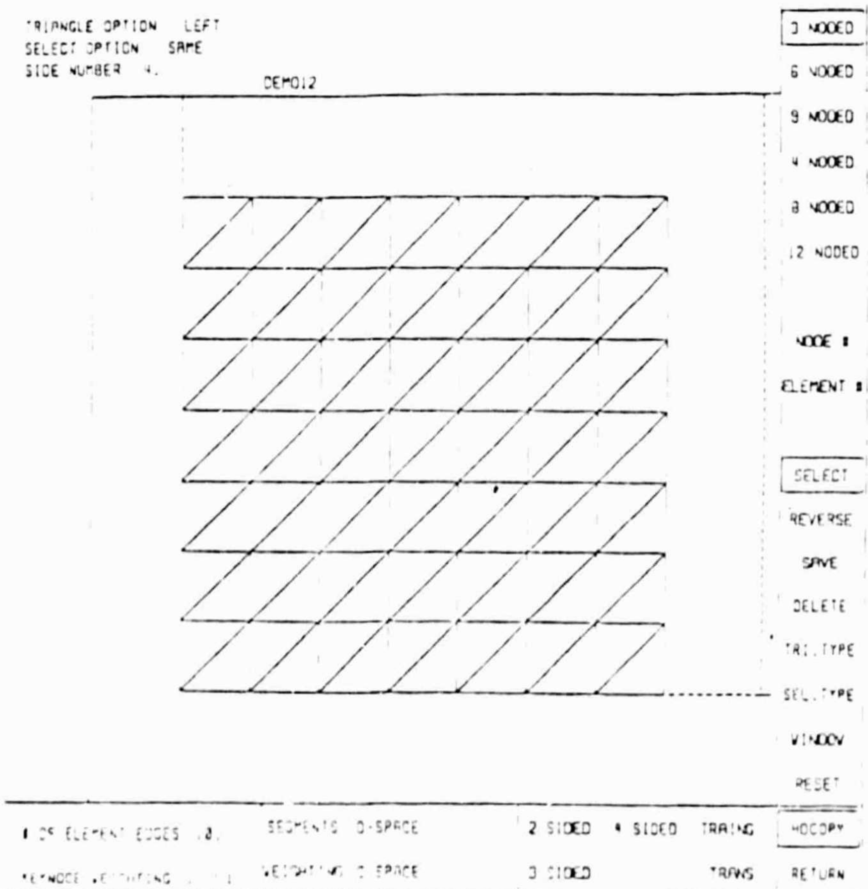

Figure 41. Fine Mesh in Lower-left Corner

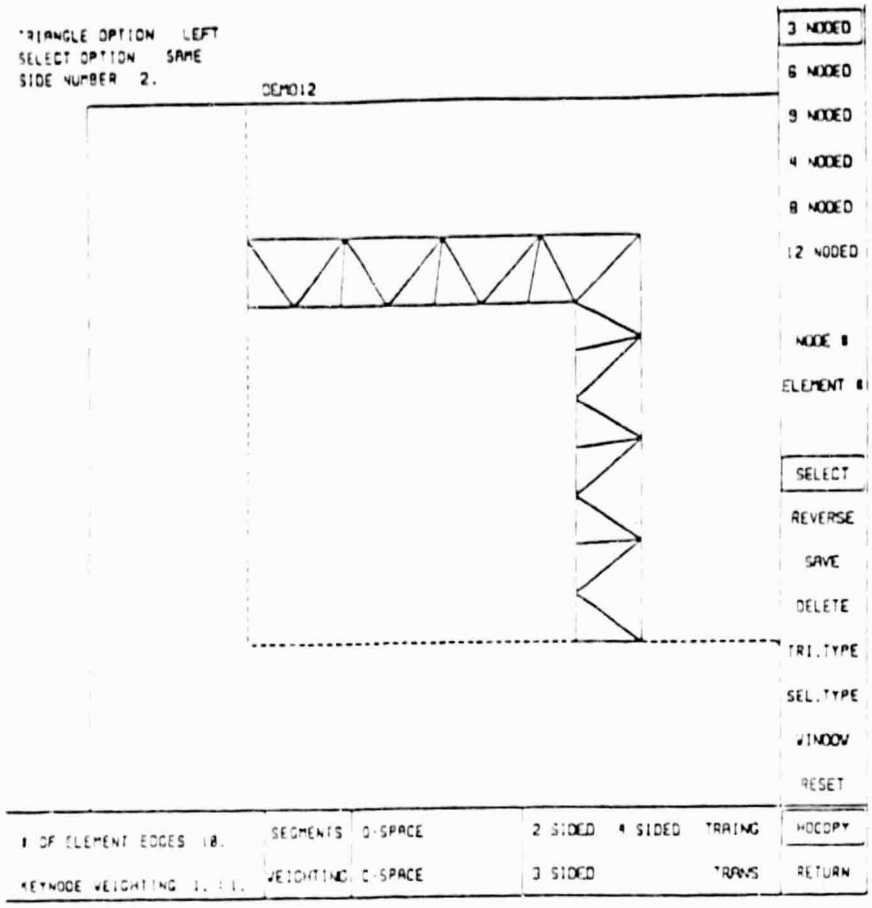

Figure 42. One Element Deep Transition Region

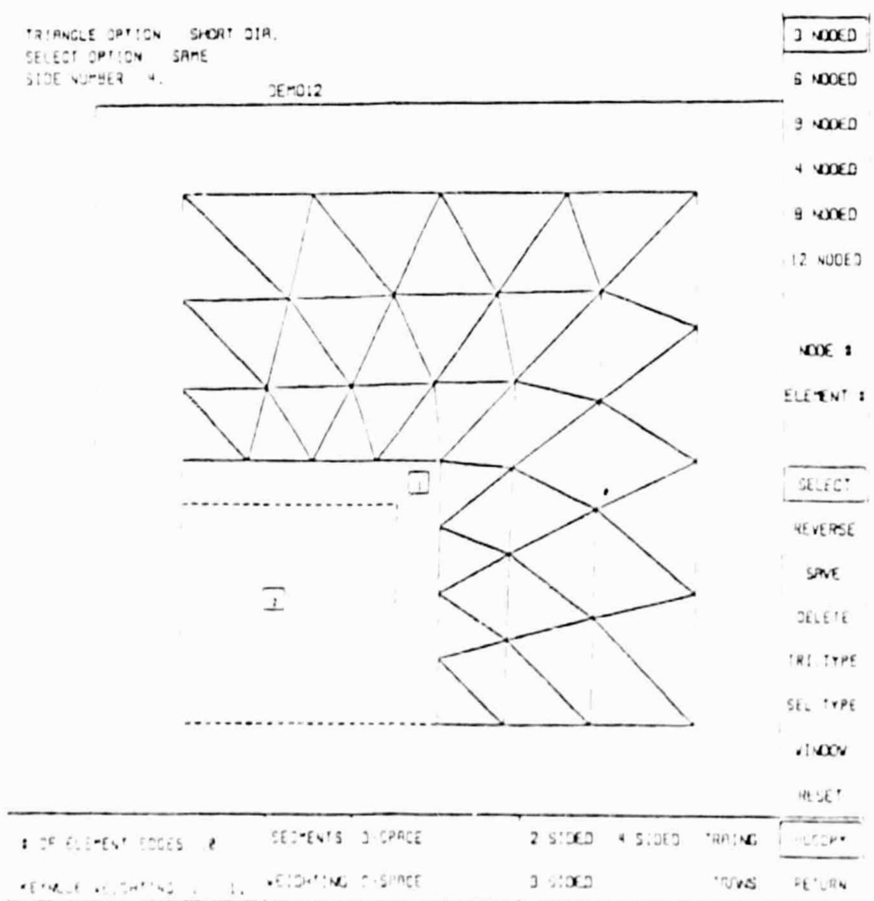

Figure 43. Four-sided Mesh to Fill the Rest of the Square

(Note: Two of the sides contain slope discontinuities, i.e., "corners".)

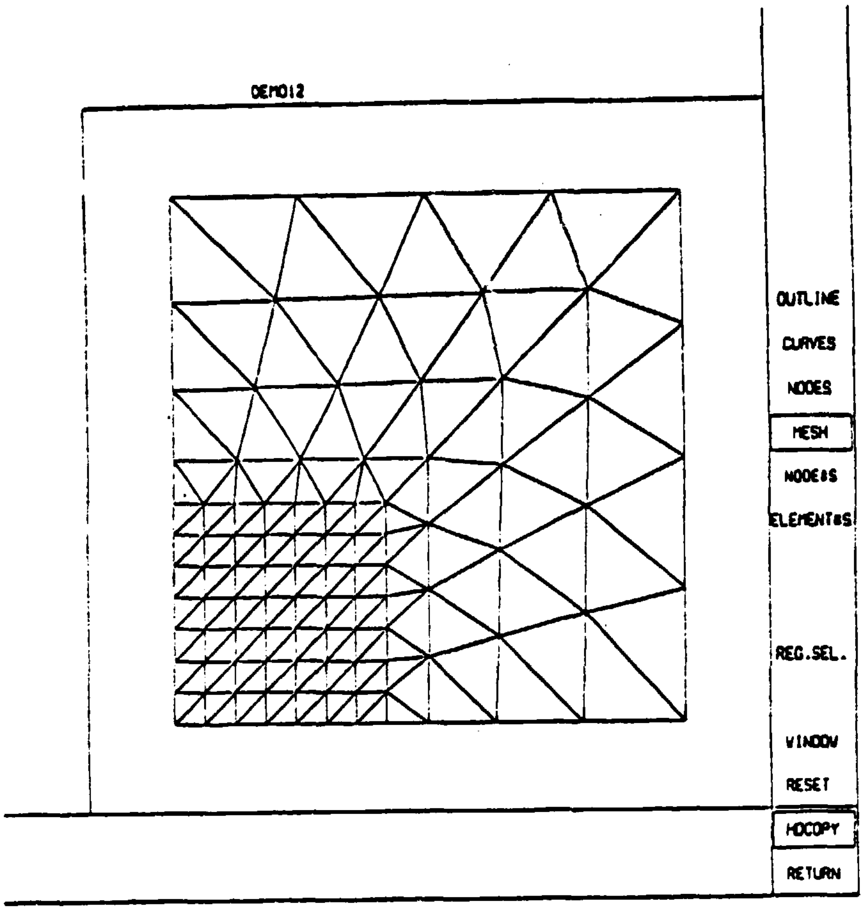

Figure 44. Final Mesh

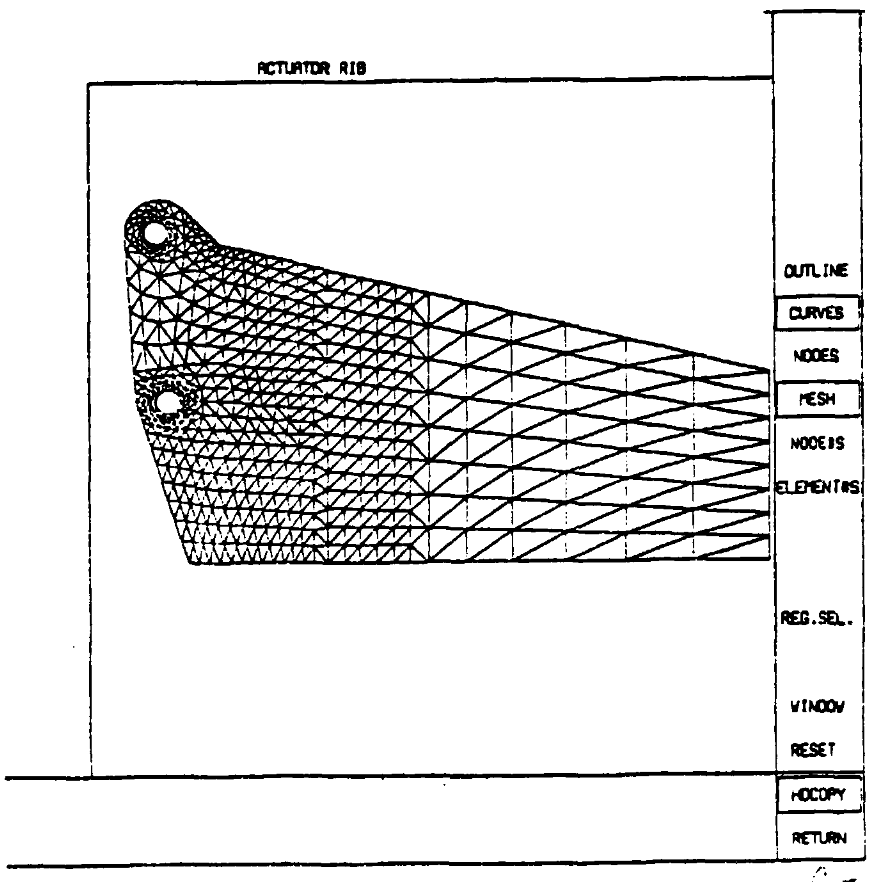

Figure 45. Finite Element Mesh for the Berg Design of the Actuator Rib

C-2

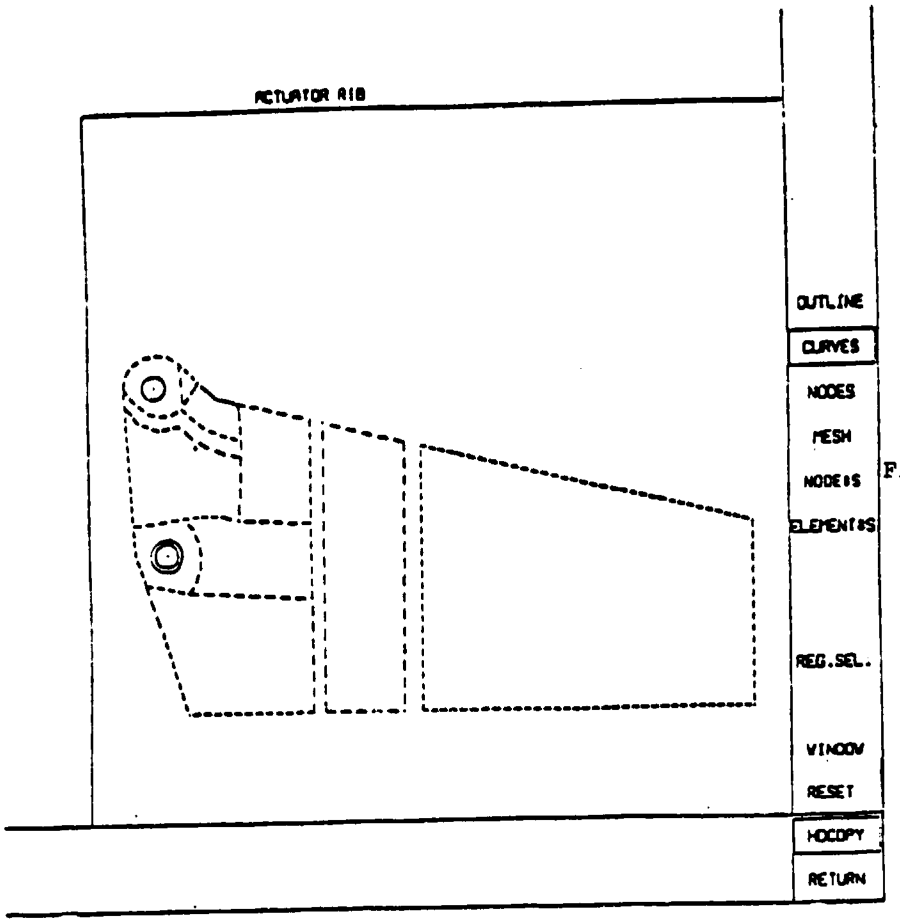

Figure 46. Subregion Boundary Curves Used in the Generation of the Actuator Rib Mesh

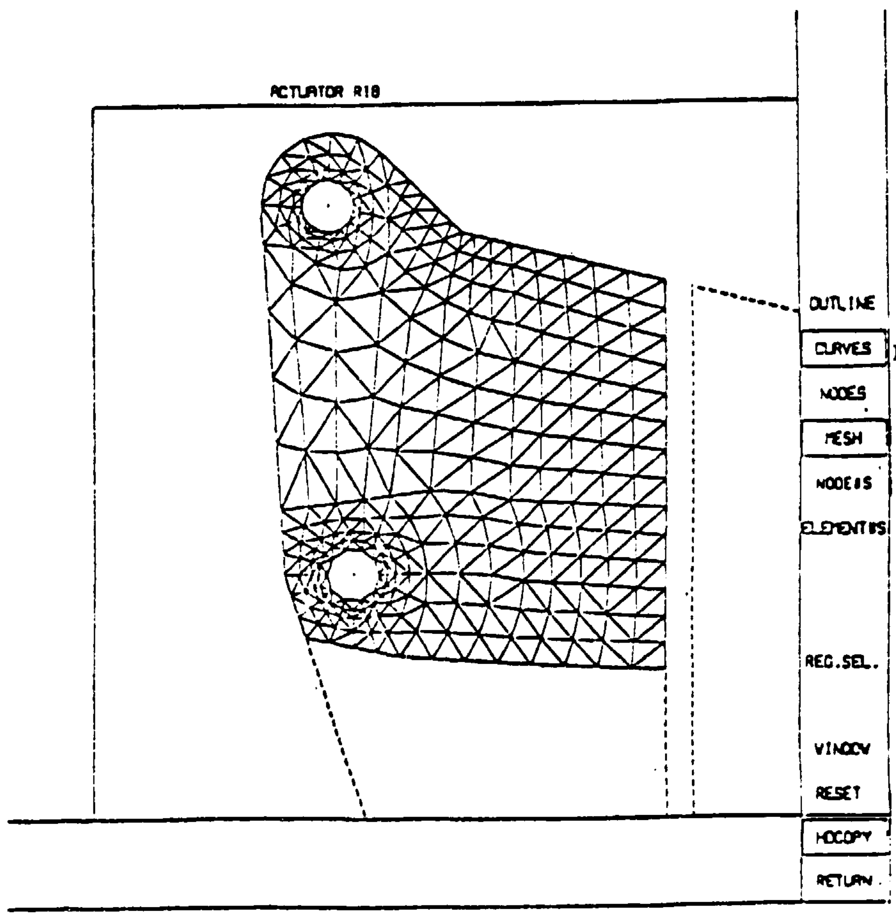

Figure 47. A Close-up of the Upper Left-hand Portion of the Actuator Rib

dimensional stiffness elements. One dimensional elements, with two-, three- or four nodes per element, can be generated, either one element at a time or along an entire curve, by activating the GEN.BAR option and pointing to the curve of interest (indicated in Figure 48). Individual elements can be deleted by activating the DEL.EL. option and pointing at the elements to be deleted, as shown in Figure 49. Nodes can also be interactively repositioned by activating the DRAG function and pulling the desired node to its new position. Figure 50 shows the mesh of Figure 49 after one of the nodes at the edge, created by the deleted elements, was pulled down and to the right. Elements can also be input by interactively inputting their node points. In Figure 51, the hole created by deleting the triangles has been filled by two quadrilateral elements input in the fashion described above.

During this reporting period some effort was also expended on our two inhouse analysis programs. Both programs have a general design and, at this time, are capable of only linear static stress analysis employing limited element libraries. However, each of these programs employes a unique feature in their design which makes them efficient on the computer on which they run.

The first program, which runs on RPI's IBM 3033, employs true dynamic array allocation. True dynamic allocation "allows" the program to set up, with the use of some special system utilities, arrays of the exact size indicated by the input information. In this way, only the amount of high

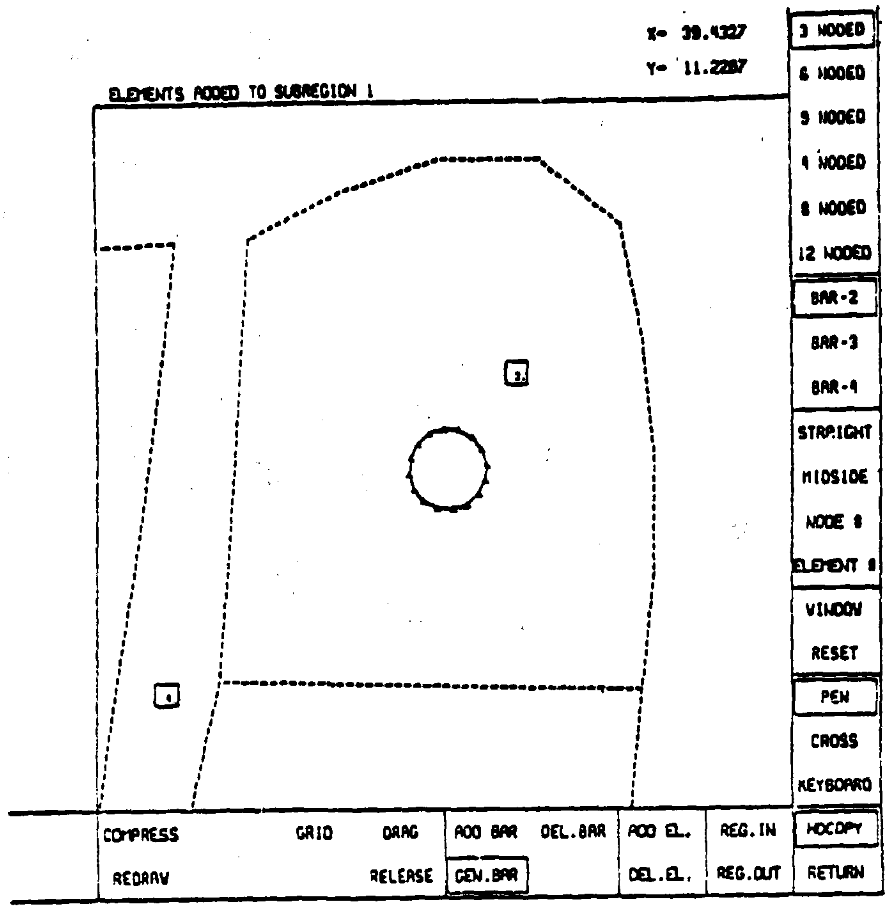

Figure 48. Generation of Stiffness Elements With Element Editor

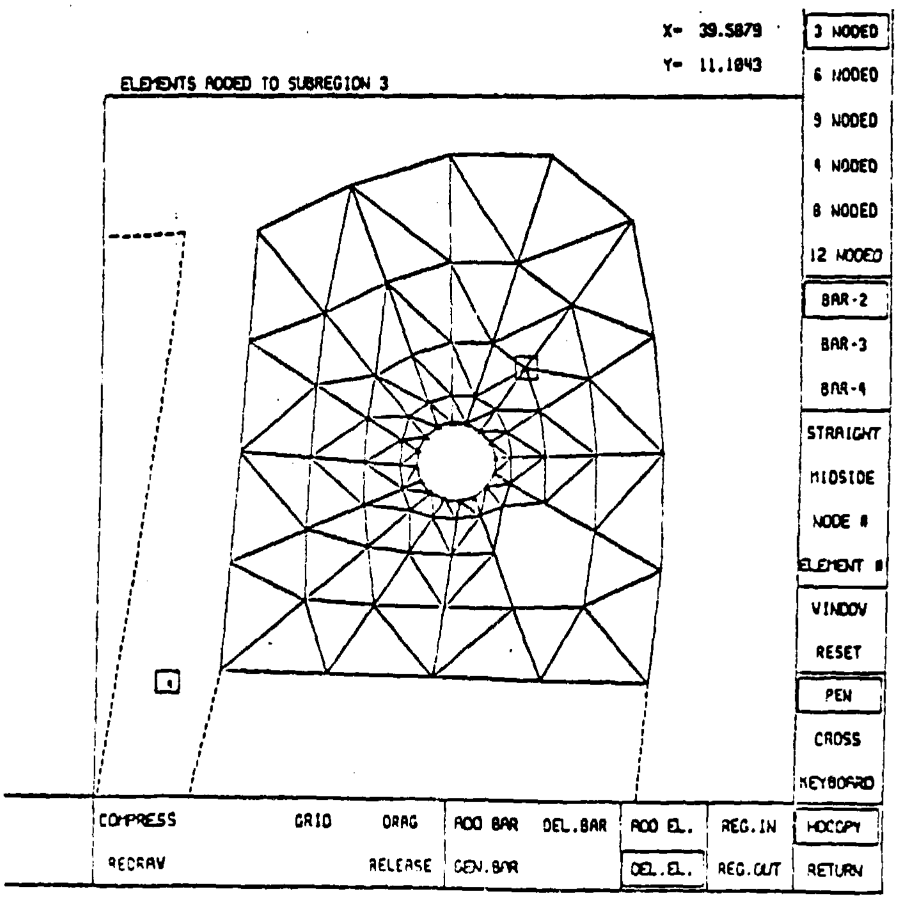

Figure 49. Deletion of Selected Elements

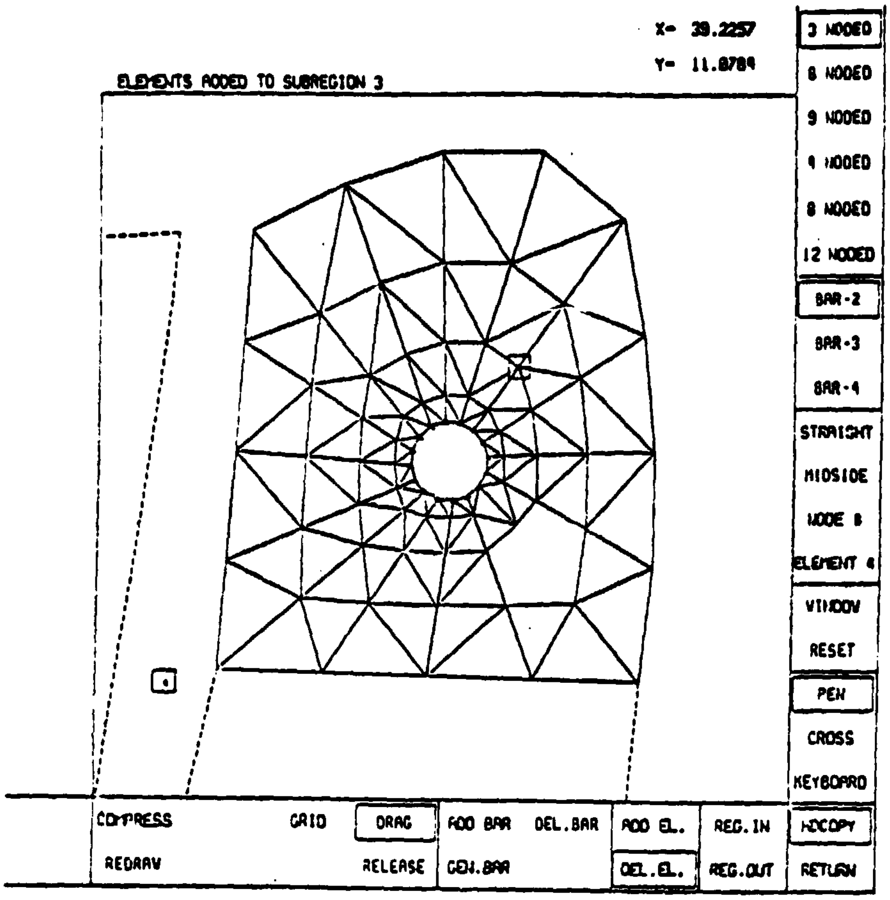

Figure 50. Dragging a Node Point

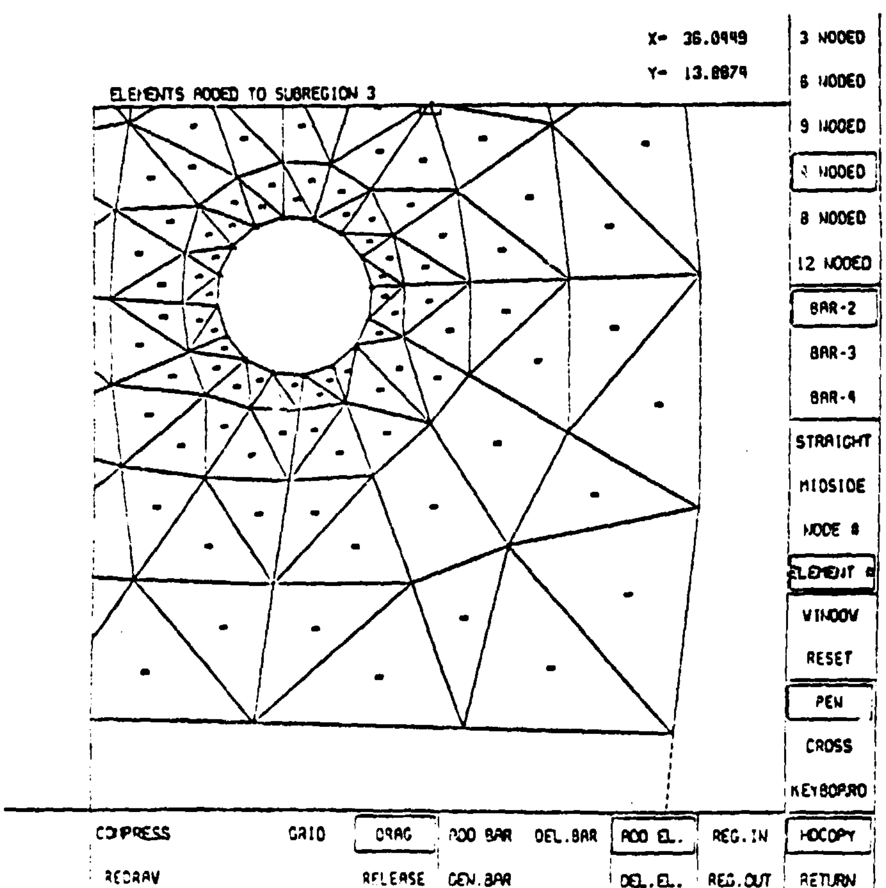

Figure 51. Adding Quadrilateral Elements in Area Where Triangular Elements were Deleted

speed storage required for the current problem is used. Therefore, small problems only require a small amount of high speed storage.

The second program runs on the PRIME 500 computers in RPI's interactive computer graphics laboratories. In the design of this program, it was assumed that the program would receive its information from an interactive preprocessor. It was also assumed that the program would be used for small to medium sized problems. Since I/0 times represent a major portion of total time for small problems, substantial improvements in efficiency can be made by making the I/0 more efficient. The steps taken to do this were;

1. to employ only binary I/0,
2. transfer as much information as possible in a single read or write and
3. to eliminate the use of scratch files as much as possible.

The resulting program has been found to be substantially faster than the canned programs available on the PRIME for small problems and somewhat faster for medium size problems (accurate statistics have yet to be worked out).

The next major portion of the finite element preprocessor to be written is a set of interactive attribute editors for specifying loads, material properties and boundary conditions. There is a need, however, to be able to use the currently available software before the attribute editors are written. Therefore, at this time, some relatively simple link programs have been written that will take the geometric information generated by the preprocessor, allow the user to specify boundary conditions, materials properties and loads and reformat the data as required to represent input for an analysis program. The preprocessor has been linked in this way to SAP4, SPAR and FEPROQ (our inhouse analysis program on the PRIME).

PART IV

INSURE (Innovative and Supporting Research)

Progress on composites research is reported in the individual write-ups on the succeeding pages in the following areas:

- Advanced Structural Analysis Methods for Composites
- Ultrasonic Non-Destructuve Testing of Composite Structures
- Optimum Combination of Hardeners in the Cure of Epoxy
- Fatigue in Composite Materials
- Resin Matrix Characterization and Properties
- Postbuckling Analysis of Curved Laminated Composite Panels
- Acoustic Emission Testing of Composite Tensile Specimens

ADVANCED STRUCTURAL ANALYSIS METHODS FOR COMPOSITES

Senior Investigator: E. J. Brunelle

Three areas of research were selected for investigation during this reporting period and are in various states of completion.

The first area demonstrates the existence of a functional dependence $n^p f\left(\frac{a_o n}{b_o m}\right)$, where p is a plus or minus integer, which is of central importance to many composite plate problems for buckling, vibration and deflection analysis. This previously unnoticed functional dependence allows general trends in solution behavior to be clearly seen with an attendent decrease in needed computer time in contrast to the usual "straightforward" analysis by various authors. This functional dependence has been verified for the cases of specially orthotropic laminates (and hence the specially orthotropic plate), antisymmetric cross-ply laminates and antisymmetric angle-ply laminates in problems of buckling, vibration and deflection (most of which had been previously investigated in the "straightforward" fashion). The simpliest way to reveal this dependence is by presenting results for the simply-supported specially orthotropic plate with uniaxial compression; biaxial loading makes the results too cumbersome for pedogogical clarity. The governing equation

$$D_{11}\frac{\partial^4 w}{\partial x^4} + 2(D_{12} + 2D_{66})\frac{\partial^4 w}{\partial x^2 \partial y^2} + D_{22}\frac{\partial^4 w}{\partial y^4} + P\frac{\partial^2 w}{\partial x^2} + \rho h\ddot{w} = q(x,y,)$$

is affinely transformed to yield

$$\frac{\partial^4 w}{\partial x_o^4} + 2D^* \frac{\partial^4 w}{\partial x_o^2 \partial y_o^2} + \frac{\partial^4 w}{\partial y_o^4} + \frac{P}{\sqrt{D_{11}}} \frac{\partial^2 w}{\partial x_o^2} + \rho h \ddot{w} = q(x_o, y_o)$$

where $D^* = \dfrac{D_{12} + 2D_{66}}{(D_{11}D_{22})^{\frac{1}{2}}}$.

We now examine the results for (i) buckling, (ii) vibration and (iii) static deflection.

<u>(i) Buckling</u>: Defining the buckling coefficient as

$k_0 = \dfrac{P}{(D_{11}D_{22})^{\frac{1}{2}}}\left(\dfrac{b}{\pi}\right)^2$ we find, $k_o - 2D^* = \left(\dfrac{a_o}{mb_o}\right)^2 + \left(\dfrac{mb_o}{a_o}\right)^2$.

This yields the simplest (and actually degenerate) functional dependence $f_1\left(\dfrac{a_o}{mb_o}\right)$ which is the same as for classical plate theory.

<u>(ii) Vibration</u>: Defining a non-dimensional frequency by the relation $\Omega_{mn}^2 = \rho h\left(\dfrac{b_o}{\pi}\right)^4 \omega_{mn}^2$ we see a more interesting and extremely useful functional dependence $n^2 f_2\left(\dfrac{a_o n}{b_o m}\right)$ appearing in the solution for Ω_{mn}, which is:

$$\frac{\Omega_{mn}}{n^2} = \left[\left(\frac{b_o m}{a_o n}\right)^4 + 2D^*\left(\frac{b_o m}{a_o n}\right)^2 + 1\right]^{\frac{1}{2}} .$$

It is noted that Ω_{mn}/n^2 may be plotted versus $\dfrac{a_o n}{b_o m}$ as a one-parameter family of curves in D^* (and that all curves are asymtotic to unity). In other words the <u>entire</u> classical frequency spectrum for <u>any</u> specially orthotropic material and <u>any</u> a/b ratio is presented on a single graph.

<u>(iii) Static Deflection</u>: Expressing w and q in terms of x_o, y_o space double-Fourier sine expansions,

$$w(x_o,y_o) = \sum_{m=1}^{\infty} \sum_{n=1}^{\infty} a_{mn} \sin\frac{m\pi x_o}{a_o} \sin\frac{n\pi y_o}{b_o}$$

$$q(x_o,y_o) = \sum_{m=1}^{\infty} \sum_{n=1}^{\infty} q_{mn} \sin\frac{m\pi x_o}{a_o} \sin\frac{n\pi y_o}{b_o}$$

we find the functional dependence $\frac{1}{n^4} f_3\left(\frac{a_o n}{b_o m}\right)$ between the Fourier coefficients as follows:

$$\frac{a_{mn}}{q_{mn}} \frac{n^4}{\left(\frac{b_o}{\pi}\right)^4} = \frac{1}{\left(\frac{mb_o}{na_o}\right)^4 + 2D^*\left(\frac{mb_o}{na_o}\right)^2 + 1} .$$

This allows deflections at any point x_o, y_o due to a given $q\,(x_o, y_o)$ pressure distribution (a commonly calculated deflection is the maximum deflection) to be plotted versus a_o/b_o as a one-parameter family of curves in D^*. Furthermore, if discrete loadings $q = q_{mn} \sin\frac{m\pi x_o}{a_o} \sin\frac{n\pi y_o}{b_o}$ are utilized (as they are in much of the literature), then the maximum deflection (say) can be plotted versus $\frac{a_o n}{b_o m}$ as a one-parameter family of curves in D^*. Both of these procedures yield much more information than the usual analysis techniques.

The second area, which is the core of a nearly completed doctoral thesis supervised by this investigator, provides uniaxial buckling coefficients k_o for any specially orthotropic rectangular plate which is simply-supported on the loaded edges and has arbitrary (specified) combinations of boundary conditions on the unloaded edges. The end product of this investigation is a collection of master plots for buckling coefficients k_o versus a_o/b_o as a one-parameter family in D^*. When one (or both) of the unloaded edges is a free edge (i.e., a natural boundary condition as opposed to a geometrical boundary condition), then a representative Poisson-like parameter ε = .2 and .3 has been used. It is to be emphasized that (i) these solutions are valid for any combination of elastic constants and that (ii) they provide upper k_o bounds for corresponding composite plates. The reader is reminded that this investigation, and any others similar to it (such as general vibration and static deflection studies of such plates), could not have been carried out with such sweeping generality without the introduction of the affine transformation concept into the initial problem formulation.

The third area started as an intended brief overview of the affine transformation technique as applied to "anything orthotropic". Obvious examples would be temperature and moisture diffusion problems in orthotropic materials (governed by second order partial differential equations) and orthotropic elasticity problems where a stress function can be introduced (most stress function problems are governed by fourth order partial differential equations). A simple but very important problem of this type is the diffusion of a concentrated load into an orthotropic sheet (plate, strip, stringer, etc.). It is recalled that the stress function approach in isotropic elasticity is used not only for plane stress, plane strain and generalized plane strain but also for torsion, axisymmetric motion and for half-space problems. Thus, utilizing the affine transformation technique, any problem solved by the stress function method in isotropic elasticity can be solved for any specially orthotropic material. As one broad class of examples, we look at the plane stress problem of orthotropic elasticity expressed in terms of stress function ϕ. The rather cumbersome equation (as derived in the literature)

$$\frac{1}{E_2}\frac{\partial^4\phi}{\partial x^4} + \left(\frac{1}{G_{12}} - \frac{2\nu_{12}}{E_1}\right)\frac{\partial^4\phi}{\partial x^2\partial y^2} + \frac{1}{E_1}\frac{\partial^4\phi}{\partial y^4} = 0$$

is affinely transformed into

$$\frac{\partial^4\phi}{\partial x_o^4} + 2H^*\frac{\partial^4\phi}{\partial x_o^2\partial y_o^2} + \frac{\partial^4\phi}{\partial y_o^4} = 0$$

where $H^* = (E_1E_2)^{\frac{1}{2}}\left(\frac{1}{2G_{12}} - \frac{\nu_{12}}{E_1}\right)$ and varies from $H^* = 1$ (the isotropic case) to roughly $H^* = 6$ for materials of interest. This equation, with just H^* as a parameter, allows one to solve plane stress problems with simplicity and great generality that Lekhnitski (among many others) did not even attempt to solve. A typical statement in the literature regarding even this simple problem is "this class of problems has not been brought to the point of numerical results"; such statements reflect the fact that the original (untransformed) equation is extremely unwieldly to use in specific problem formulations and solutions. On the other hand, the transformed equation (with just H^* as a parameter) makes specific problem formulation and solution a quite simple and straightforward procedure. An educated guess is that, using the affine transformation techniques, Lekhnitski's classical text on the subject could be rewritten with one-tenth of the pagination besides presenting master curves that definitively solve, once and for all, a wide variety of useful problems.

ULTRASONIC NON-DESTRUCTIVE TESTING OF COMPOSITE STRUCTURES

Senior Investigators: H. F. Tiersten
P. Das

It was mentioned in the last semi-annual report that ultrasonic images of composite materials were obtained using a doubly focussed acoustic imaging system as shown in Figure 52. The image data was obtained using a Z-80 microprocessor controlled data acquisition system. The system triggered the transmitting transducer and sampled the received ultrasonic signal which had been transmitted through the composite material. The received signal was then stored on a floppy disk as an 8 bit number representing the received ultrasound intensity. This process was repeated as the composite sample was scanned under the microprocessor control. These images were displayed on a storage oscilloscope from which a black and white print can be obtained. However, the quality of the images was poor.

In the last six months, great improvement in the image quality has been obtained through use of i) a high resolution display monitor and ii) color-coding of the intensity data. To obtain high quality color-coded images, the raw stored data is transferred to the Image Processing Laboratory which has a DEANZA image processor with a PRIME host computer as shown in the block diagram of Figure 53. The transferred data is stored in the PRIME file system. For display or processing, the data is transferred to the image refresh

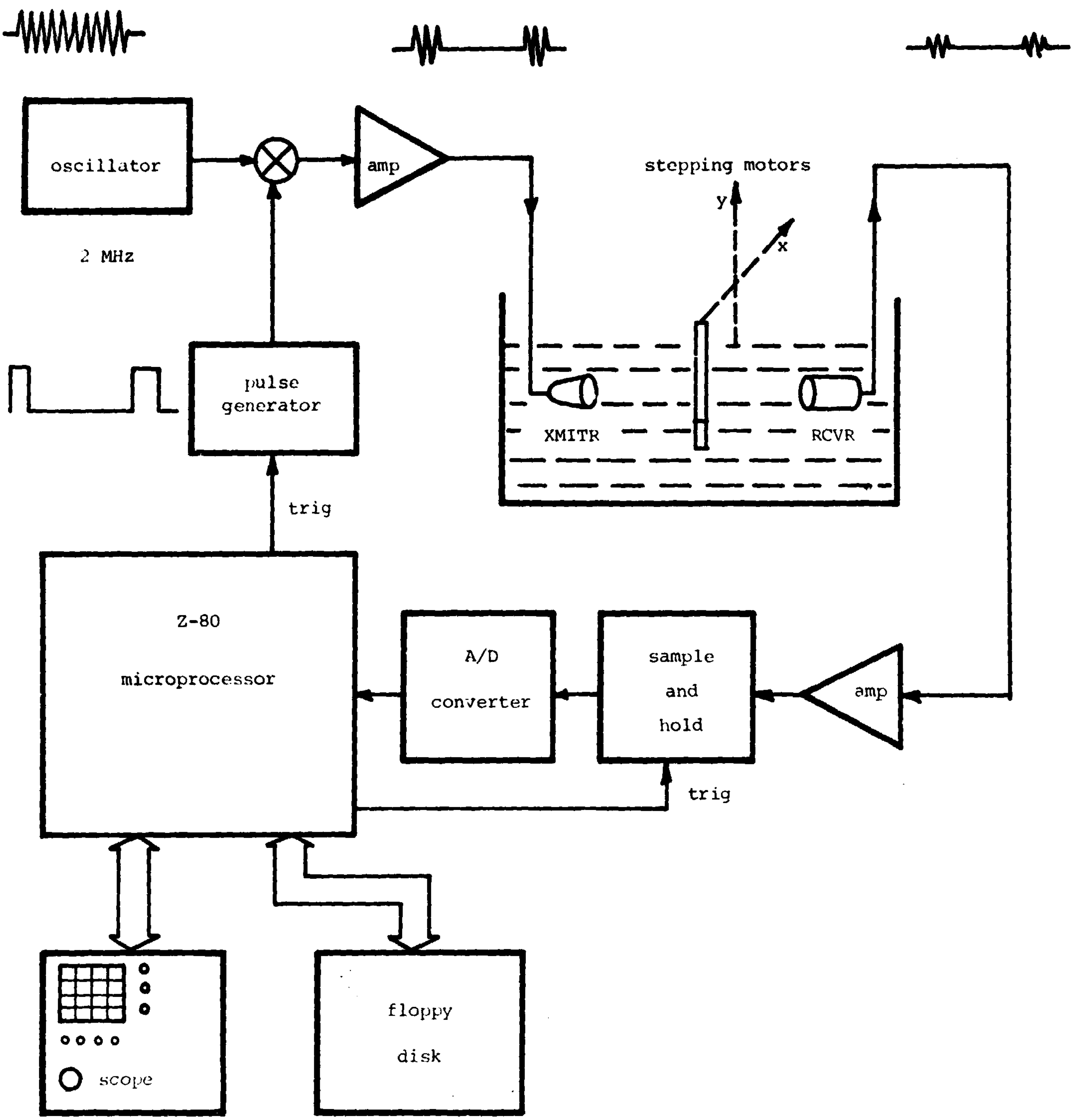

Figure 52. Block Diagram of Data Acquisition System for Ultrasonic Imaging of Composite Materials

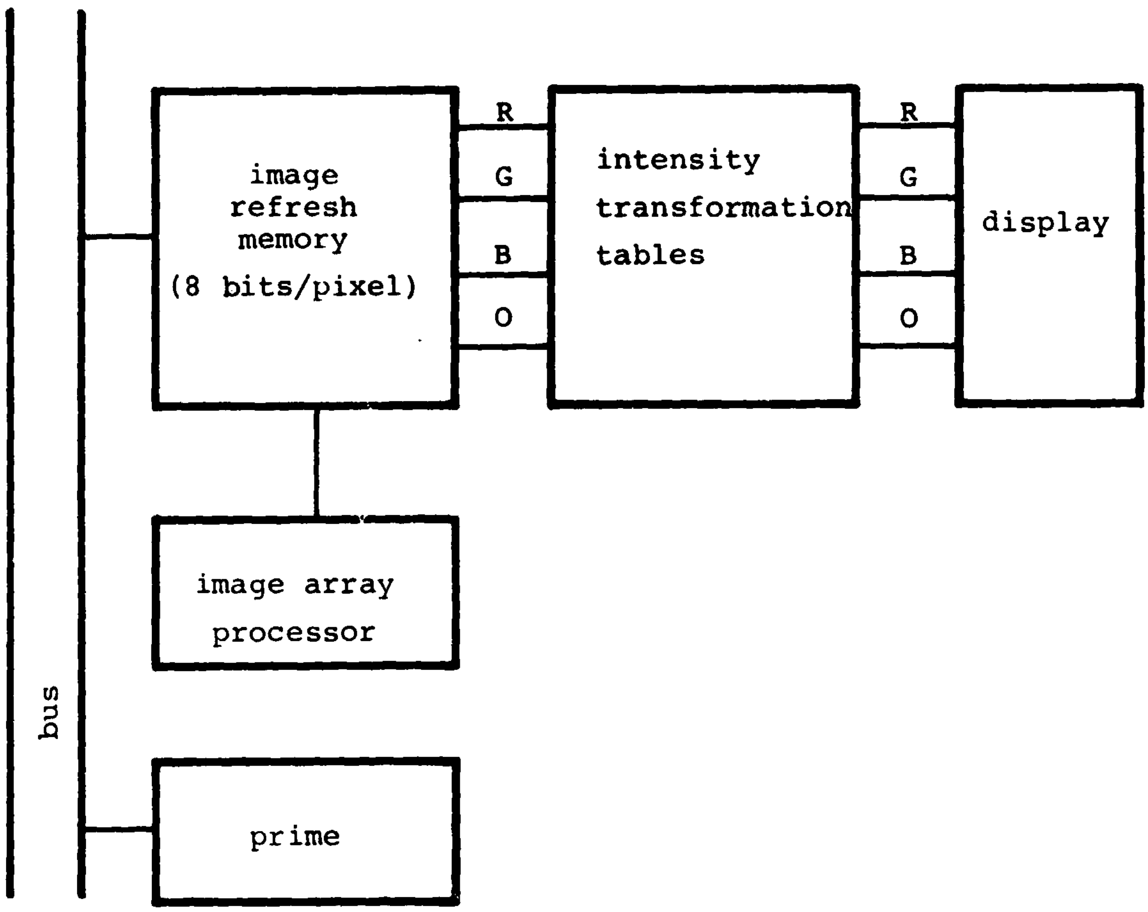

Figure 53. Block Diagram of the DEANZA PRIME Image Processor

memory. The color coding of the data can be achieved through a programmable intensity transformation table. The image is displayed in color on a high resolution monitor with zoom and scroll capability. Some idea of the improvements achieved is given by comparisons among Figures 54 through 59. Figures 54 and 55 are the early pictures which are described in the second of two papers referenced at the end of this section. Figures 56 and 57 are the same pictures using a better black and white monitor. Figures 58 and 59 are the same pictures using color coding and a color monitor.

A second aspect of this project concerns the improvement of trapped energy mode mosaic ultrasonic transducers. Both experimental and theoretical progress has been made in this area. These results have been elaborated in the following two papers:

1. "Increased Bandwidths and Mode-shapes of the Thickness-Extensional Trapped Energy Mode Transducer Array", 1979 Ultrasonic Symposium Proceedings, IEEE Publication No. 79 CH 1482-9, pp. 148-152, 1979.

2. "Ultrasonic Imaging Using Trapped Energy Mode Fresnel Lens Tranducers", Acoustical Imaging, Vol. 9, Plenum Press, to be published. This paper was presented in the Ninth International Symposium on Acoustical Imaging, Houston, Dec. 3-6, 1977.

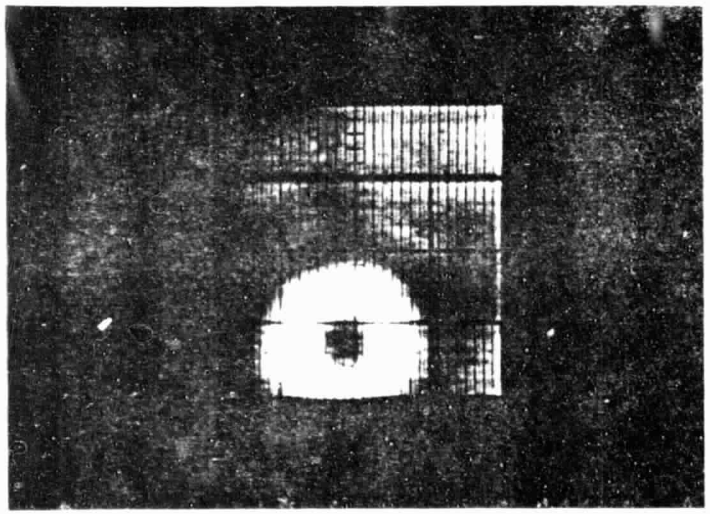

Black and White Ultrasonic
Image of Delamination Around
a Hole (Specimen #1)

Figure 54

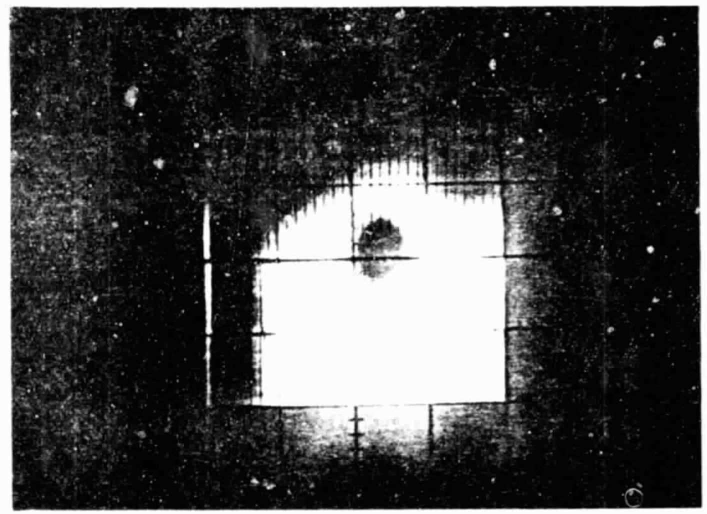

Black and White Ultrasonic
Image of Delamination Around
a Hole (Specimen #2)

Figure 55

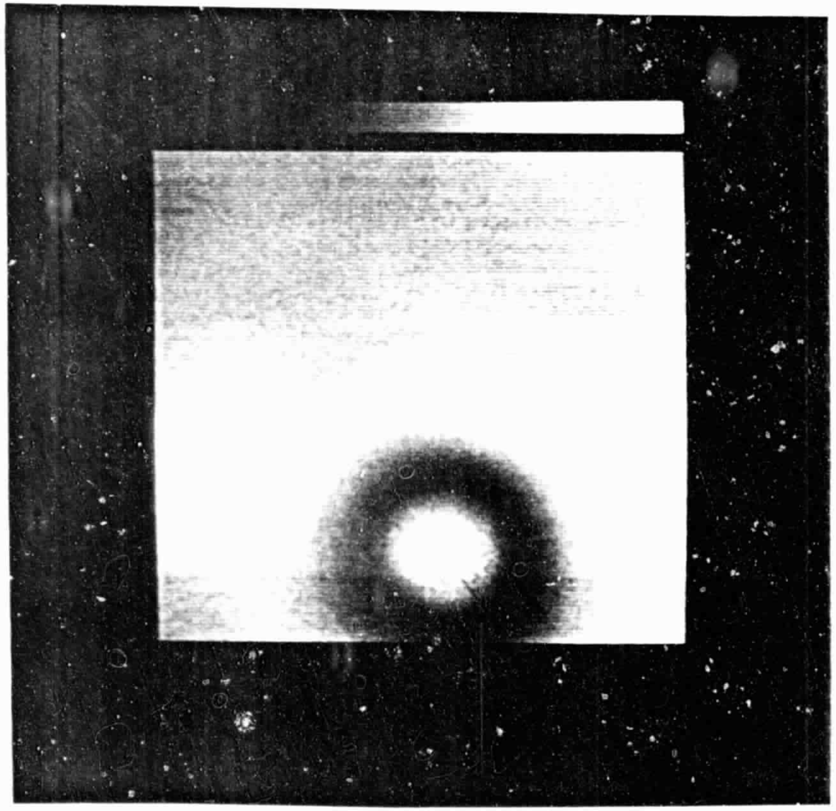

Monotone Ultrasonic Images of Delaminations Around a Hole from Monitor with Improved Definition (Specimen #1)

Figure 56

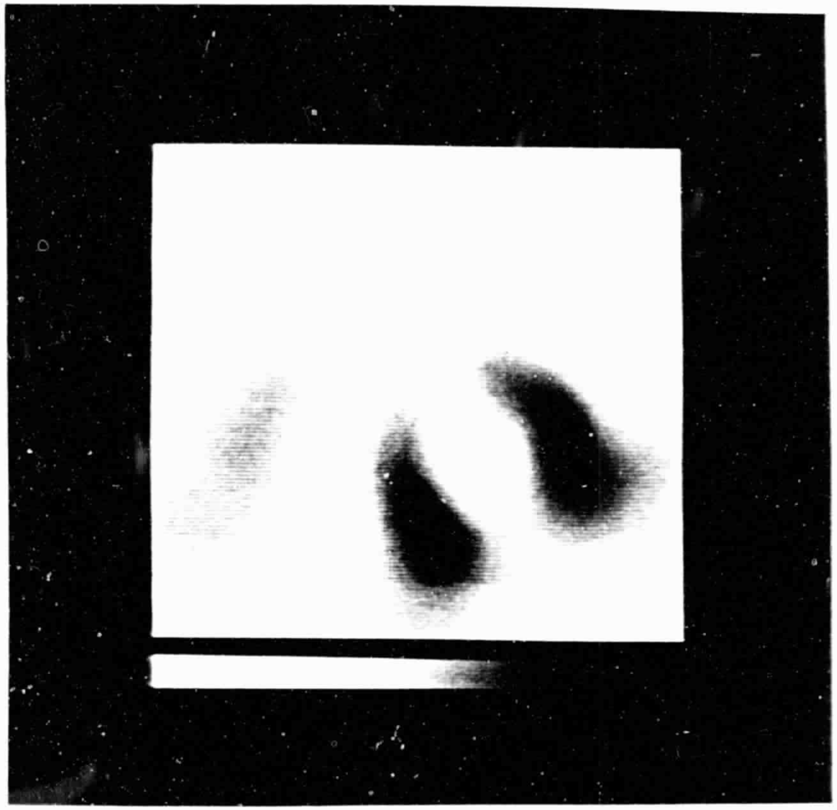

Monotone Ultrasonic Images of Delaminations Around a Hole from Monitor with Improved Definition (Specimen #2)

Figure 57

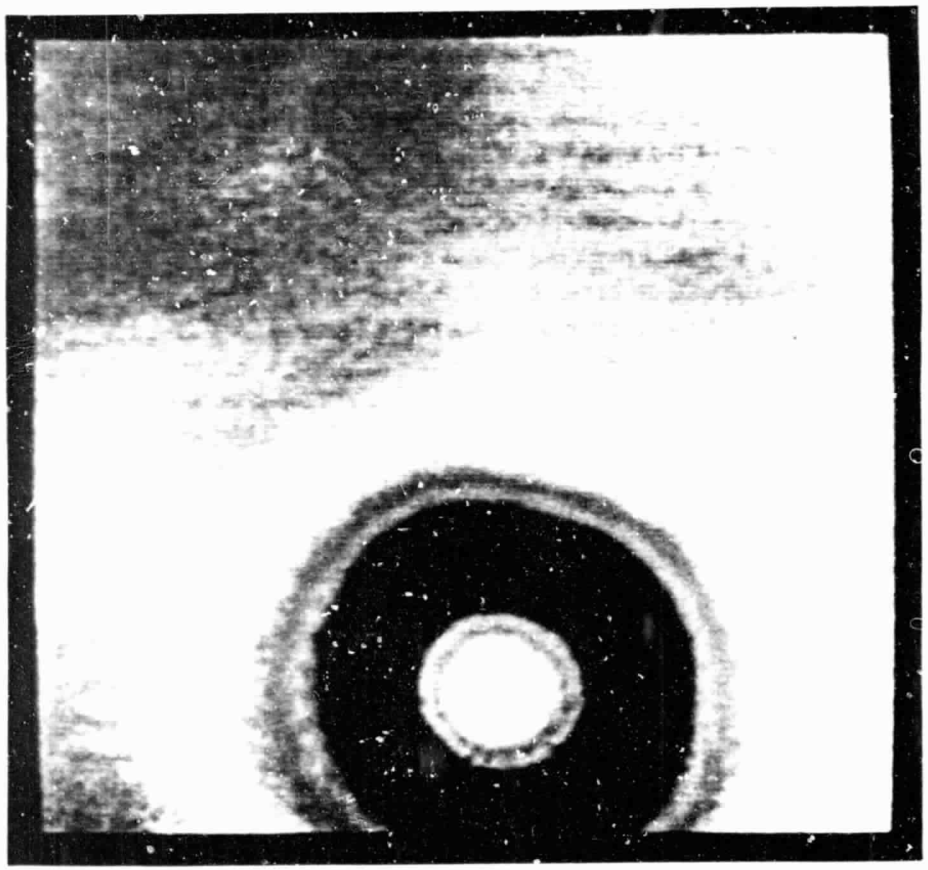

Color Photograph of Enhanced Ultrasonic Images of Delaminations Around a Hole (Specimen # 1)

Figure 58

Color Photograph of Enhanced Ultrasonic Images of Delaminations Around a Hole (Specimen # 2)

Figure 59

OPTIMUM COMBINATION OF HARDENERS IN THE CURE OF EPOXY

Senior Investigator: R. J. Diefendorf

There is a need for a room-temperature cure, epoxy hardener system since quite often, in wet lay ups, size and/or nature of material combination may not permit a heat cure. The resin system should not only have low viscosity for easy spreading, sufficiently long pot life and low but sufficient exotherm temperature for good cure, it should also have adequate cured properties to meet the requirements of its intended use.

Plain Bisphenol A base epoxies, such as Epon 828 and Aradite 6010 cured with polyamines like DTA or TETA, do not meet the above requirements because they are limited by their relatively short pot life and high exotherm temperature.

For structural work at RPI, Aradite 509 resin and hardener XU-224 [Ciba Geigy] (Table XI) appear to be excellent candidates for room temperature applications, because of their relative low viscosities and desirable exotherm temperature.

Since XU-224 is compatible with rapid curing aliphatic polyamines like XU-225, combinations of XU-224 and XU-225 can be used to obtain pot lives between the two extremes. The manufacturer's data for various combinations of XU-224 and XU-225 curing agents with 509 resin are shown in Table XII.

TABLE XI
TYPICAL RESIN AND HARDENER PROPERTIES*

	A-509	XU-224	XU-225
Viscosity at 25°C CPS	500 - 700	50 - 100	-----
Active Hydrogen Equivalent AHE	-----	70 - 75	143
Equivalent Epoxide/ 100g WPE	189 - 200	-----	-----
Pot Life	42 phr - 3.5 hr.	-----	76 phr < 20 min.

TABLE XII
EFFECT OF ADDING XU-225 ON GEL AND POT LIFE*

Composition Number	509 (pbw)	XU-224 (pbw)	XU-225 (pbw)	Pot (hr)	Gel (hr)
1	100	27	30	.5	.75
2	100	29	23	1.0	1.25
3	100	34	15	1.5	2.5
4	100	34	9	2.5	3.5
5	100	42	0	3.5	6.0

* Supplied in Ciba Geigy brochure.

Batches with the same ingredient quantities as in Table XII were made up, and it was observed that very poor cure resulted from all the mixtures. After three weeks, all the batches were still soft and pliable. The difficulty was that the composition of the corresponding batches of ingredients were not listed. Each batch would be expected to result in slightly different cured properties. The objective of this study was to evaluate the variation in the supplier's specification and to determine the optimum blend that will give good cured properties for the CAPGLIDE project.

For computing mixing ratios, our basic assumption was that hardeners XU-224 and XU-225 are miscible in all proportions.

Avg. Active Hydrogen Equivalent XU-224 = 72.5
Avg. Equivalent Epoxide Weight A-509 = 194.5

For XU-224: $\frac{72.5}{194.5} \times 100 = 37.2$ phr* A-509.

Similarly, for XU-225: $\frac{143}{194.5} \times 100 = 73.5$ phr* A-509.

There is uncertainty over the actual epoxy content of A-509, since the actual content of epoxy may differ significantly from the value supplied in the literature. Accordingly, 25 gm samples of A-509 were cured with XU-225 (phr varied from 30 to 50 phr at intervals of 2) to determine the combination that results in the best cure hardness.

After four days, XU-224 cured A-509 with 42 phr, produced the best cure and highest cured hardness. This

---

* phr: parts per 100 parts of resin.

suggested that either the active hydrogen equivalent (AHE) of XU-224 was actually lower than the literature value or that the average epoxy content was over estimated. Correspondingly, XJ-225 required 80.0 phr for optimum cure.

Using the new values for equivalents, a series of specimens were prepared as described in Table XIII and listed below.

1) The required weights of A-509, XU-224 and XU-225 were measured.
2) The mixture was hand mixed until liquid became homogeneous.
3) The mixture was degassed for three minutes in a desiccator.
4) .3 gm of catalyst DMP-30 was added into each batch.
5) Catalyst was thoroughly blended into resin for at least five minutes.
6) Mixture was degassed.
7) About 25 gm of the blend was poured into a cup arrangement to measure exotherm temperature and time. The results are shown in Table XIV.
8) The rest of the resin was poured into a mold.

The samples were then prepared as follows:

9) After one week, the mold samples were cut using a water-cooled carbide blade.
10) Cut samples were milled to 2" diameter specimens, 1/4" to 3/8" thickness, for ASTM (D-732)-35 shear strength test.

TABLE XIII
BLEND RATIO FOR A-509 EPOXY RESIN WITH XU-224 AND XU-225 HARDENERS

Composition Number	X_2	XU-225	XU-224	XU-224/XU-225	A-509	DMP30 Catalyst
1	0.05	2	40.9	20.45	100	.3
2	0.1	4	39.9	9.98	100	.3
3	0.15	6	38.8	6.47	100	.3
4	0.2	8	37.8	4.73	100	.3
5	0.25	10	36.7	3.67	100	.3

All weights in grams

TABLE XIV

PROPERTIES OF A-509 EPOXY RESIN CURED WITH VARIOUS RATIOS OF XU-224/XU-225

Samples	Composition phr A-509 XU-224/XU-225	Microhardness Knoop Hardness #	Shear Strength kpsi	Remarks
Batch 1	20.45	8.7	16.0	Two samples tested Range 908 psi - Fracture not brittle
Batch 2	9.98	8.0	17.2	Two samples tested Range 433 psi - Fracture not brittle
Batch 3	6.47	9.2	17.9	Two samples tested Range 431 psi - Fracture not brittle
Batch 4	4.73	6.8	16.0	Two samples tested Range 2 psi - Fracture not brittle
Batch 5	3.67	6.4	15.6	Three samples tested Range 746 psi - Fracture not brittle

11) After shear test, samples were cut through their diameter and polished.

12) Microhardness of sheared zone and unsheared region was measured.

The shear and microhardness test results are shown in Table XV.

A close analysis of the data supplied by Ciba Geigy, as shown in Table XII, suggests that except for Composition 5, either excess or insufficient hardeners have been used to cure Aradite 509 in the preliminary test samples. This may have caused our cure problems as the excess hardener or epoxy may have resulted in the plasticization of the cured product. Furthermore, comparison of the ratio of XU-224/ XU-225 used in the Ciba GEigy data with those in Figures 60 and 61, clearly shows that improved cures and properties could be obtained only close to the optimum value of 6.5 obtained in the RPI calorimetry experiment. Consequently, care should be taken to determine the equivalents for each received batch of resin and hardeners, and enough XU-225 added to achieve a sufficient exotherm to obtain a proper cure without seriously degrading pot life. It is also worthy of note, that addition of DMP-30 catalyst did help attain a higher extent of reaction, as measured by differential scanning calorimetry.

Measurement of shear strength and hardness shows that the XU-224 and XU-225 blend cured A-509 has properties which differ from those of A-509 cured with only XU-224, by as much as a factor of 1.30 higher.

TABLE XV

EXOTHERM BEHAVIOUR OF A-509 EPOXY RESIN CURED WITH VARIOUS RATIOS OF XU-224/XU-225 HARDENERS

Samples	Composition phr A-509 + .3g Cat. 064 Hardeners Ratio XU-224/XU-225	Time to Reach Exothermic Temperature	Exothermic Temperature	Dwell Time Exothermic Temperature
Batch 1* Mass = 26.8g Thickness = 0.725"	20.45	113.0 min.	46.0°C	28.5 min.
Batch 2 Mass = 27.0g Thickness = 0.722"	9.98	89.0 min.	88.0°C	4.3 min.
Batch 3 Mass = 28.6g Thickness = 0.774"	6.47	97.6 min.	95.8°C	3.5 min.
Batch 4 Mass = 25.6g Thickness = 0.7"	4.73	74.3 min.	95.0°C	3.5 min.
Batch 5 Mass = 26.3g Thickness = 0.738"	3.67	81.5 min.	88.0°C	3.4 min.

* Sample was observed not to gel even after dwell at exotherm.

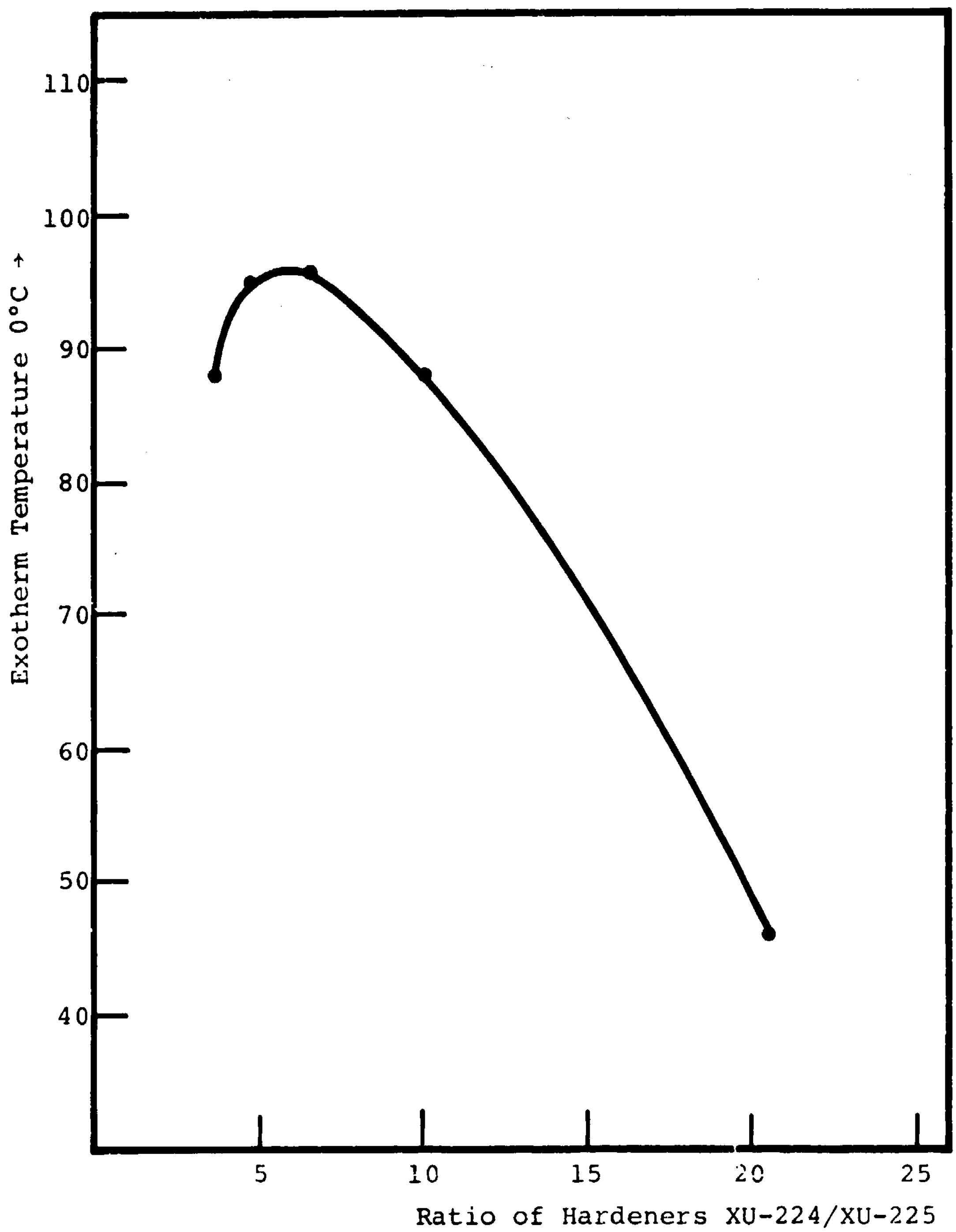

.gure 60. Dependence of Exotherm Temperature on Ratio of Hardeners XU-224/XU-225

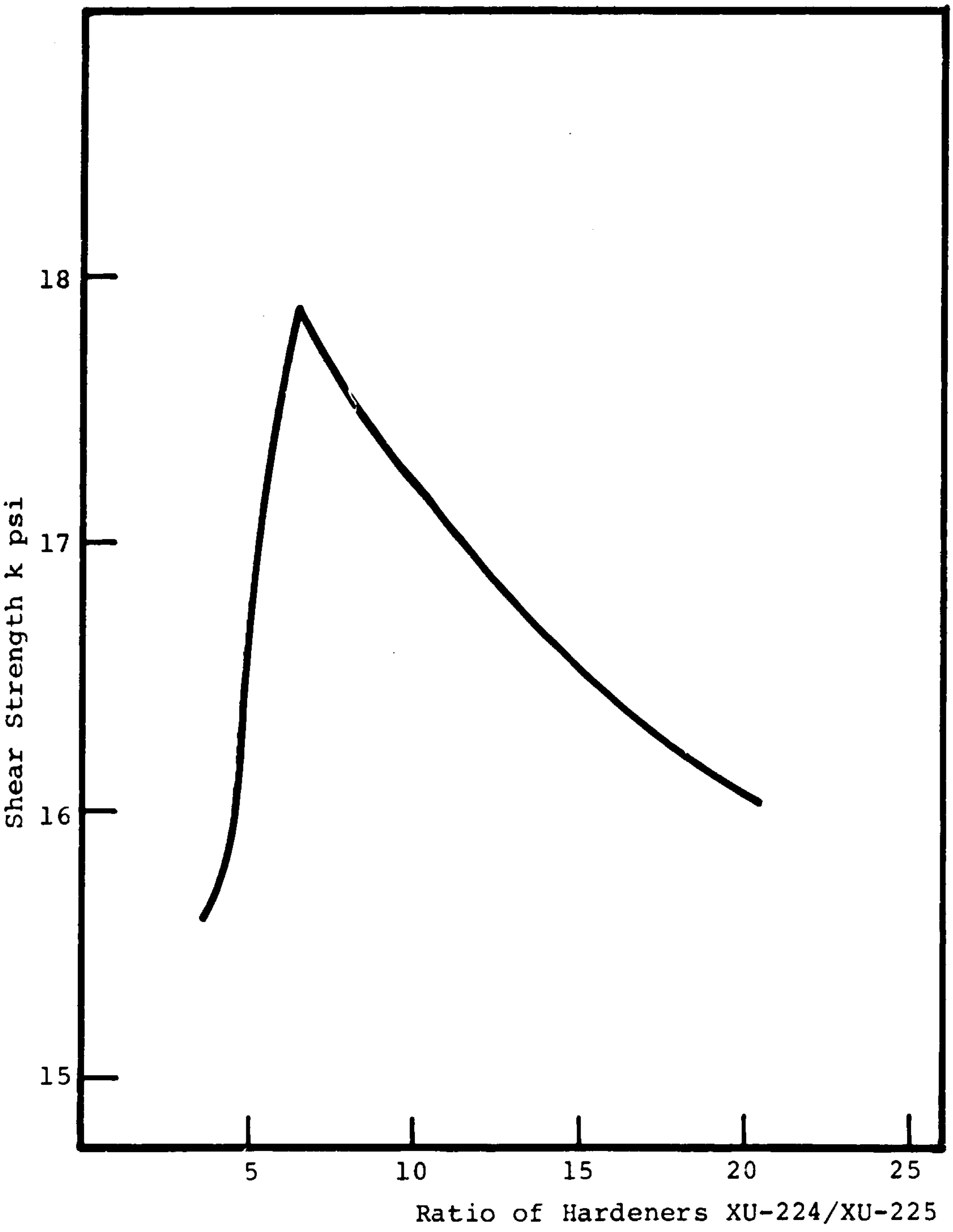

Figure 61. Change in Shear Strength of Aradite 509 Epoxy Cured With XU-224 and XU-225 Modified Aliphatic Amines

The study suggests that past problems with ambient temperature cures can be eliminated by quality control of the incoming resins and hardeners and by system optimization. Better pot lives, improved processibility and improved mechanical properties could be obtained thereby. In thin sections, because of low exotherms, use of a catalyst is recommended.

FATIGUE IN COMPOSITE MATERIALS

Senior Investigator: E. Krempl

Work continued on the biaxial fatigue test specimen and fixture, on the uniaxial fatigue testing of laminates and on a model for cumulative damage.

Machining of the fixture shown in Figure 32 of Reference 1* was completed, and eight specimens (Figure 31 of Reference 1) were manufactured using a wraparound technique. The straight section of the tube consists of four layers of $[\pm 45°]_s$ graphite-epoxy laminates.

Fixture and tube have been checked out and have performed fully satisfactorily under monotonic loading. Results are given in Table XVII which lists Young's Modulus E, Shear Modulus G and the ultimate strength in tension σ_{max}, as well as the ultimate shear strength τ_{max}. Since no data on tubes was available, results from two other investigations on plates are listed for qualitative purposes. No direct comparison of the data is intended.

The quantities E and G were determined from stress-strain plots and are consistent. The strain readings were obtained from a biaxial Instron clip-on extensometer attached to the uniform section of the specimen.

The fixture was tested with and without the auxiliary hydraulic pressure for gripping of the specimen. Initial

---

* All reference numbers in this section refer to Table XVI.

TABLE XVI
REFERENCES: FATIGUE

1. 37th Semi-Annual Report, "Composites Structural Materials", NASA/AFOSR, December 1979.

2. Yang, J. N. and D. L. Jones, "Statistical Fatigue of Graphite-Epoxy Angle-Ply Laminates in Shear", Journal of Composite Materials, 12, 1978, pp. 371-389.

3. Whitney, J. M., "Fatigue Characterization of Composite Materials," AFML-TR-79-4111, October 1979.

4. Ostergren, W. J. and E. Krempl, "A Uniaxial Damage Accumulation Law for Time-Varying Loading Including Creep-Fatigue Interaction", Trans. ASME, Journal of Pressure Vessel Technology, 101, 1979, pp. 118-124.

5. Advanced Composites Design Guide, Vol. 1, "Design", 3rd Edition, Structures Division, Air Force Flight Dynamics Laboratory, September 1976, Section 1.2.1.2.

6. Nguyen, N. Q. and J. L. Kardos, "Fatigue Failure of Composite Laminates", AFML-TR-79-4035, April 1979.

TABLE XVII
STATIC PROPERTIES COMPARISONS

	E (GPA)*	G (GPA)	σ_{max} (MPA)**	τ_{max} (MPA)
RPI Samples				
Gr/E thin-walled tube #2	11.8***	26.5***	---	132
Gr/E thin-walled tube #3	12.7***	27.6***	125	---
Gr/E thin-walled tube #4	12.7***	25.7***	---	169
Average	12.4	26.6	---	151
Samples From References				
Plates (45°)$_s$ Reference 5**** Intermed. strength	16.5	31.0	158	346
Plates (45°)$_s$ Reference 6**** High strength AS/3501-5A	16.1	----	183	---

* Geiga Pascal (GPA)

** Mega Pascal (MPA)

*** Determined from readings of biaxial extensometer attached to uniform section of specimen.

**** Reference number refers to Table XVI in this section.

leakage problems have been corrected.

Uniaxial fatigue tests were performed in the Instron servocontrolled testing machine using Type C, $\{0/(\pm 45)_2/90\}_s$, and Type D, $\{90/(\mp 45)_2/0\}_s$, 12-ply laminates for an R-ratio of .666. The frequency was varied between 1 Hz and 10 Hz. Figure 62 shows the results. The straight lines represent least square fits to the respective data points. The influence of layup sequence and frequency is less than the scatter of the data.

The modeling of damage accumulation in composites was studied, with specific reference to the residual strength degradation model (References 2 and 3) and others. It was found that the basic equations proposed in Reference 2 are very similar to the one proposed in Reference 4 and applied to high-temperature, low-cycle fatigue. Differences between References 2 and 3 and Reference 4 exist. In Reference 4, time is introduced as the fundamental variable (not cycles as in References 2 and 3) so the Reference 4 is applicable to arbitrary loading (constant amplitude loading <u>is</u> required for References 2 and 3). For periodic constant amplitude loading, the time-to-failure calculated in Reference 4 can be easily transformed to cycles-to-failure to obtain the usual representation. The basic formulation of Reference 4 includes rate-dependence but can be reduced to the rate-independent case considered in References 2 and 3. The approach in Reference 4 is deterministic and must be extended to include the statistical distribution of fatigue life.

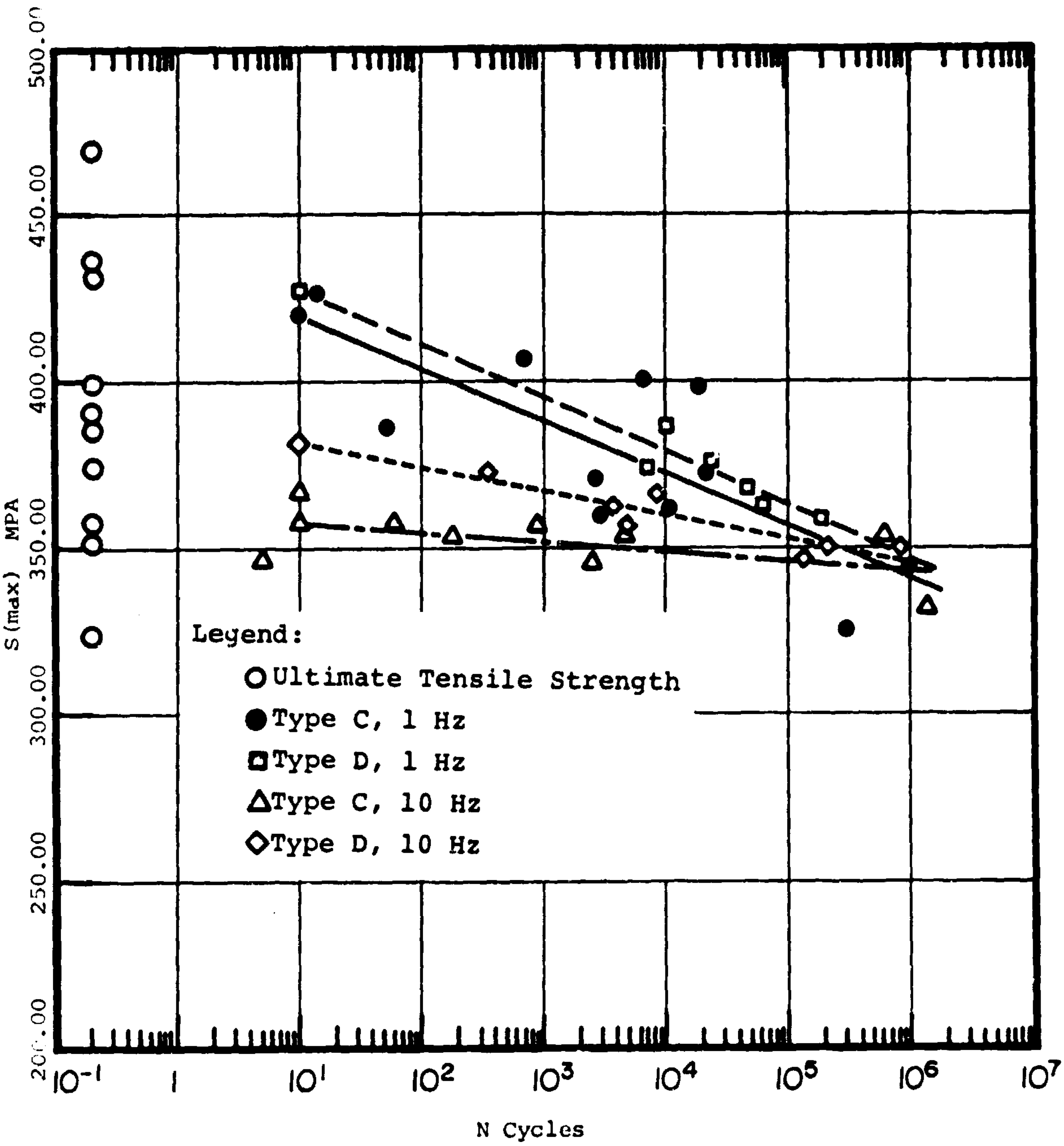

Figure 62. S-N Plots for Tension-Tension Fatigue of Graphite-Epoxy Laminates, (R Ratio = .667 at Room Temperature)

RESIN MATRIX CHARACTERIZATION AND PROPERTIES

Senior Investigator: S. S. Sternstein

Three areas of research are being pursued as indicated below:

1. Inhomogeneous Swelling and the Effects of Moisture

The inhomogeneous swelling theory, previously developed by Sternstein for application to filled elastomers, has been modified to cylindrical geometry for the analysis of water induced stresses in carbon-epoxy composites. A constitutive relation has been developed from literature data, in order to describe the thermodynamics of water interaction with epoxy resins. A key feature of this model is the incorporation of a two network system of crosslinks, one of which is chemical and permanent, and the other which is labile and a function of water content. The latter feature results in a strongly water dependent modulus of elasticity which plays a major role in the stresses, strains and water concentration gradients at the fiber-matrix interface.

Various temperature and relative humidity boundary conditions have been used to develop moisture, stress and strain profiles about a carbon fiber in an epoxy matrix. Swelling instability and predictions are currently under investigation. A finite element scheme is currently being formulated by Professor Shephard (Civil Engineering) in order to solve the many fiber boundary value problems both with and without external stresses.

2. Characterization of Epoxy Neat Resins

Neat resin samples have been conditioned at 70°C for one year to achieve equilibrium water content. These samples are now being tested using dynamic mechanical spectroscopy, creep and stress relaxation techniques in order to determine the effects of combined temperature and moisture effects on the viscoelastic properties and primarily the glass transition region.

In the course of the moisture conditioning, it was determined that organic compounds are leeching from the samples. Chromatography techniques are currently being used to attempt to identify the materials leeching out. It is of particular concern to us to determine whether or not prolonged moisture exposure at 70°C has resulted in hydrolytic degradation of the epoxy resin.

3. Interlaminar Failure of Composites

Interlaminar failure is primarily governed by the epoxy resin and can be caused by planar impact or out-of-plane loads or moments. We are attempting to develop a biaxial out-of-plane test to investigate various stacking sequences. The results may be useful also for assessing the susceptibility of various stacking sequences to impact damage. However, our primary goal is to determine the interlaminar failure tolerance of the epoxy layers between adjacent plies.

In this regard, we are currently examining the nonlinear plate theories developed by Whitney and by Christensen.

These theories should enable us to better calculate the shear and normal stresses acting on the epoxy layers between plies.

POSTBUCKLING ANALYSIS OF CURVED LAMINATED COMPOSITE PANELS

Senior Investigators: N. J. Kudva
T. A. Weisshaar*

The present study is concerned with the buckling and postbuckling analysis of curved panels made of laminated composite materials and subjected to axial compression. Attention is restricted to geometrically perfect, midplane symmetric, cylindrical panels of constant curvature.

A finite element procedure is used for the analysis. The finite element used is a singly curved, four node element with 12 degrees of freedom at each node. The degrees of freedom at each node are - the displacements U,V,W in the X, Y and Z directions respectively and the derivatives $U_{,x}$; $V_{,x}$; $W_{,x}$; $U_{,y}$; $V_{,y}$; $W_{,y}$; $U_{,xy}$; $V_{,xy}$ and $W_{,xy}$ - the X coordinate is the axial coordinate, and the Y coordinate is along the circumference. Bicubic Hermite polynomials are used for interpolation within an element. Linear elastic material behavior is assumed and Donnell's form of the strain-displacement relations is considered. Since the present investigation is confined to shallow panels -representing less than a quarter part of a complete cylinder - these strain-displacement relations are adequate.

In contrast to most previous investigations in the field, nonlinear prebuckling deformations and exact boundary

---

* This is a continuation of the work begun by N. J. Kudva with T. A. Weisshaar while at VPI.

conditions are taken into account. In the prebuckling range, the full nonlinear equations of equilibrium are solved to determine the equilibrium points. The equilibrium equations are solved using a generalized Newton-Raphson technique. The buckling load of a perfect panel, corresponding to the lowest bifurcation point of the equilibrium equations, is characterized by a singular tangent stiffness matrix. This is determined by linearizing the equilibrium equations about an equilibrium point close to the bifurcation point.

The postbuckling path is determined using the amplitude of the buckling mode as an independent parameter. The Newton-Raphson technique is also used to determine equilibrium points on the postbuckling path. However, to ensure that the solution proceeds along the required secondary path, the orthogonality condition given below is imposed.

$$q = \varepsilon Y + W \quad ; \quad Y^T W = 0$$

where q is the displacement vector consisting of all the degrees of freedom,

ε is the amplitude of the buckling mode,

Y is the buckling mode vector,

superscript T indicates the transpose of the matrix

and W is a vector determined from the above equations.

The loading is imposed by uniform edge displacement along the curved edges. Results were obtained for a few typical graphite-epoxy curved panels with a $[90°|\theta°|-\theta°|0°]_s$ layup. The panels have aspect ratio equal to unity, length to radius ratio of 0.2 and clamped boundary conditions on all sides with no tangential displacements permitted. The fiber orientation angle, θ, was varied from 0° to 90° and was found to have a significant effect on the buckling load, buckling mode shape and postbuckling behavior. The coupling terms D_{16}, D_{26} caused nonlinear prebuckling deformations. In the postbuckling region, the analysis was carried far enough to determine a local minimum, if any, on the secondary path. For the panels considered, $\theta = 45°$ gave the highest buckling load as well as the largest drop in the equilibrium load level in the postbuckling region. The results obtained in this analysis have not been found in the established or the current literature.

ACOUSTIC EMISSION TESTING OF COMPOSITE TENSILE SPECIMENS

Senior Investigators: H. Otsuka
H. A. Scarton

The objective of this research was to apply the acoustic emission technique to monitor the crackling sounds emitted from fracturing composite materials. Specimens were designed to accomodate two acoustic emission transducers. The materials used were ±45° and 0-90° carbon-cloth-ply-epoxy composites. Figure 63 shows typical test specimens. Figure 64 shows the acoustic emission results obtained with a critically active (see Reference 1, Table XVIII) 0-90° specimen. Here the term "count" implies a single acoustic emission signal whose amplitude is above some previously set threshhold. The "time" used on the abcissa scale corresponds to load, since the testing machine has been set in these tests at a steadily increasing load (i.e., fixed load application rate).

The sharply increasing slope with increasing load noted on this curve, is typical of what occurs just prior to failure. The repetitiveness of this sequence of events verifies the usefulness of the acoustic emission tool in providing a reliable precursor to actual failure. Characteristic acoustic emission amplitude distributions obtained from ±45° and 0-90° carbon-cloth-ply-epoxy specimens under a monotonically increasing tension load are shown in Figure 65. Previous work (Reference 2, Table XVIII), as well as *in situ* observation, allows us to speculate that the lowest

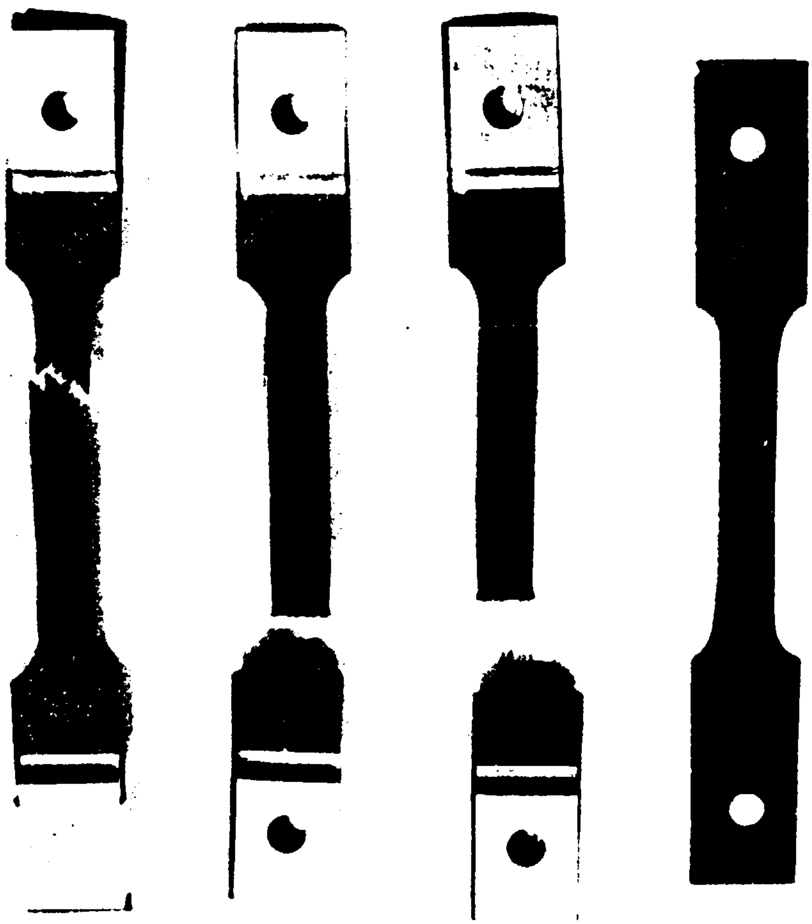

Figure 63. Sample carbon cloth-ply-epoxy composites test specimens: (a) ± 45° specimen after failure, (b) and (c) 0-90° specimens after failure, (d) 0-90° specimen ready for application of the reinforcing mounting end tabs.

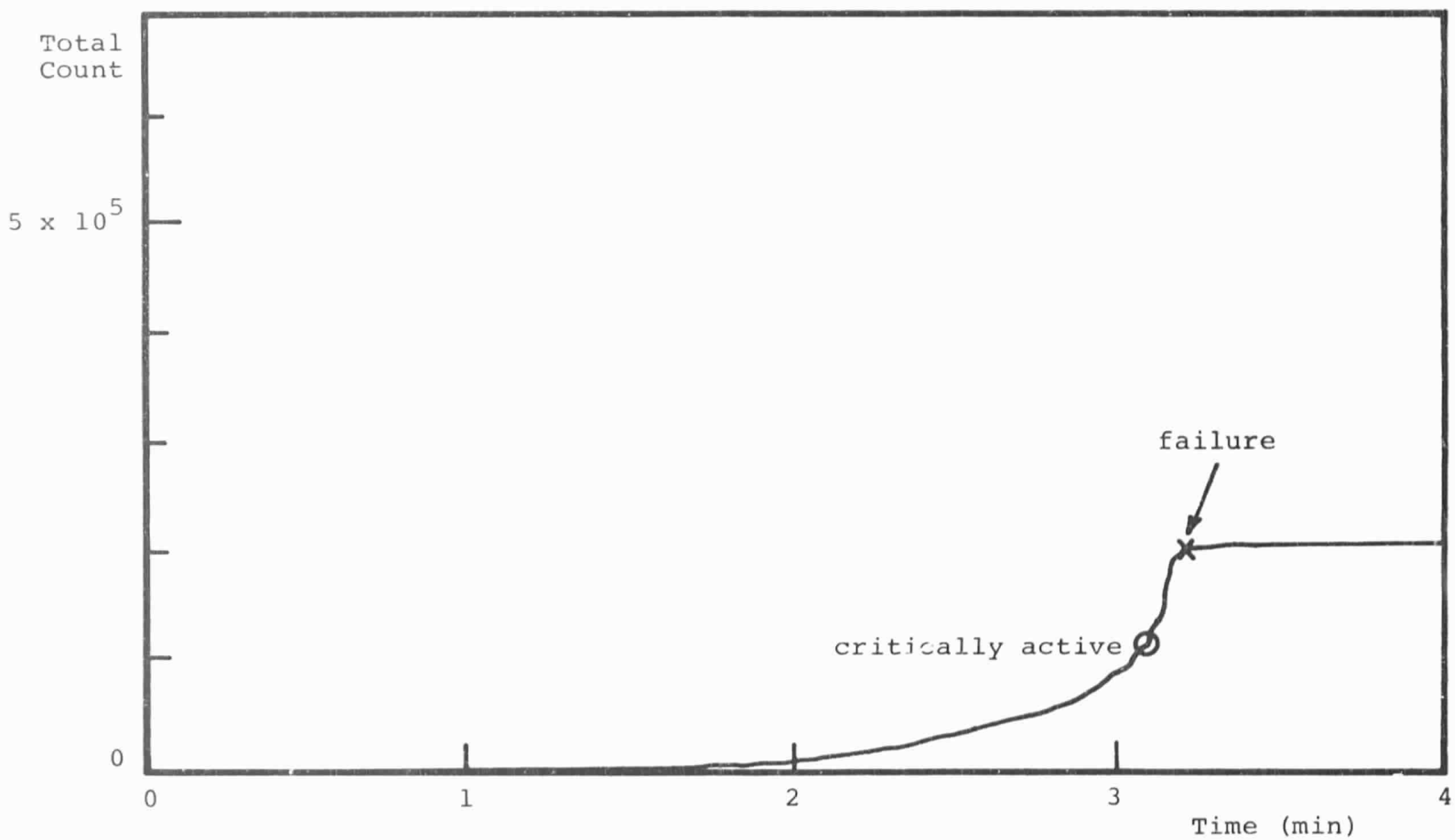

Figure 64. Total Counts Versus Time (Load) for 0-90° Specimen

TABLE XVIII
REFERENCES: ACOUSTIC EMISSIONS

1. ASTM "Standard Recommended Practice for Acoustic Emission Monitoring of Structures During Controlled Stimulation", E 569-76, September 1976, pp. 617-620.

2. Otsuka, H. and H. A. Scarton, "Variations in Acoustic Emission between Graphite- and Glass-Epoxy Composites", Journal of Composite Materials, submitted for publication July 1980.

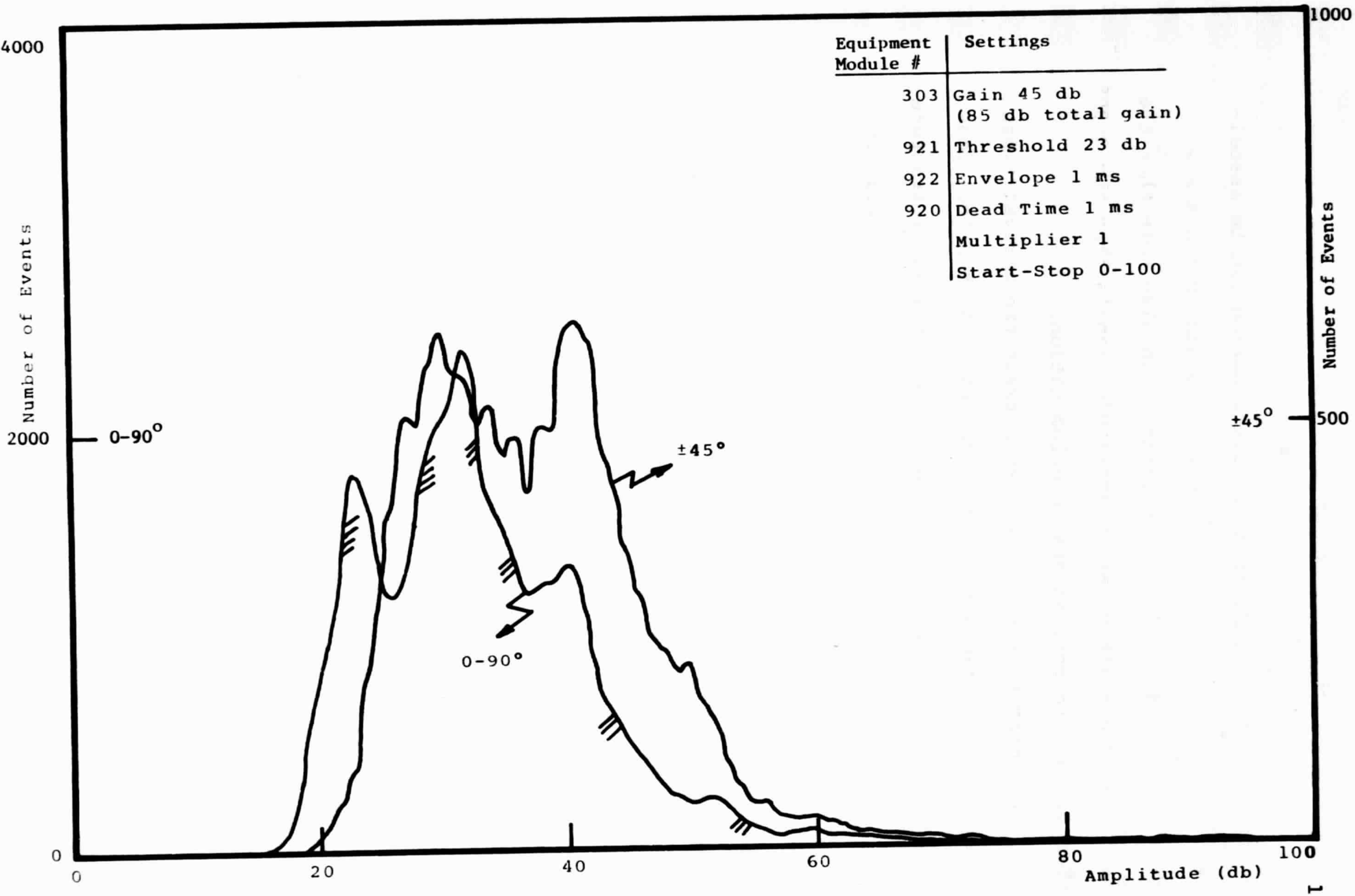

Figure 65. Amplitude Distributions of Acoustic Emissions from ±45° and 0-90° Specimens.

amplitude peak of this trimodal distribution can be associated with matrix crazing, while the two higher peaks are from delamination and fiber breakage. We also note that the ±45° specimen emitted larger amplitude signals than the 0-90° specimen due to more extensive delamination.

By comparing the differences between the arrival times of signals from two separated AE transducers, the locations of the sources of the signals and, hence, the local fracture sites can also be recorded. A plot of the source location versus number of acoustic emission events for ±45° material at failure is shown in Figure 66. The distribution of locations of observed local fracture (and failure) sites coincides with the AE source locations. Continuing work is now being done to further investigate the implications of the acoustic emission signal statistics to the fracture of composite materials. It is our hope that these highly localized data will increase our understanding of the manner in which composite materials fail. This knowledge will improve our abilities to design new composite materials and discover incipient failure in existing composite structures or large scale specimens under test.

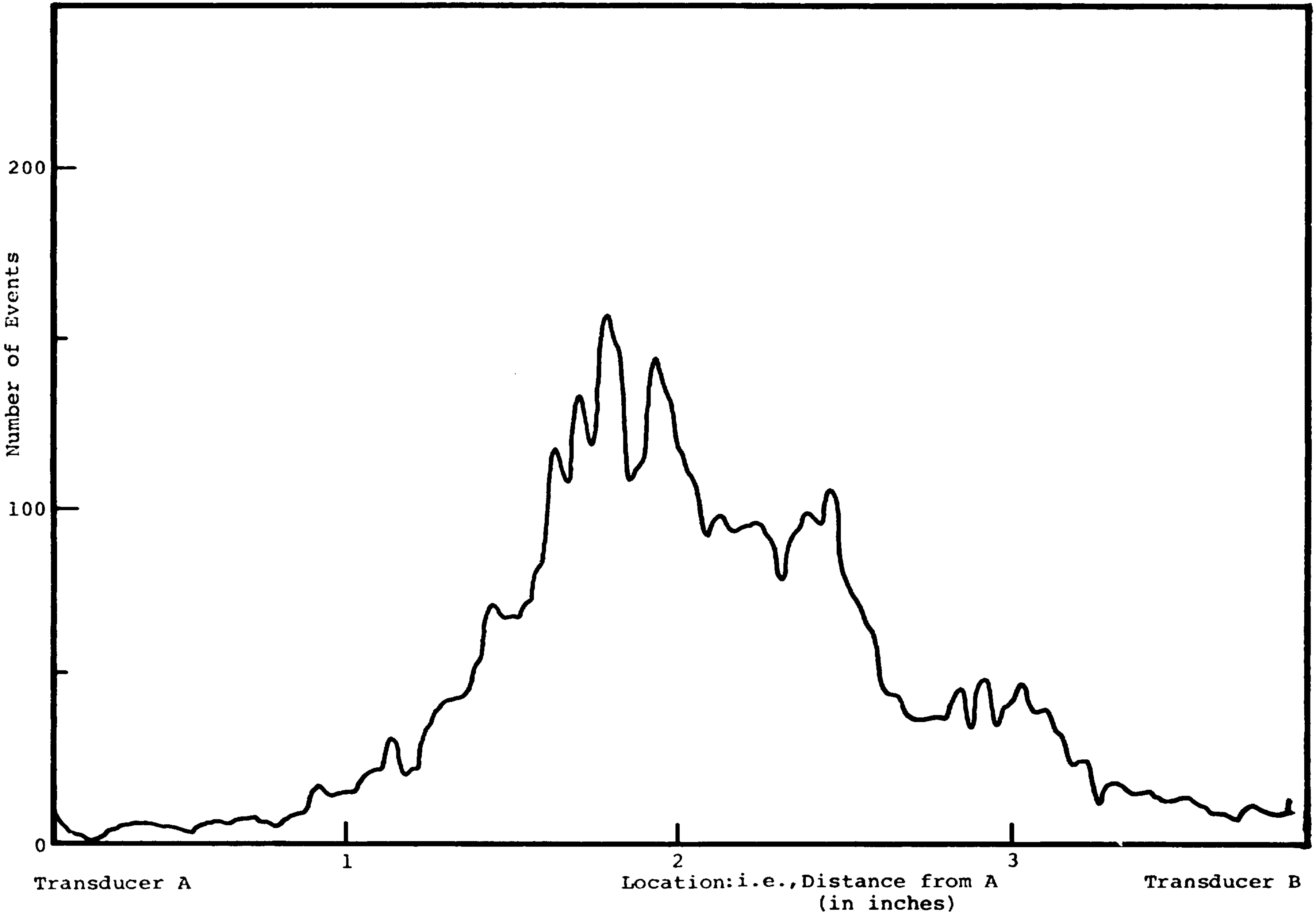

Figure 66. Location Distribution of Acoustic Emissions at Failure (±45°)

PART V

PERSONNEL

AUTHOR INDEX

PERSONNEL

Senior Investigators

Brunelle, E. J., Jr., Sc.D. (Aeroelastic and structures design and analysis)*	Associate Professor of Aeronautical Engineering
Das, P. K., Ph.D. (Non-destructive evaluation, research)*	Professor of Electrical and Systems Engineering
Diefendorf, R. J., Ph.D. (Fabrication, CAPGLIDE, fiber behavior, research)*	Professor of Materials Engineering
Feeser, L. J., Ph.D. (Computer applications and graphics, computer aided design, optimization)*	Professor of Civil Engineering
Hagerup, H. J., Ph.D. (Aerodynamics, configuration, pilot accommodation, CAPGLIDE)*	Associate Professor of Aeronautical Engineering
Helwig, G., Dr.Ing. (Finite element methods, computer aided design, composite structure optimization, CAPGLIDE)*	Research Assistant Professor of Aeronautical Engineering
Hoff, N. J., Ph.D. (Structural design and analysis, CAPGLIDE)*	John A. Clark and Edward T. Crossan Professor of Engineering
Krempl, E., Dr.Ing. (Fatigue studies, research)*	Professor of Mechanics and Director of Cyclic Strain Laboratory
Scarton, H., Ph.D. (Acoustic emission NDE)*	Associate Professor of Mechanical Engineering and Mechanics
Shephard, M., Ph.D. (Computer graphics, finite element methods)*	Assistant Professor of Civil Engineering

* Fields of Speciality

Sternstein, S. S., Ph.D. (Failure analysis, matrix behavior, research)*	William Weightman Walker Professor of Polymer Engineering
Tiersten, H. F., Ph.D. (Non-Destructive evaluation theory, research)*	Professor of Mechanics

Contributing Faculty

Kudva, N. J., Ph.D. (Postbuckling behavior)*	Assistant Professor of Aeronautical Engineering
McDonald, J. J., Ph.D. (NDE signal processing)*	Associate Professor of Electrical Engineering

Research Staff

Manager & Master Technician, Composites Laboratory

Paedelt, Volker

Research Associates

Otsuka, Hiromitsu, M.S.

Webster, R. T., M.S.

Graduate Assistants

Altman, Carl, B.A.
Chen, Lien-Wen, M.S.
Ely, Dale, B.A.
Helmer, James, B.S.
Herbert, Paul, B.S.
Kim, Wonsub, B.S.
Lumban Tobing, Frida, M.S.
Muser, Cristoph, Dipl.Mech.Ing.
Niu, Tyan-Min, M.S.
Taggart, David, B.S.
Uzoh, Cyprian, B.S.
Yang, Phillip, B.S.

* Fields of Speciality

Undergraduate Assistants - Seniors

Biddlecorn, Charles
Borfitz, Michael H.
DeFazio, Richard
Emmel, John E.
Fortune, James
Kearns, Thomas M.
McGuire, Paul T.
Mirales, Nicholas
Naylor, Dennis L.
Reilly, Dominic R.
Riker, Steven
Schmidt, David
Shaefer, Paul
Simkulet, Michael
Thomas, Scott
Van Elten, Charles
Venner, Joseph
Winckler, Steven
Zahorsky, John

Undergraduate Assistants - Juniors

Cappella, Michael
Cawthorne, Matthew
Coffed, Steven
Cronin, Catherine
Dalzell, Scott
Dormady, Daniel
Dunlap, Daniel
Fox, Peter
Grant, Peter
Leonard, Peter
Luth, Jim
McDermott, Dennis
Merritt, Mark
Murawski, Michael
Paige, Ron
Paige, Russell
Pretak, David
Ryan, Jody
Ryan, Kenneth
Wetzel, Eric

AUTHOR INDEX

Semi-Annual Progress Report

September 1979 - April 1980

COMPOSITE STRUCTURAL MATERIALS

Air Force Office of Scientific Research

and

National Aeronautics and Space Administration

Grant No. NGL 33-018-003

Co-Principal Investigators:

George S Ansell
Dean, School of Engineering

Robert G. Loewy
Institute Professor

and

Stephen E. Wiberley
Professor of Chemistry

Rensselaer Polytechnic Institute

Troy, New York 12181

NASA Technical Officer

Leonard A. Harris
Materials and Structures Division

NASA Headquarters

38th Semi-Annual Report **June 1980**

Semi-Annual Progress Report

September 1979 - April 1980

COMPOSITE STRUCTURAL MATERIALS

Air Force Office of Scientific Research

and

National Aeronautics and Space Administration

Grant No. NGL 33-018-003

Co-Principal Investigators:

George S Ansell
Dean, School of Engineering

Robert G. Loewy
Institute Professor

and

Stephen E. Wiberley
Professor of Chemistry

Rensselaer Polytechnic Institute

Troy, New York 12181

NASA Technical Officer

Leonard A. Harris
Materials and Structures Division

NASA Headquarters

38th Semi-Annual Report June 1980

CONTENTS

LIST OF TABLES

LIST OF FIGURES

INTRODUCTION

INTRODUCTION

The promise of filamentary composite materials, whose development may be considered as entering its second generation, continues to generate intense interest. Such interest is well founded, having been generated by the possibility of using brittle materials with high modulus, high strength, but low density in composites which fail in a non-catastrophic manner. Such fiber reinforced composite materials offer substantially improved performance and potentially lower costs for aerospace hardware. While much progress has been achieved since the initial developments in the mid 1960's, however, only a very few applications to primary aircraft structure have been made, and those are in a material-substitution mode and on military aircraft.

To fulfill the promise of composite materials more completely, requires a strong technology base. NASA and AFOSR have realized that to fully exploit composites in sophisticated aerospace structures the technology base must be improved. This, in turn, calls for expanding fundamental knowledge and the means by which it can be successfully applied in design and manufacture. Not the least of this effort is to learn how to design structures specifically to capitalize on the unique properties of composite materials. It also calls for expanding the body of engineers and scientists competent in these areas. As part of their approach to accomplishing this, NASA and AFOSR have funded the current composites program at Rensselaer. The purpose of the RPI composites program is to develop advanced technology in the areas of physical properties, structural concepts and analysis, manufacturing, reliability and life prediction. Concommitant goals are to educate engineers to design and use composite materials as normal or conventional materials. A multifaceted program has been instituted to achieve these objectives. The major elements of the program are:

1. CAPCOMP (Composite Aircraft Program Component). CAPCOMP is primarily a graduate level project being conducted in parallel with a composite structures program sponsored by NASA and performed by a private, aerospace manufacturing contractor. The first component redesign is being done in conjunction with the Boeing Commercial Airplane Company. The main spar/rib region on the Boeing 727 elevator, near its actuator attachment point, was selected, with Boeing's advice and the concurrence of NASA/AFOSR, for study in CAPCOMP. The magnitude of the project - studying, designing, fabricating and testing of a relatively small but highly stressed region on the elevator - is both consistent with Rensselaer's capabilities and a significant challenge. The selection of a portion of a full-scale flight hardware structure assures relevance to this project's direction.

Visits to Boeing were conducted in the Fall of 1978 by Professor Hoff and several of his students, and the first serious design work began shortly thereafter. Two alternative designs were pursued to the point of preliminary analysis and testing. One of these was selected for more detailed analysis, redesign, complete fabrication and testing. Further progress on fabrication planning and fabrication facilities and test fixture development is reported in Part I.

2. CAPGLIDE (Composite Aircraft Program Glider). This undergraduate demonstration project has as its objectives the design, fabrication and testing of a foot-launched, ultralight glider using composite structures. A flight vehicle was selected to maximize student interest and to provide the students with a broad-based engineering experience. For those students continuing with graduate work at RPI, CAPGLIDE is intended to provide natural progression to CAP-COMP. The progress on the CAPGLIDE project to date has been very good. Seven professors and approximately 30 students were actively engaged in the project during this period; that is, the '79-'80 semesters. High point of the project to date was final assembly of the complete glider, dubbed "RP-1", and its exhibition during the site visit to Rensselaer by a team of scientists/engineers from NASA and industry. A description of the status of the CAPGLIDE project to the end of the current reporting period is given in Part II.

3. COMPAD (Computer Aided Design). A major thrust of the composites program is to develop effective and efficient tools for the analysis and design of composite structures. Rensselaer and NASA Langley have jointly implemented the use of the SPAR code on minicomputers, and the work at Rensselaer

has made "virtual memory" available to those using SPAR. Attention for the current period has continued to be focused on preprocessor developments; details are reported in Part III.

4. Composites Fabrication and Test Facility. Structural design engineers, educated only by course work and design projects limited to paper, often fail to sense or appreciate problems involved in fabrication. The actual fabrication and testing of composite structural components provides this training and the final validation for the designs in our CAP projects. RPI's Composites Fabrication and Test Facility is located in the laboratory and high bay areas of the Jonsson Engineering Center. Equipment is available for compression molding parts as large as 19" x 19" and vacuum bagging parts of much larger size. Panels approximately 4' x 20' have been made by vacuum bagging. Specifics are given in Part II, CAPGLIDE. A pressure vessel for small parts and spars has been designed and built. A second one capable of higher pressures was designed and parts ordered in the current period; assembly of all components but air circulation is now complete. More information on this development is contained in Part I, CAPCOMP.

5. INSURE (Innovative and Supporting Research). The criteria for selection of research projects to be conducted under this program are (a) that they must anticipate critical problem areas which may occur in the CAP or NASA/AFOSR programs or (b) that solutions to existing problems are not

yet satisfactorily in hand. During the reporting period seven such projects were conducted as part of the program. Results from the ongoing projects are reported in Part IV.

6. Curriculum Revisions. The goal of educating engineers to think of composites as normal or conventional materials has required changes in curriculum. Since the initiation of this program, almost all Rensselaer engineers take introductory courses which incorporate the concepts of anisotropy and composite materials. In addition, six specialized courses in composites have been offered during the past three years to develop those special skills required of students involved in the composites program. A new course was introduced in the Fall of '78 semester on composite design and analysis using programmable hand calculators, a central mini and full frame computers. A new graduate level advanced topics course with the title "Advanced Finite Elements"was offered for the first time in September 1979.

The additions of the SAP and SPAR computer codes and the growing availability of interactive computer graphics under our COMPAD program element have reached the point where our engineering students are using these facilities as everyday working tools for design, analysis and visualization purposes. We have thus achieved one of the principal goals of the curriculum development activities.

7. Technical Interchange.

a) Mr. Hiromitsu Otsuka joined the faculty at RPI as a Visiting Research Associate. Mr. Otsuka is a member of the staff of the Industrial Products Research Institute of the Ministry of International Trade and Industry where he was engaged in developing a light weight wheelchair of fiber reinforced plastic materials. At RPI he has been conducting acoustic emission studies of composites under load, together with RPI's Professor H. Scarton, during this period.

b) Technical Meetings: Technical meetings, on- and off-campus, provide important opportunities for interchange of technical information. Because of the large number of composites meetings, a central catalog with all upcoming meetings is being maintained and distributed periodically. In this way we help assure that a Rensselaer staff member will participate in important meetings. The calendar for this reporting period is shown in Table I. Meetings attended by RPI composites program faculty/staff during the reporting period are shown in Table II. Some meetings particularly relevant to composites, held on-campus with off-campus speakers, are listed in Table III. A list of composite-related visits to relevant organizations by RPI faculty/staff/students, with the purpose of each visit outlined, is presented in Table IV.

In summary, the NASA/AFOSR Composites Aircraft Program is a multi-faceted program whereby aeronautical, mechanical and materials engineers must interact to achieve its goals. "Hard-nosed" engineering of composite aircraft structures is balanced against research aimed at solving present and future

TABLE I
CALENDAR OF COMPOSITES-RELATED MEETINGS
for the period September '79 to April '80

1979	
10/1-3	Tests Methods and Design Allowables for Fibrous Composites, Dearborn, Mi. "Sponsored by ASTM."
10/7-10	Fall Meeting of Society for Experimental Stress Analysis, Mason, Oh.
10/8-11	Advanced Techniques in Failure Analysis Symposium and Exposition, Los Angeles, Ca.
10/10-11	Conference on Engine Structures, NASA Lewis Research Center.
10/10-12	3rd SAE International Conference on Vehicle Structural Mechanics, Troy, Mi. "Sponsored by SAE."
10/16-18	50th Shock and Vibration Symposium, Colorado Springs, Co.
10/22-23	Grumman/University Technical Forum, Bethpage, N. Y. "Sponsored by Grumman."
10/23-25	SAMPE Technical Conference, Boston, Ma. "Sponsored by SAMPE."
10/28	Annual Meeting of the Society of Rheology, Boston. Ma.
10/30-11/1	5th Annual Mechanics of Composites Review, Dayton, Oh. "Sponsored by the Air Force Materials Lab."
10/30	U. S. National Committee for Theoretical and Applied Mechanics, Boston, Ma.
11/6-8	Helicopter Propulsion System Specialists' Meeting, Williamsburg, Va. "Sponsored by AHS."
11/13-16	Supersonic Cruise Research Conference, Hampton, Va. "Sponsored by NASA Langley."
12/2	9th International Symposium on Acoustical Imaging, Houston, Tx.
12/2-7	ASME Winter Annual Meeting, N. Y. C., N. Y. "Sponsored by ASME."

TABLE I (continued)

1980	
1/6-11	Engineering Foundation Conference on Fatigue Crack Initiation, Asilomar, Ca.
1/14-16	18th Aerospace Sciences Meeting, Pasadena, Ca. "Sponsored by AIAA."
1/20-26	Gordon Research Conference on Deformation and Failure in Composites, Santa Barbara, Ca.
2/4-8	35th Annual Reinforced Plastics/Composites Institute Conference, New Orleans, La. "Sponsored by the Society of Plastics Industry.
2/10-13	3rd Annual Meeting of Adhesion Society, Savannah, Ga.
2/24-26	109th AIME Annual Meeting, Failure Modes in Composites V, Las Vegas, Ne. "Sponsored by AMMRC."
3/25-27	Specialists Meeting on Fatigue Methodology, St. Louis, Mo. "Sponsored by AHS."
4/14-15	Symposium on Short Fiber Reinforced Composite Materials, Minneapolis, Mn. "Sponsored by ASTM/SAE/ASCE."
4/14-18	Practical Applications and Design of Fibrous Composites, Los Angeles, Ca. "Sponsored by UCLA."
4/22-24	Conference on Propeller Propulsion, Dayton, Oh. "Sponsored by University of Dayton, AIAA, AHS, Society of Auto Engineering."

TABLE II

COMPOSITES-RELATED TECHNICAL MEETINGS ATTENDED OFF-CAMPUS

for the period September '79 to April '80

1979	
10/1-3	ASTM Meeting on Test Methods and Design Allowables for Fibrous Composites (Prof. Helwig), Dearborn, Mi.
10/10-11	Conference on Engine Structures (Prof. Loewy), NASA Lewis Research Center.
10/28	Annual Meeting of the Society of Rheology, (Prof. Sternstein and D. Taggart), Boston, Ma.
10/30-11/1	Mechanics of Composites Review (Prof. Kudva), Dayton, Oh.
10/30	U. S. National Committee for Theoretical and Applied Mechanics (Prof. Hoff), Boston, Ma.
12/2	9th International Symposium on Acoustical Imaging (Prof. Das), Houston Tx.
1980	
1/6-11	Engineering Foundation Conference on Fatigue Crack Initiation (Prof. Stoloff), Asilomar, Ca.
1/20-26	Gordon Research Conference on Deformation and Failure in Composites (Profs. Diefendorf and Sternstein*), Santa Barbara, Ca.

* Presented a paper titled, "Swelling Stress in Epoxy Composites".

TABLE III
COMPOSITES-RELATED MEETINGS/TALKS HELD AT RPI

(September '79 - April '80)

Topic	Date	Speaker(s)
Aromatic Polyamides: Development and Uses	10/10/79	Paul W. Morgan, formerly Research Associate, E. I. duPont de Nemours and Co.
New Methods in High Temperature Structural Design	10/11/79	Donald Griffin, Westinghouse Corp.
World Trends in Computer-Aided Manufacturing	10/25/79	M. Eugene Merchant, Director of Research Planning, Cincinnati Milacron, Inc.
Effects of Moisture on Epoxy Composites	11/29/79	James B. Whiteside, Head, Applied Mechanics Laboratory, Grumman Aerospace Company
An Integrated Shell Analysis System with Interactive Computer Graphics	11/13/79	John F. Abel, Cornell University
New Thoughts on the Problem of Bending and Twisting of Beams	12/13/79	Eric Reissner, University of California at San Diego
Microscopic Fracture of Fibrous Composites	1/15/80	Byron Pipes, Director, Center for Composite Materials, University of Delaware
Some Topics of Low-Cycle Fatigue Design of Heavy Duty Components	1/17/80	Y. Asada, University of Tokyo
Preliminary Design Study of a Space Telescope Using Composites	2/7/80	Donald E. Skoumal, Lead Engineer, Structural Development, Boeing Aerospace Co.
Acoustic Scattering in Random Inhomogeneous Media	2/18/80	Mark Beran, Tel-Aviv University
Challenges of Opportunities of In-situ Composites	3/6/80	F. Lemkey, United Technologies Corp.
Forces Acting on Lattice Defects in Generalized Coordinates	3/13/80	Richard K. T. Hsieh, Royal Institute of Sweden
Reacting to Things That Fall Apart in Service	4/17/80	Oscar Orringer, Transportation Systems Center, Department of Transportation, Cambridge, Ma.

TABLE IV
COMPOSITES-RELATED VISITS TO RELEVANT ORGANIZATIONS
by RPI Faculty/Staff/Students

Visited	Date	by Prof(s)	Purpose
ASTM Committee Meetings E-9 and E-24, Pittsburgh, Pa.	10/30-11/1	N. Stoloff	Meetings concerning fatigue toughness and fracture toughness testing
Lockheed California Co.	11/6	S. Sternstein	To discuss processing science aspects of curing composites
Boeing Commercial Airplane Company: J. L. Lundry Supervisor-Aero Methodology	11/12-13	G. Helwig H. Hagerup	To apply Boeing Airfoil Composite Design Methodology to CAP-GLIDE RP-2
NASA Langley: Structures Division	4/9/80	N. Hoff	To present results of theoretical developments regarding stresses around holes in composites

problems. In the following sections, detailed descriptions of the CAPCOMP, CAPGLIDE, COMPAD and INSURE programs are presented.

PART I

CAPCOMP (Composite Aircraft Program Component)

CAPCOMP (Composite Aircraft Program Component)
(N. Hoff, R. Loewy)

CAPCOMP is a program to design flight critical structures to take the maximum advantage of composite materials. By combining the efforts of experienced faculty with bright and well trained but inexperienced graduate students in an environment relatively free of traditional design and manufacturing processes, we intend to devise new and hopefully useful design concepts.

There is sufficient information available to prove that many structural elements can be made lighter by using advanced composites today than by using metals. But if such elements have to be joined by methods other than adhesive bonding, difficulties and uncertainties arise which can be eliminated only through conservative designs with their attendent penalties in weight or by extensive and expensive programs of "cut and try". This stands as one important impediment to full adoption of composites by the aerospace industry.

On the basis of these considerations Rensselaer Polytechnic Institute began, as the first task aimed at new structural concepts, the design using composites of a joint used in an airplane elevator. To make the design realistic, an existing metal airframe component was chosen for redesign in composites. The existing design chosen was that of the Boeing 727 elevator actuator attachment. We conceive of this work as carrying forward a Structures Demonstration Program using the joint of the 727 elevator, paralleling that of NASA and its aerospace engineering contractor, the Boeing Commercial Airplane Company. Our design, fabrication and test effort emphasizes design ideas specifically suited to advanced composite construction for the purpose of minimizing the weight of the structure, but on a scale consistent with the university context and funding level. The staff of RPI is very grateful to the Boeing Company and its engineers for their wholehearted support of the work at RPI.

During the reporting period, one of two different designs reported previously (July and December 1979) as suitable for replacing the largely metal attachment produced by Boeing was selected for further analysis, redesign, fabrication and testing. We call it the "Berg Design", and it makes use of quasi-isotropic, graphite-epoxy laminates. The second design, called the "Muser Design", which made a deliberate attempt to use uniaxial graphite-epoxy tape to as great an extent as possible, was suspended. It has led, however, to more generic research efforts to maximize the load carrying ability of pin-loaded holes in composite membranes and plates. These efforts are directed at improving the design of the attachment of the rib flanges to the elevator skin through mechanical (i.e., pin-type) fasteners and at maximizing the efficiency of the movable, heavily loaded, actuator attachment points in CAPCOMP. In addition, however, and increasingly, these generic effects are motivated by the general and widespread utility that will result from improvements in pin-loaded hole designs for composites.

These efforts have been jointly directed by Dr. Nicholas J. Hoff, in part time arrangement and by Dr. Robert G. Loewy. They are further described in the following paragraphs.

1. The Elevator and Its Attachment

To place the progress reported here in proper context, some descriptions used in earlier reports are repeated. The conventional aluminum alloy elevator of the Boeing 727 is shown in the upper half of Figure 1. The lower half of the figure is the new version of the elevator redesigned by Boeing in graphite epoxy; it is evident from the pictures that the latter is composed of fewer parts than the former. However, the actuator fitting of the new design is still manufactured of aluminum alloy. This fitting is shown in Figure 2. The fitting is attached to outboard and inboard portions of a new graphite-epoxy spar and to a graphite-epoxy nomex-honeycomb rib as indicated in Figure 3.

The attachment was designed by Boeing to carry loads up to 19,000 pounds. The direction of the load varies as the elevator rotates over an angle of 28 degrees from the full-down to the full-up position.

2. Berg's Design

Berg's design is shown in Figures 4 and 5. The first of these figures compares the Boeing composite design with

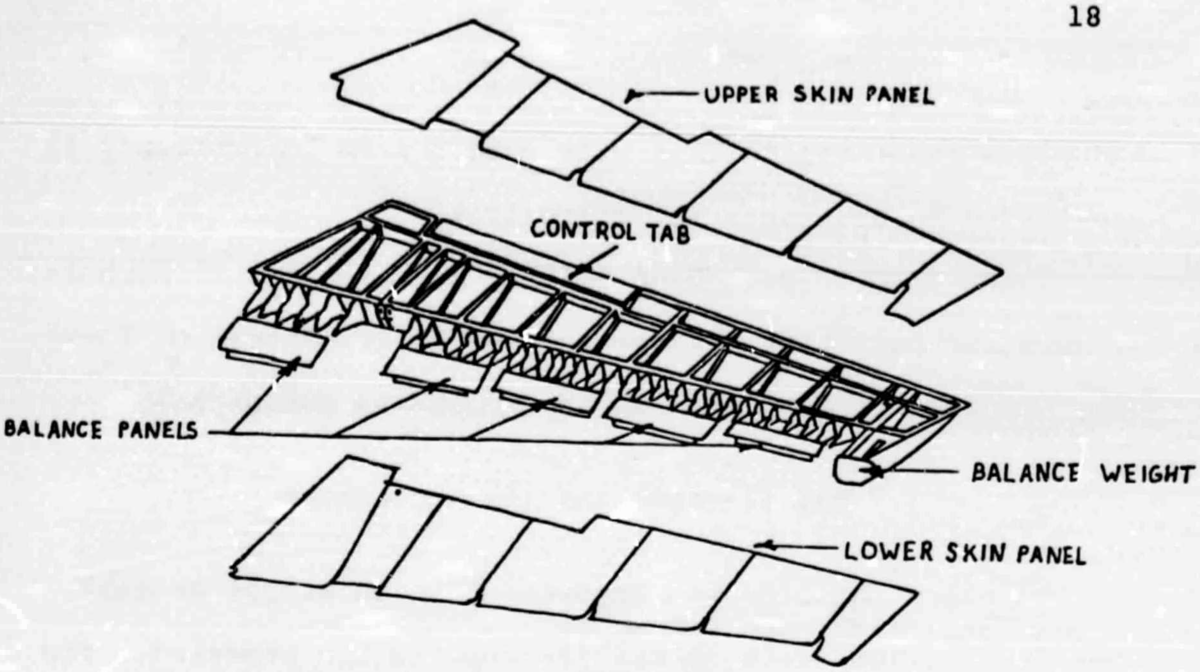

Conventional Aluminum Elevator

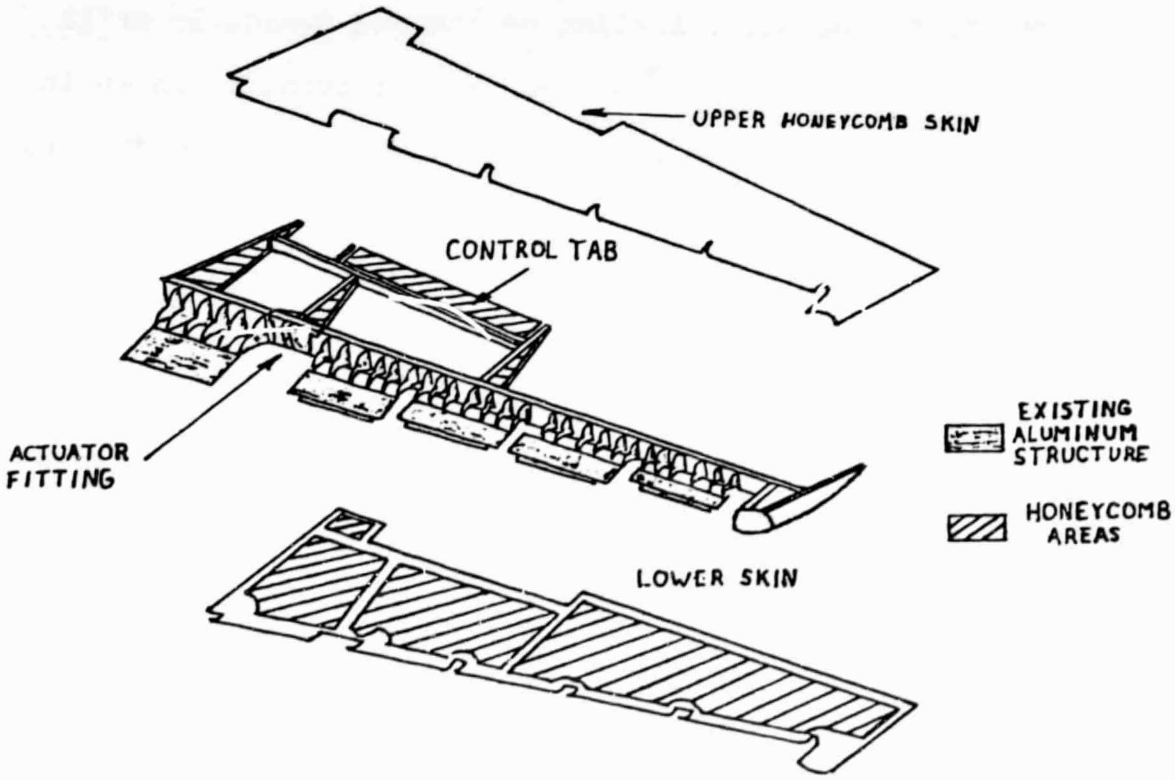

Advanced Composite Elevator

BOEING ELEVATOR ASSEMBLY

Figure 1

ALUMINUM ACTUATOR FITTING (Boeing Design)

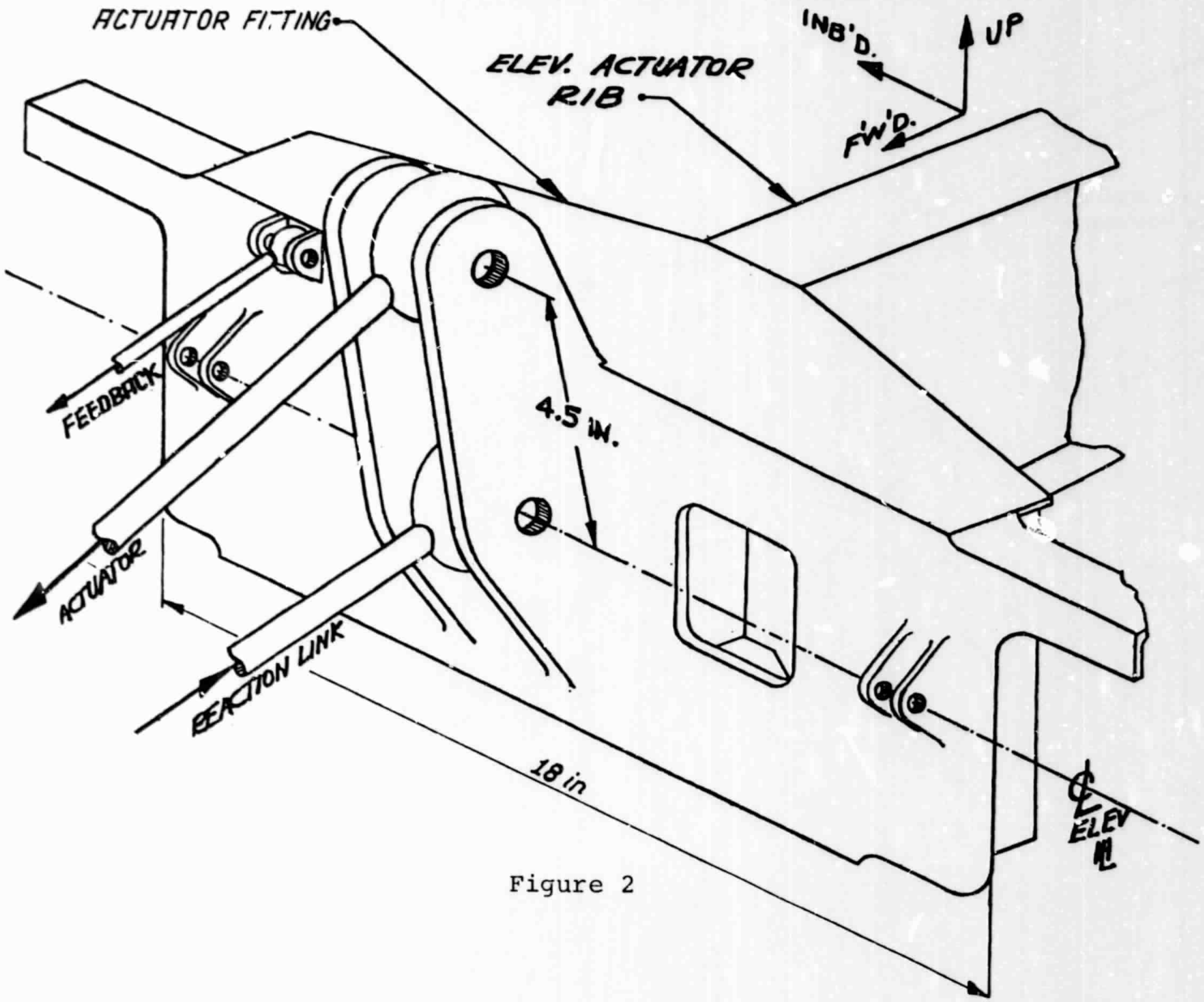

Figure 2